I

Master of Science Thesis

Experimental investigation of artificial boundary layer transition

A comparison of different tripping devices

R.A.C.M. Slangen

March 2009

Faculty of Aerospace Engineering

Delft University of Technology

Abstract

Nowadays there is a wide variety of applications for forced transition. They are all based on introducing disturbances to the flow and increasing its momentum thickness. Forced transition or bypass transition as it is also called is used to manipulate the flow by setting the transition point in such a way that the required/better flow situation is achieved.

There is a variety of types of transition devices in use such as a simple wire, sandpaper, surface steps and zigzag tape. All of them have their own characteristics. In this report an investigation of the last two has been given. From practical experience it is known that the zigzag tape produces transition to turbulence with less height of the obstacle. This implies that the zigzag strip produces turbulence more efficiently than a two-dimensional roughness. The difference in efficiency suggests that there may be differences in the mechanism creating turbulence behind these two kinds of devices. What happens in the transition phase of the flow over these obstacles has been investigated.

For this investigation hot wire anemometry has been used to locate and quantify turbulence and particle image velocimetry to visualize structures in the flow. The results confirm the different behaviour (efficiency) of the two tripping device types. A clear difference is revealed in the flow comparing the zigzag strip to the two-dimensional roughness element composed of a strip of rectangular cross-section. The zigzag strip causes streamwise vortices which interact with the outer flow to create turbulence through mixing. This explains why it is more efficient. These vortices persist quite far downstream, hence the turbulent flow is only slowly moving to a uniform state. This means the flow is not completely uniform. The surface step creates a spanwise vortex which causes the mixing. This vortex doesn’t trail far behind the strip and thus creates a more homogeneous turbulent flow downstream of it.

Preface

This report represents the Master thesis of my study. I did this research within the chair of Aerodynamics of the faculty of Aerospace engineering of the Delft University of Technology. For the last twelve months I have been working on the low speed boundary layer flow over a flat plate, using several devices to trigger transition from laminar to turbulent flow.

I would like to thank dr.ir. B. W. van Oudheusden, prof. dr. F. Scarano and dr.ir. L.L.M. Veldhuis for their supervision and advice. Also I would like thank Gerrit Elsinga for his advice on PIV and hot wire anemometry. A word of gratitude also goes out to technical staff of the Aerodynamics group for helping me in setting up the experiments and providing me with the required computer necessities. I also would like to thank Roeland de Kat and Ferry Schrijer for helping me out during experiments. Furthermore I would like to thank everybody in the Aero-basement for the nice discussions and necessary relax breaks during the days.

Above all I would like to thank my parents, sister and my friends for their support during my study and last but not least my girlfriend for her endless support during my study.

Delft, March 2009

Roel Slangen

List of symbols

a	Overheat ratio; Seeding particle radius
c_p	Specific heat
C_w	Heat capacity of the hot wire
d	Diameter
d_{diff}	Diameter of Airy disc
d_p	Particle diameter of seeding
D_a	Aperture diameter
d_τ	Particle image diameter
E_a	Acquired voltage
E_c	Thermal energy of the hot wire
E_{corr}	Temperature corrected voltage
f	Focal length
$f_\#$	Aperture number
h	Height i.e. y
H	Shape factor $\left(\frac{\delta^*}{\theta}\right)$; heat removed from hot wire
I	Electrical current
k	Heat conductivity
k_f	Heat conductivity of the fluid
L	Kolmogorov length scale
Nu	Nusselt number
M	Magnification factor
P	Pressure
q	Heat transfer rate; width of zigzag strip
R_w	Electrical resistance hot wire
Re	Reynolds number
Re_{crit}	Critical Reynolds number for amplification of TS-waves
Re_{tr}	Reynolds number based on point of transition
Re_δ	Reynolds number based on boundary layer thickness $\left(\frac{U_\infty \delta}{\mu}\right)$
Re_Θ	Reynolds number based on momentum thickness $\left(\frac{U_\infty \theta}{\mu}\right)$
S_k	Particle Stokes number
t	Time; Thickness of the strip
T	Temperature
T_s	Temperature of the fluid surrounding hot wire
T_w	Hot wire temperature
T_0	Ambient temperature
Tu	Turbulence intensity
u, v, w	Velocity in x, y, z-direction respectively
$\bar{u}$, $\bar{v}$, $\bar{w}$	Average velocity in x, y, z-direction respectively
U_{mean}	Average velocity
U_{RMS}	Root mean square of velocity
U_∞	Freestream velocity

V_f	Fluid velocity
V_p	Seeding particle velocity
w	Total width of the strip
W	Electrical energy produced in the hot wire
x, y, z	Coordinate axis
z_0	Distance between lens and image plane
Z_0	Distance between object and lens
α	Top angle of zigzag strip
α_0	Sensor temperature coefficient
δ	Boundary layer thickness
δ_z	Focal depth
δ^*	Displacement thickness
$\delta_{99\%}$	Boundary layer thickness based on $u = 0.99U_\infty$
θ	Momentum thickness
λ	Wavelength of the laser light
λ_{TS}	Wavelength of TS-wave
λ_x, λ_z	Length of Λ-vortices in x and z-direction respectively
μ	Dynamic viscosity
ν	Kinematic viscosity
ρ	Density
ρ_f	Fluid density
ρ_p	Density of seeding particles
τ	Boundary layer shear stress
τ_f	Characteristic time of the flow
τ_p	Particle response time
ψ	Stream function

Contents

1. Introduction

Looking at the flow over a smooth surface, especially at the thin layer near the surface (i.e. the boundary layer) one can see the flow starting as a smooth flow with near parallel streamlines up till some point were small disturbances start to become unstable and amplify until the flow will become fully chaotic. The first phase is called laminar flow and the latter is called turbulent. The phase in between is called transition (figure 1.1). This transition is still regarded as a very complex phenomenon in modern fluid dynamics research. It will be very useful to know how the transition mechanism in the boundary layer works. You can use this knowledge to develop devices to delay or to initiate transition more effectively. In this field already quite some research has been done, both experimental as well as numerical (CFD). Different transition devices have been developed ranging from simple passive 2-dimensional wires to active means like the application of speakers.

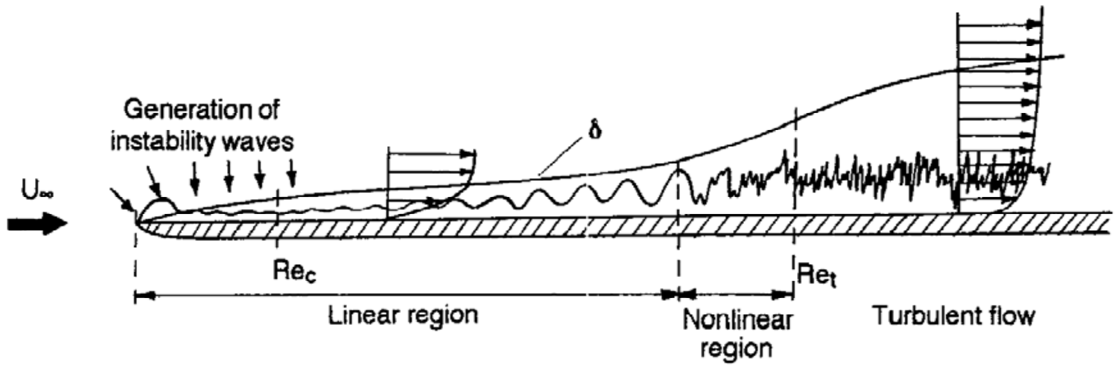

figure 1.1 Sketch of turbulence development (Kachanov, 1994)

1.1 Transition devices in use

Transition devices are used to alter the state of the boundary layer over/around an object. They can be found in wind tunnels during experiments (eg. Klebanoff,1955) to create turbulence at a shorter distance than naturally would occur. In this case this may be usefull, because space may be limited in a windtunnel. On airfoils they are used to tune some of the performance parameters eg. triggering boundary layer transitions can reduce the laminar bubble (reference 2: Aerodynamic tuning of a nimbus 4D model). On speed-skating suits they decrease the drag (based on the same principle as the golf ball).

On sailplanes the zigzag strips are used to create a turbulent boundary layer in order to postpone separation which would cause a substantial drag increase. An example of this use is shown in figure 1. 2.

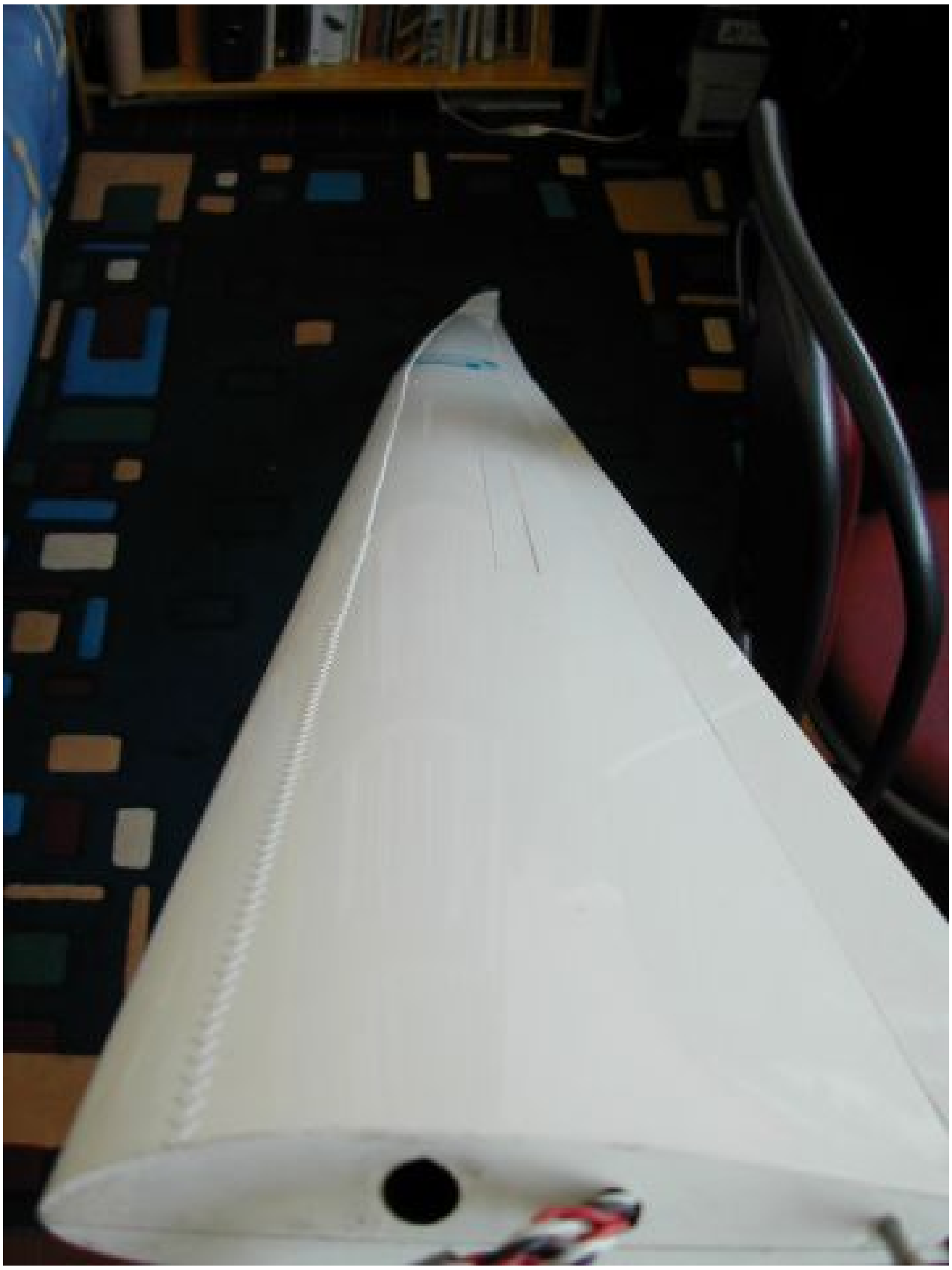

figure 1.2 Sailplane wing with zigzag strip (Aerodynamic tuning of a nimbus 4D model)

Not all transition devices are equally effective (for comparable height) in triggering turbulence. For instance a forward facing step is less effective than a backward facing step. But most important for this investigation: a rectangular strip (2-dimensional) is not as effective as a zigzag strip (3-dimensional) (Aerodynamic tuning of a nimbus 4D model). This difference suggests that the flow in the boundary layer behind these strips should be different.

1.2 Existing research on transition devices

Research on transition devices or bypass transition varies from experimental and theoretical research in the 1950s of Preston [1957] (roughness, circular wire, surface step), Braslow [1960](sandpaper roughness) and Klebanoff [1955] (research on transition in general but used sandpaper to trigger transition) via Smith [1983] (circular rod) to the numerical research of more recent dates [Brandt, 2002]. However most research done on this topic so far has been done on either very simple devices such as sandpaper roughness, wires and steps or on rather complex devices such as acoustic speakers and vibrating ribbons. In this report we are going to take a look at the straight rectangular strip and zig zag strip which are easy to use. A comparison in transition mechanism between these two has been made.

1.3 Goals for this investigation

The goal of this investigation is to get a better understanding of the transitional flow, caused by artificial transition, in the boundary layer. In this graduation work primarily particle image velocimetry (PIV) is used to visualise and analyse the low speed flow over a flat plate using two different transition devices (straight and zigzag strip).

1.4 Outline of the report

Chapter 2 of this report will deal with turbulence and transition to turbulence in general. The used experimental setup is explained in chapter 3. Chapter 4 shows the results from which the conclusions in chapter 5 have been found. The final chapter 6 gives some recommendations for further investigation

2. Transition and Turbulence

From the leading edge the boundary layer starts of as an ordered smooth parallel 2-dimensional flow. Viscous forces at the wall slow the flow down from the bottom upward. The boundary layer is that part of the flow where the velocity is less than 99% of the free stream velocity. This influence on the flow reaches ever higher above the plate the further you get from the leading edge and so the boundary layer will grow in thickness. More phenomena happen in this part of the flow, which will be discussed in this paragraph.

2.1 Theoretical approximations

From theoretical aerodynamics several models for a laminar boundary layer are known. A very common one is the Blasius equation. This equation gives the following results (White, 1991)

$$\delta_{99\%} \approx \frac{5x}{\sqrt{\mathrm{Re}_x}} \tag{2.1}$$

$$\mathrm{Re}_\theta \approx \frac{0.664}{\sqrt{\mathrm{Re}_x}} \qquad \text{where } \mathrm{Re}_\theta = \frac{U\theta}{\mu} \tag{2.2}$$

In figure 2.1 and 2.2 the theoretical development of the laminar boundary layer in streamwise direction is shown. These plots are used later on make a good estimation of the strip position and its height, to make sure the strip doesn't protrude the boundary layer.

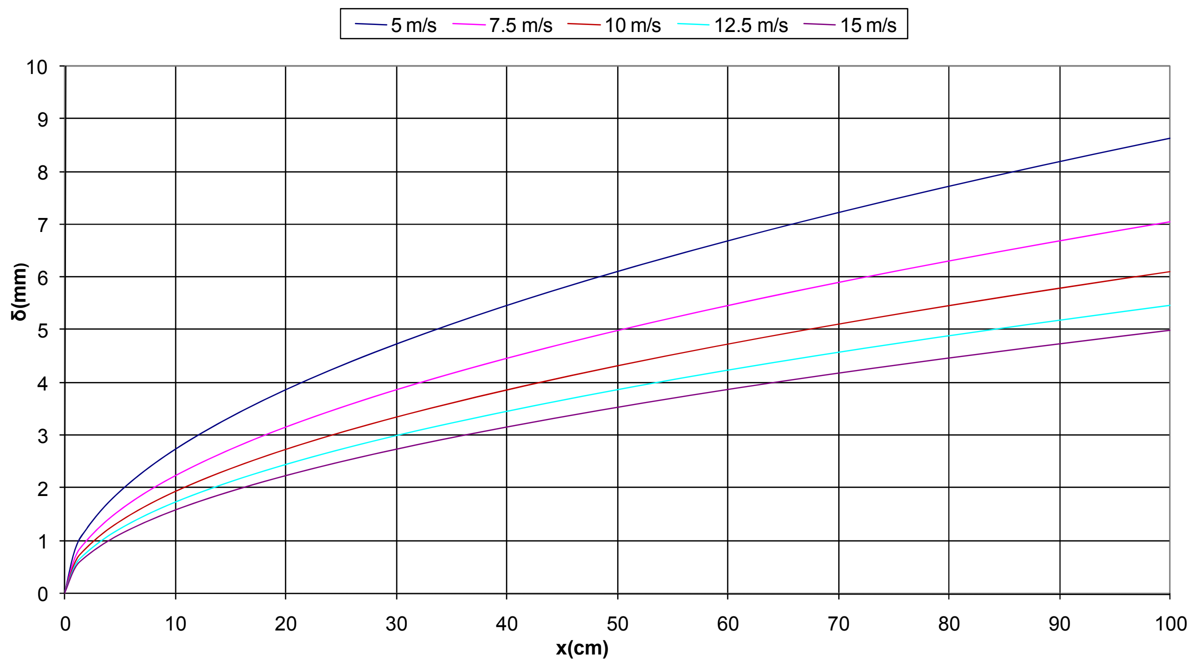

figure 2.1 Boundary layer thickness on a flat plate, with zero-pressure gradient; μ=1.8*10^{-5} kg/ms

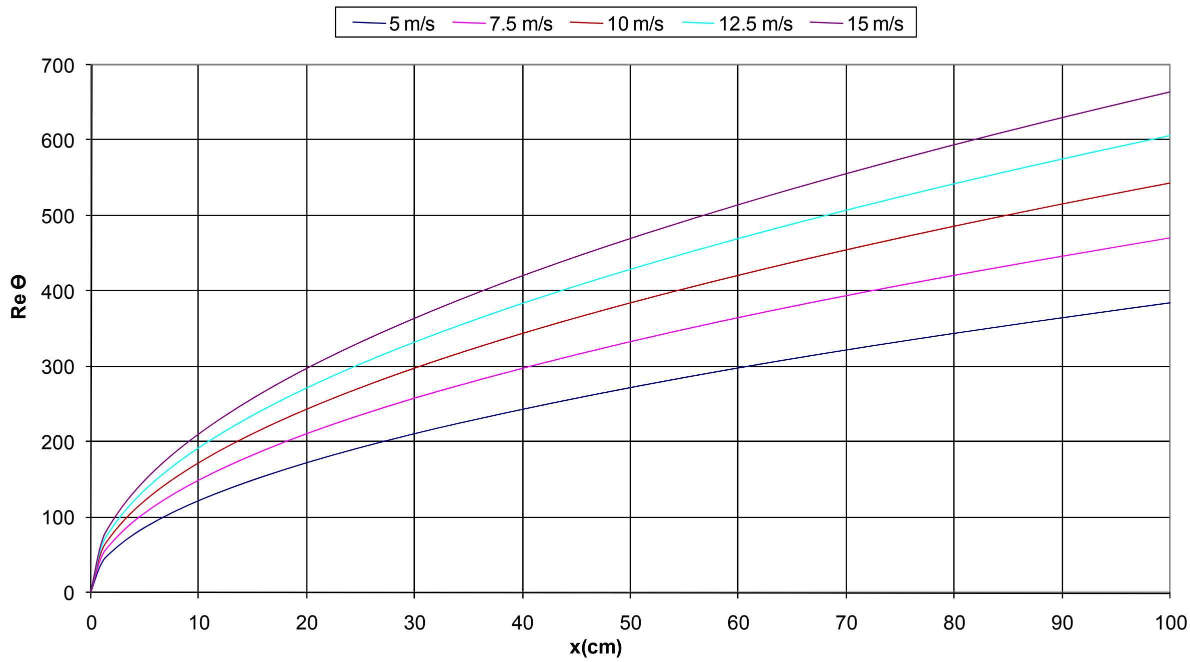

figure 2.2 Momentum thickness on a flat plate with zero-presure gradient; μ=1.8*10^{-5} kg/ms

2.2 Transition to turbulence

The flow over a flat plate in a homogeneous parallel flow will develop a boundary layer starting to grow at the leading edge. At first the flow will be laminar, because all disturbances (like Tollmienn-Schlichting waves) are damped sufficiently. So the flow will be smooth.

At larger downstream locations disturbances aren't damped sufficiently anymore. From here the disturbances will continuously grow and will develop into so called Λ-vortices. At first these Λ-vortices are inline and later staggered [White,1991] .

At some point these Λ-vortices start to rise from the surface. Once these horseshoe vortices reach the flow outside the boundary layer they will cause a lot of turbulence. This phase is called bursting.

This causes a turbulent spot. From this point the flow in this part of the flow is turbulent. These spots grow until the complete flow is turbulent. This transition to turbulence can occur naturally or it can be forced by means of a transition device.

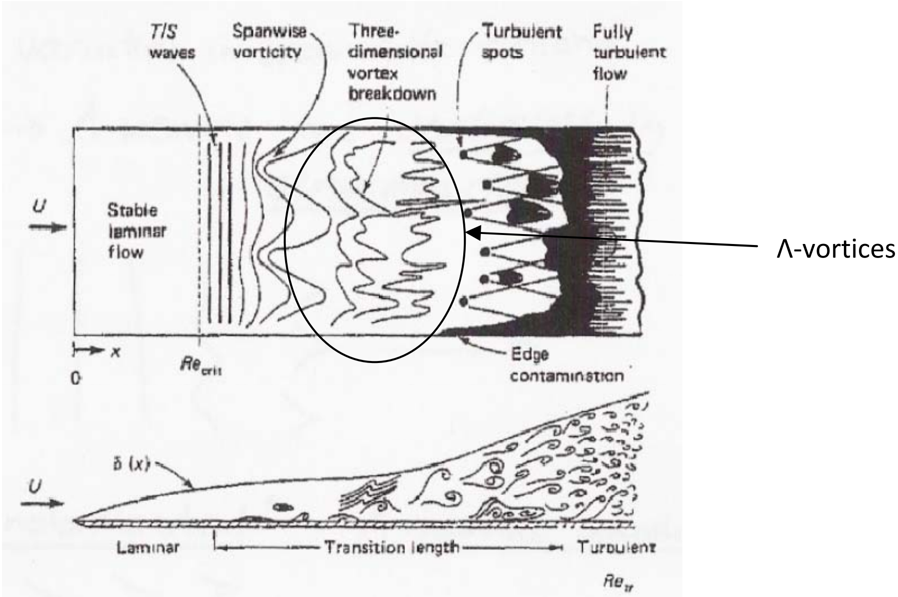

figure 2.3 Sketch of transition process (White, 1991)

2.2.1 Natural transition

Under normal circumstances the flow goes through several stages during transition. In this section these stages are described.

Tollmienn Schlichting waves
Tollmienn Schlichting waves are very small instability waves which form in the boundary layer. These waves are at the frequency which is damped the worst; hence they can grow and get a 3-dimensional structure, with peaks and valleys in spanwise direction (White). There is no point going into more detail for now since these waves are hard to detect (because of their small amplitude) and their small significance for this study, since the focus of this report is on artificial transition. According to Preston the minimum momentum thickness in order to have amplification of disturbances: $Re_\theta = 162$

Hairpin vortices
The Tollmienn-Schlichting waves develop into spanwise vorticity and strong spanwise variations in streamwise velocity. These waves break down into so-called Λ-vortices which can be divided in three distinct forms:

type	Fluctuations (% of U_∞)	$\frac{\lambda_x}{\lambda_{TS}}$	$\frac{\lambda_z}{\lambda_x}$	Configuration
K	1	1	0.5	Inline
C	0.3	0.5	1.5	Staggered
H	0.6	2	0.7	Staggered

Table 2.1 The different types of Λ-vortices

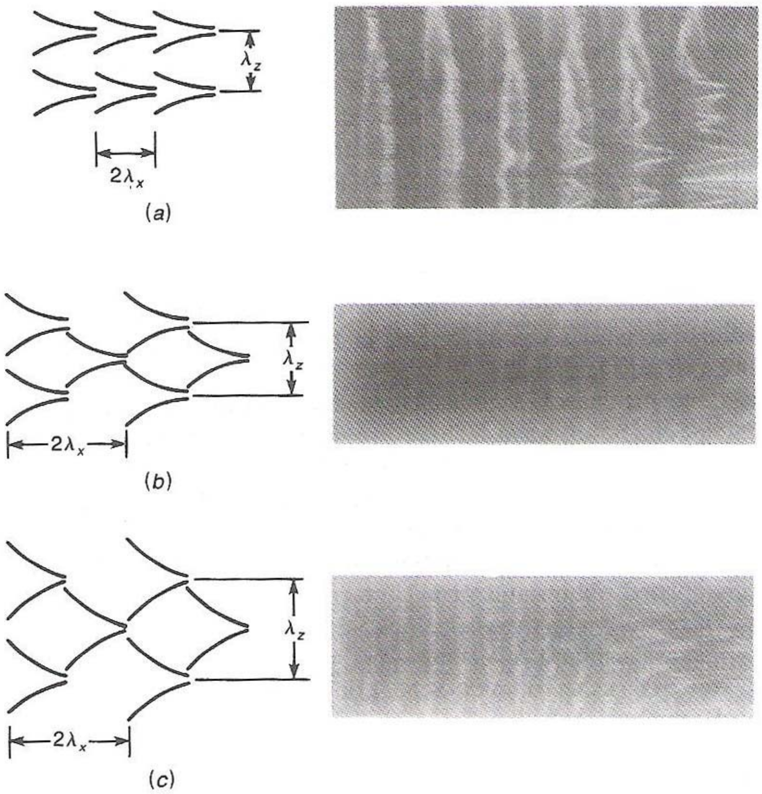

Figure 2.4 Vortex breakdown in a boundary layer: (a) K-type, (b) C-type, (c) H-type

These vortices grow and move away from the surface (with the “feet” still attached). The tips can protrude the boundary layer and in growing bigger they become more unstable until they collapse (burst) into smaller units of all frequencies and have become random. Now a turbulent spot has been formed.

Turbulent spots

The turbulent spots arise at random (within certain distance) and have a very distinct shape. From the above the spot looks like an arrowhead (figure 2.5). The spot continues to grow. Because of this growing these spots swallow the surrounding laminar flow. This effect is strongest on the top side of the leading edge. Also there are some strong instability waves at the edges.

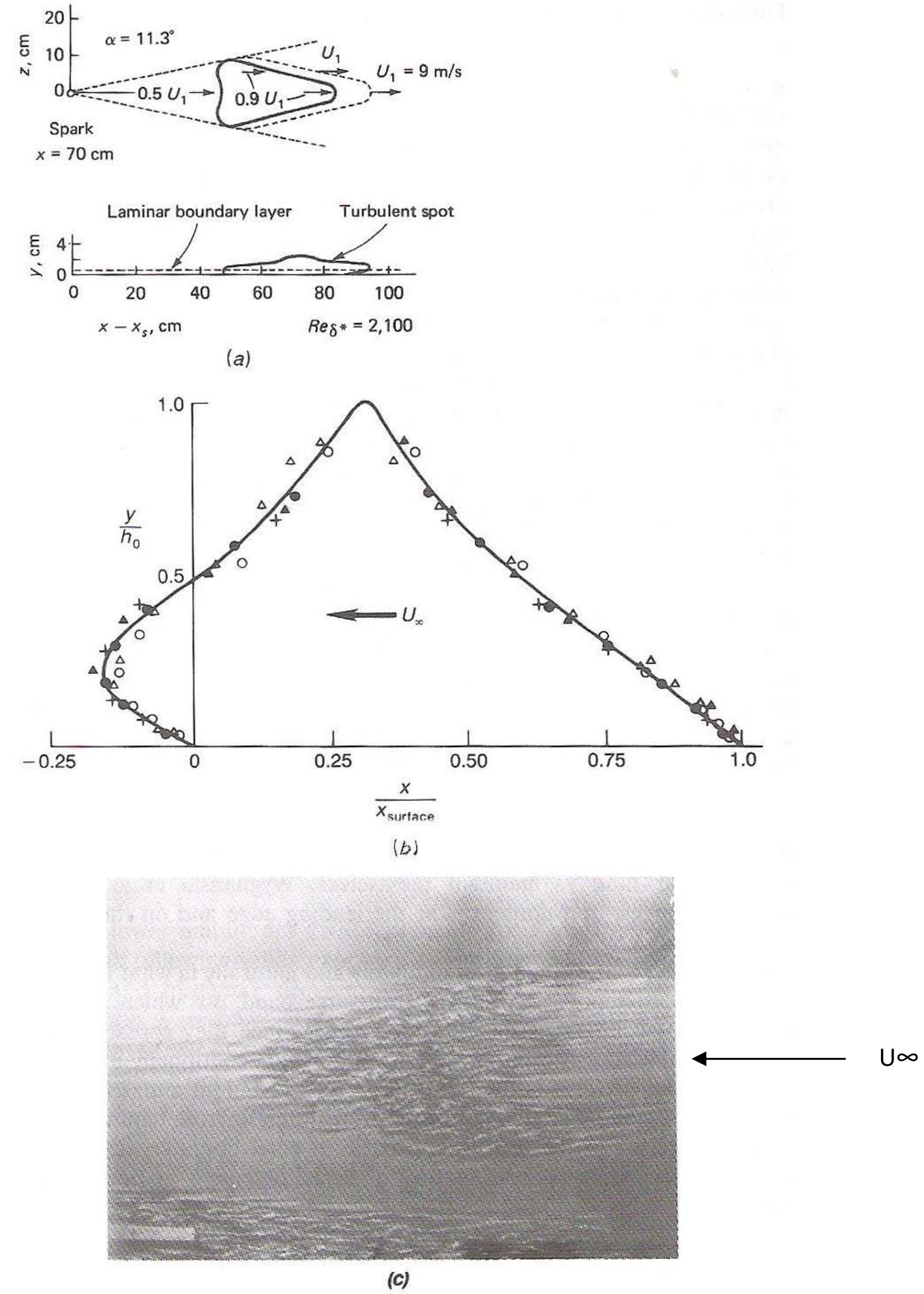

Figure 2.5 Turbulent spot in boundary layer (a) drawing of a spot; (b) side view; (c) picture of a turbulent spot (White,1991)

The turbulent spots keep on growing until the complete flow becomes turbulent and the transition phase is completed. According to Preston the minimum momentum thickness for fully developed turbulent flow: $Re_\theta = 320$, this is the absolute minimum. In practice however this number can easily go to 620, depending on what kind of disturbances are introduced.

2.2.2 Forced transition

When transition is forced the process of transition differs from the natural case. Forced transition works by introducing artificial perturbations in the flow which can quickly grow into full turbulence.

Basic concepts

The basics or forced transition lie in the fact that an obstacle in the flow introduces additional and quite strong perturbations in the flow. However this is not the only thing. According to Preston (1959) the obstacle also increases the momentum thickness. From experiments it is clear that the momentum thickness must be over a specific value in order to have fully turbulent flow. A transition device moves the location, where the minimum momentum thickness is reached, forward by its drag. Thus the onset of transition can be shifted forward by the use of some transition device. These devices use the fact that Re_{crit} , which is based on the position on the flat plate corresponds to a certain Reynolds number based on the momentum thickness of the boundary layer (Re_θ), which actually determines the stability. This $Re_{\theta\ crit}$ where the flow becomes unstable (disturbances are amplified) is 162 and for a flat plate and Re_θ for fully turbulent flow about 320. Also there should be enough disturbances in the flow to be amplified. (Preston)

So for the transition device to trigger transition it should be capable of doing two things:

- increase momentum thickness
- add disturbances to the flow

The increase in momentum thickness is related to the drag by [Preston]:

$$D = \rho U^2 \Delta\theta \tag{2.3}$$

And using:

$$D = C_D \frac{1}{2} \rho u_d^2 d \tag{2.4}$$

where u_d is the velocity at the top of the obstacle and d is its height.
Combining these two equations yields:

$$\frac{\Delta\theta}{d} = \frac{1}{2} C_D \left(\frac{u_d}{U}\right)^2$$

$$\frac{U\Delta\theta}{\nu} = \frac{1}{2} C_D \left(\frac{u_d}{U}\right)^2 \frac{Ud}{\nu}$$

This is the same as:

$$\Delta \mathrm{Re}_\theta = \frac{1}{2} C_D \left(\frac{u_d}{U}\right)^2 R_d \tag{2.5}$$

The value of the drag coefficient for a circular wire will be 0.75 in this case. The velocity at the top of the obstacle depends on its position and height.

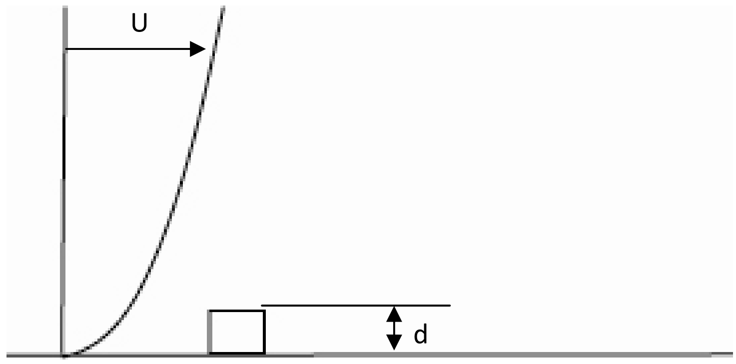

Figure 2.6 Definition of obstacle height

With this one can estimate the transition position once you know the momentum thickness in the undisturbed flow. These relations have been used in this investigation to make an estimate for the required thickness and position of the strip. The finetuning has been done using a trial-and-error technique.

Examples of forced transition

Forced transition is applied in both practical use and in experiments. The common practical use is to produce a turbulent boundary layer sooner such that separation of the flow is delayed. This is used in sail planes, speed-skating and golf balls. For these application it is usually not really necessary to know exactly how the flow behaves behind the strip as long as it produces turbulence. However this knowledge could lead to more advanced transition devices. More examples are given in figures 1.2 and 2.7.

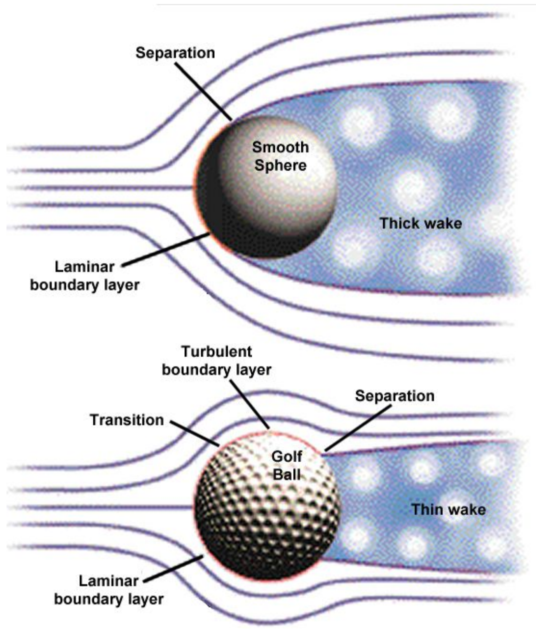

Figure 2.7 Flow separation on a sphere with a laminar versus turbulent boundary layer [Scott, 2005]

In experiments these devices are regularly used to trigger transition at the required point. Usually it is assumed that the turbulence behind the strip is homogeneous. This assumption however may not always true. As can be seen in figure 2.8.

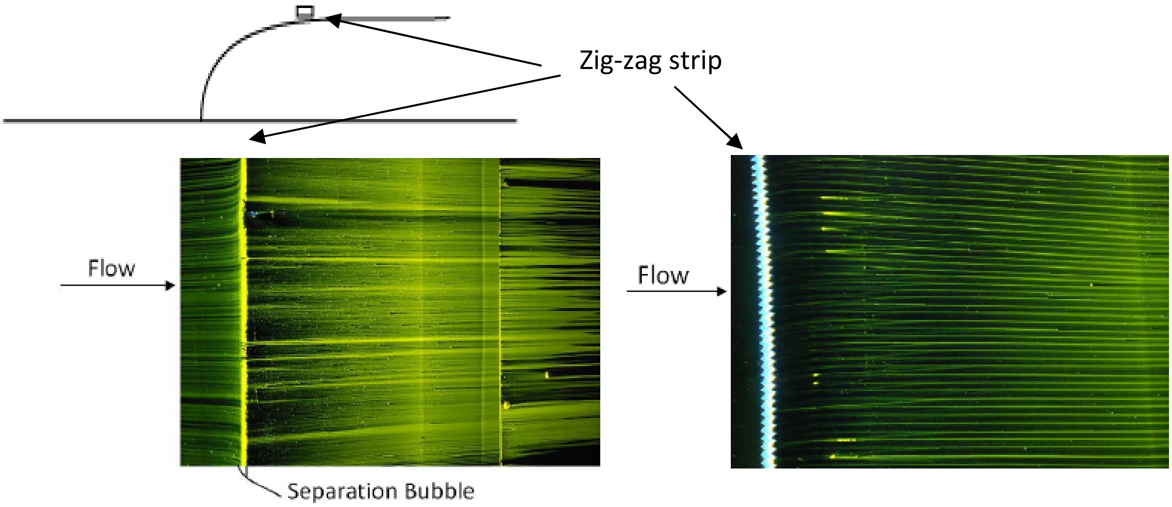

Figure 2.8 (Top) Top view of flow situation; (Bottom) Oil flow visualization on front of a bluff body. On the left clean and on the right zigzag strip. [Abbas, 2008]

In the pictures it can be seen that the trails from the zigzag strip are clearer and reach further downstream. So one could ask: How random is this turbulence? And in this case does this have consequences for the experiment?

Examples of transition devices

Commonly used transition devices are sandpaper, circular wires and zigzag strips. All of them have their own specifics. Circular wires are easy, but less effective than a zigzag strip. Sandpaper roughness will create turbulence more randomly than the other two and is also not that difficult to use, however it needs more width to create turbulence.

2.3 Turbulent flow

Once the transition phase is completed, the flow will be completely turbulent. This turbulent flow shows some characteristic phenomena:

- Fluctuations in pressure and velocity. These fluctuations are 3-dimensional and are superimposed on a mean flow value.
- Fluid eddies of all sizes (between the boundary layer thickness δ and the smallest Kolmogorov length scale, $L = \left(\frac{\nu^3 \delta}{U_\infty{}^3}\right)^{\frac{1}{4}}$. (2.6)
- Random variations in fluid properties having a continuous energy spectrum with low values at high wave numbers.
- Turbulence is self-sustaining. It sustains itself by forming new eddies compensating for the ones dissipated.
- Mixing. Eddies have a 3-dimensional organization, hence they provide more mixing of momentum, mass and energy with non-turbulent areas (diffusion).

Intermittency

Once the flow is turbulent it doesn’t mean there is a sharp edge between the turbulent part and the non-turbulent part. There is a so called region of intermittency. The easiest way to illustrate this is a sketch (figure 2.8). In the sketch the fluid flows from left to right. One can see the irregular nature of the border between both flow regimes. Would there have been a probe at say 0.8δ than the signal would have looked something like figure 2.9. In this way the two parts of the flow start to “mix”.

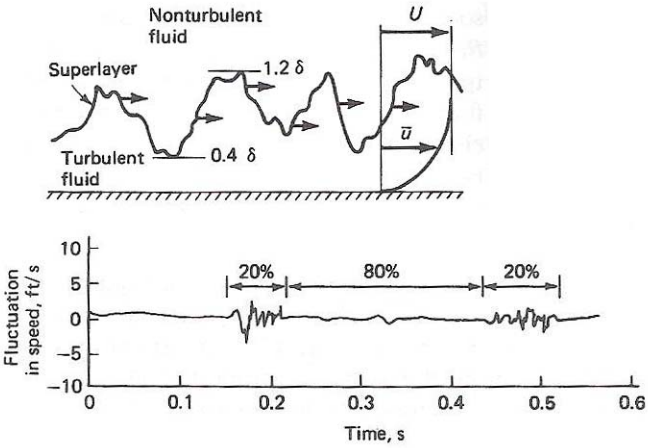

Figure 2.9 Sketch of intermittency in the flow (White, 1991)

Coherent structures

Before going any further a definition of a coherent structure is needed:

“A coherent motion is defined as a three-dimensional region of the flow over which at least one fundamental flow variable (velocity component, density, temperature, etc.) exhibits significant correlation with itself or with another variable over a range of space and/or time that is signicicantly larger than the smallest local scales of the flow.” [Robinson, 1991].

In the layer closest to the wall the streamwise velocity shows narrow streaks of relative higher and lower speed. These streaks are called high and low speed streaks. After some distance the low speed streaks are ejected (away from the surface and slightly upstream) and the high speed steaks sweep towards the wall. This is an intermittent process which causes most of the turbulence in the boundary layer. This process is called bursting.

In the outer layer packs of turbulent and non-turbulent fluid move along each other, causing mixture and giving birth to shear layers.

In the boundary layer many vorticial structures are present. Spanwise and streamwise vortices are most important in the turbulence production process since they can transport momentum and mass between the layers. Also so called horseshoe and hairpin vortices are important for the turbulence production. These vortices can be formed from spanwise vortices which roll up and start stretching and lifting from the surface. At the head of the hairpin a shear layer is formed, which becomes unstable and then bursts. Figure 2.10 shows a schematic picture of this process. Figure 2.11 shows a more detailed sketch of this phenomenon.

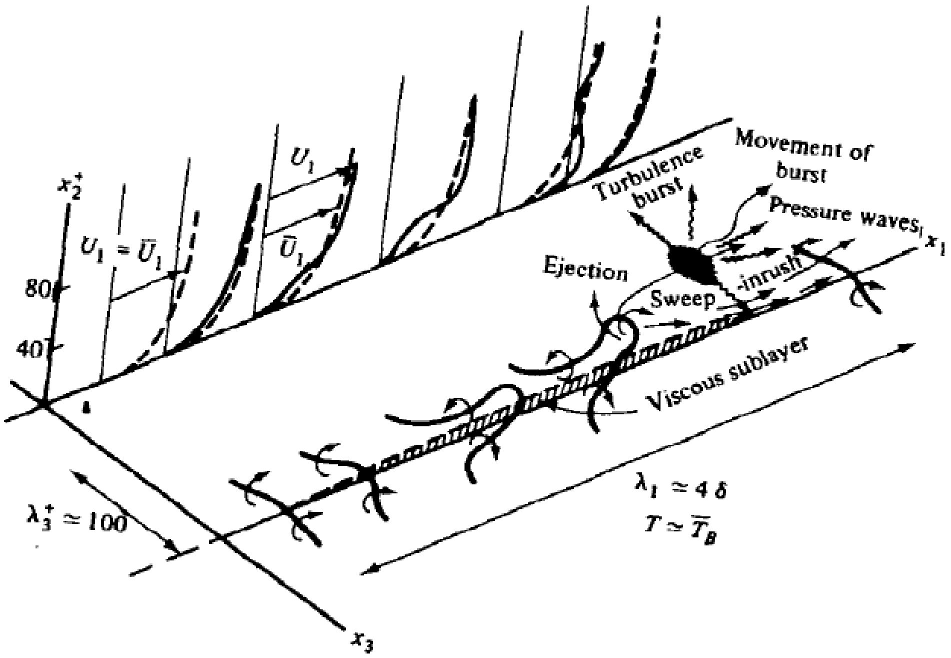

Figure 2.10 Model of near wall turbulence (Robinson, 1991)

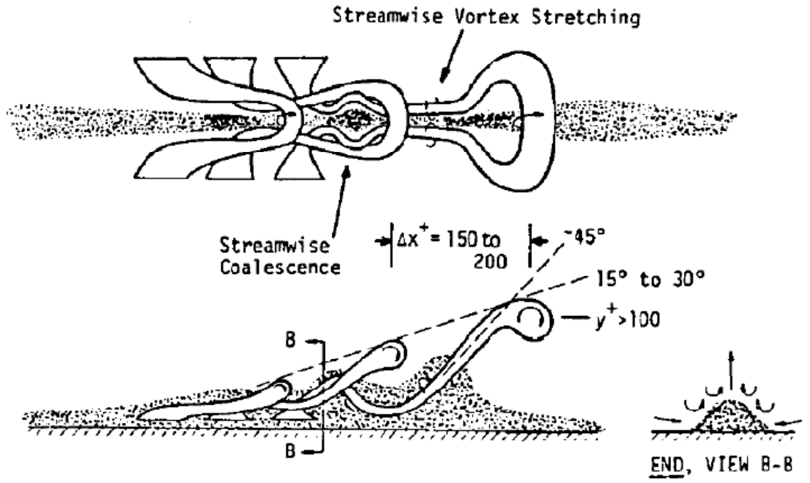

d) vortex ejection, stretching and interaction

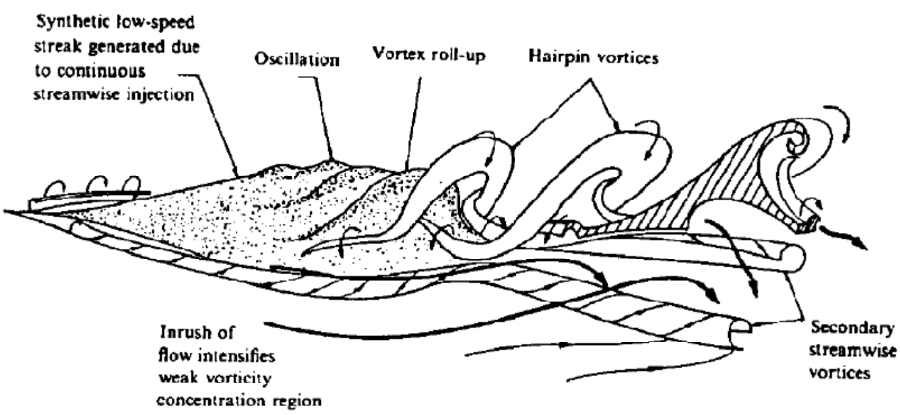

Figure 2.11 (top) Illustration of breakdown and formation of hairpin vortices (Bottom) Breakup of a synthetic low-speed streak (Robinson, 1991)

3. Experimental approach

In order to investigate the flow phenomena of interest some carefully designed experiments were performed. The first steps will be a series of experiments which should yield the exact settings in order to achieve the right flow conditions. These design parameters are flow speed, trip position and height, boundary layer thickness and length of the plate. After that the investigation will go more into the details of these specific flow conditions. All the experiments have been done in the W-tunnel of the Aerodynamics group of the Faculty of Aerospace engineering of the Technical University of Delft.

3.1 The Windtunnel

The W-tunnel is a blow down (open jet) low speed wind tunnel. It is driven by a 16.5 kW fan. Air is sucked in at the plenum (2x1.5x2m, lxwxh) and passes through the diffuser in order to slow down the air into the settling chamber, where most turbulence is removed by two gauzes. The contraction after the settling chamber will accelerate the flow into the test section and finally into the free atmosphere. The speed ranges from 0 to 35 m/s and a free stream turbulence level of 0.1%. The nozzle exit has a 400x400x400mm Perspex test-section. A view of the tunnel is given in figure 3.1.

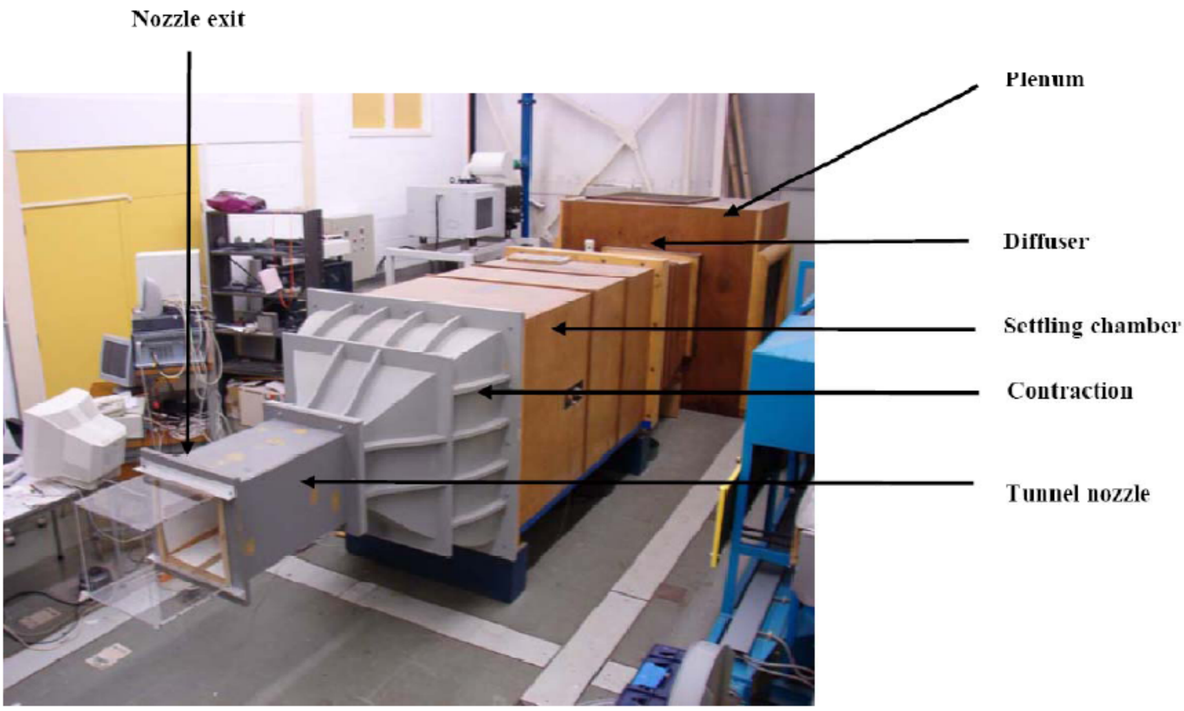

Figure 3. 1 W-tunnel at Delft University of Technology, Faculty of Aerospace engineering

3.2 The models

The tests have been done on a 50 cm aluminum flat plate and a 100 cm Plexiglas flat plate of equal thickness and nose geometry in the tunnel . A picture of the setup is given in figure 3.2.

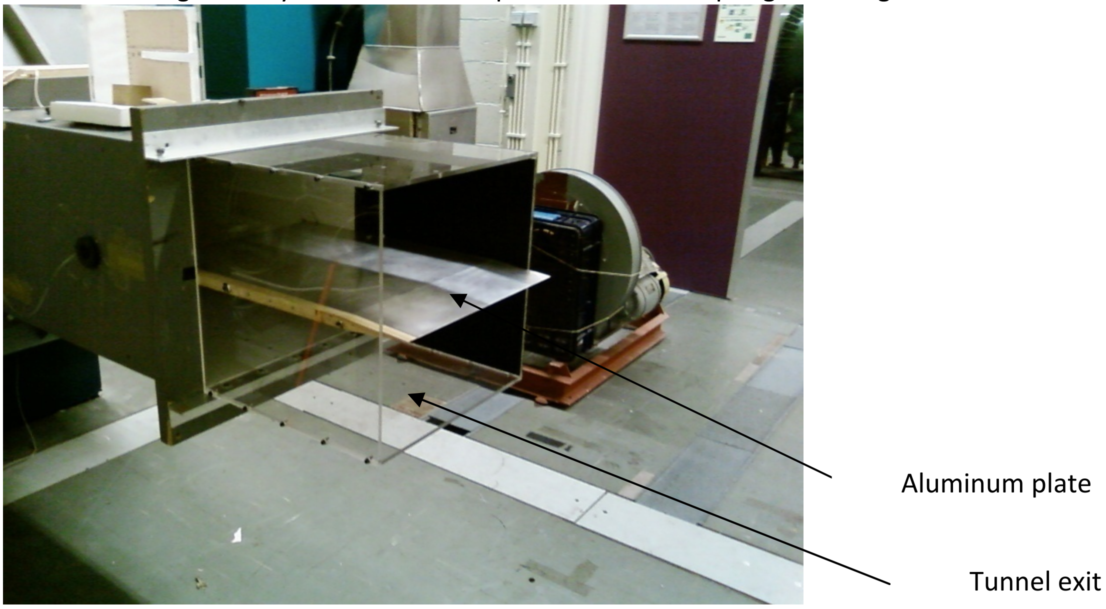

Figure 3. 2 Aluminum plate in the tunnel exit

At first athe 50 cm aluminum plate has been used, since it proofed to be to short to create a boundary layer of sufficient thickness and a large enough transition region it has been replaced by the 100 cm Plexiglas one. The basic setup is shown in figures 3.2 and 3.3 (without measuring equipment. In figure 3.3 a sketch of a typical experiment is given. In this case a transition strip is placed on the Plexiglas plate at 350mm from the leading edge.

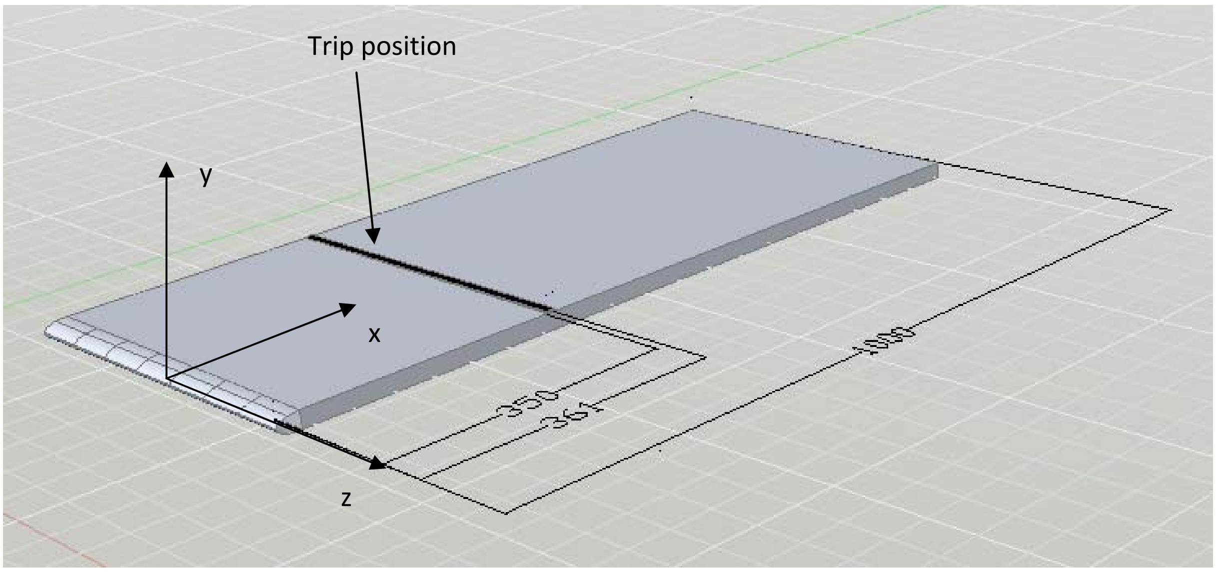

Figure 3. 3 Layout of the Plexiglas plate, main flow in x-direction

In the experiments where a transition device has been used, it was either a straight strip or a zigzag strip. In figure 3.4 both strips are shown. Both strips span the complete width of the plate.

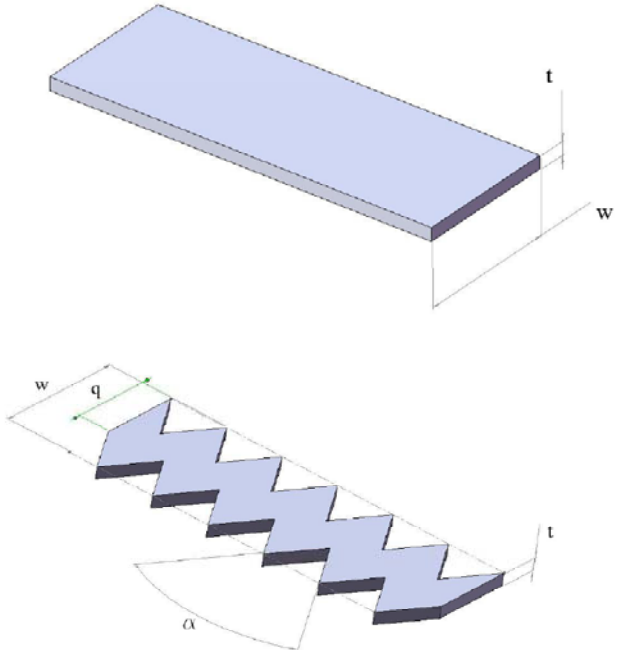

Figure 3. 4 Strips used to produce artificial transition; Straight strip (top), Zigzag strip (bottom); The variables are w=11mm, q=7mm and t=height of the strip and $\alpha = 60^o$

3.3 Experimental procedure

In this investigation four different measurement techniques have been employed. These are acoustic test using a small microphone, pressure test using a static pressure tube, hot wire anemometer (HWA) testing and Particle Image Velocimetry (PIV). The first two of them have not been used extensively (only for checking the pressure gradient on a clean plate) and are fairly simple to use, so only HWA and PIV techniques will be explained here in more detail. These two have been used for getting detailed velocity and turbulence data and visualization. In this paragraph these techniques and procedures are discussed, starting with the acoustic and pressure tests.

Verification of flow conditions: Acoustic and pressure test
The first test just involved a simple microphone connected to a headset. By listening to the acoustic signal a quick estimation about some flow properties, such as separation and onset of turbulence could be made. The pressure test was done to check the pressure distribution along the plate. This was done by putting a static pressure probe at the surface of the plate and traversing the plate as can be seen in figure 3.5.

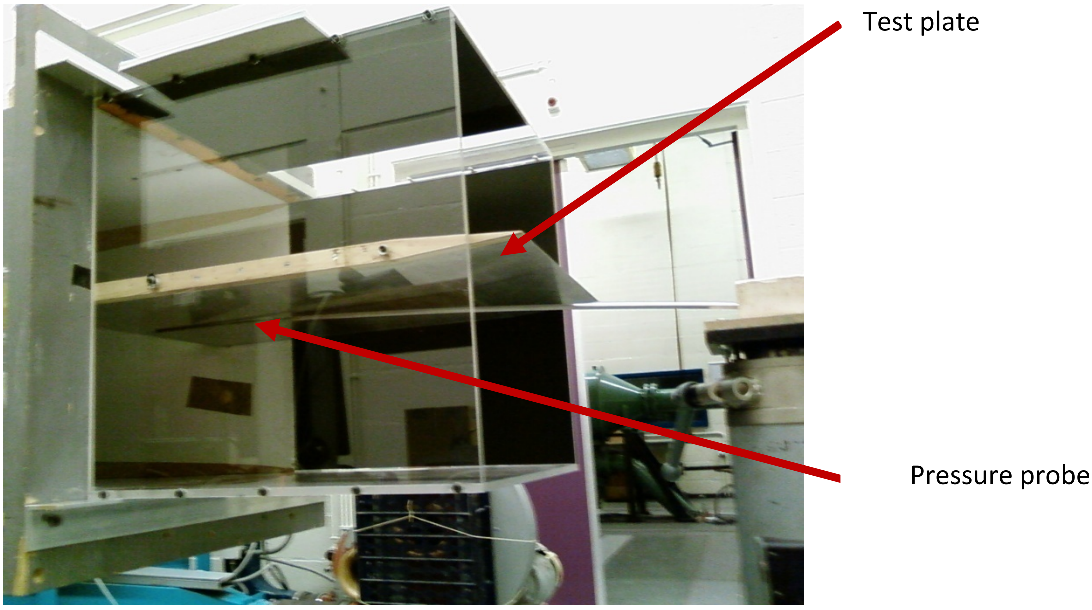

Figure 3. 5 Pressure test setup in the tunnel

The the static pressure was related to the static pressure just in front of the plate (measured by static pressure orfice in the tunnel. That is why all the pressure differences are negative. The pressure difference was displayed in real time.Ssince it was not connected to a computer the value was read from the display. Since this value fluctuated these results give a more qualitive picture of the flow, although numbers are given. This high accuracy and reproducibility are not needed at this stage of the research as this is only a rough check for flow conditions. The results are presented in figure 3.6.

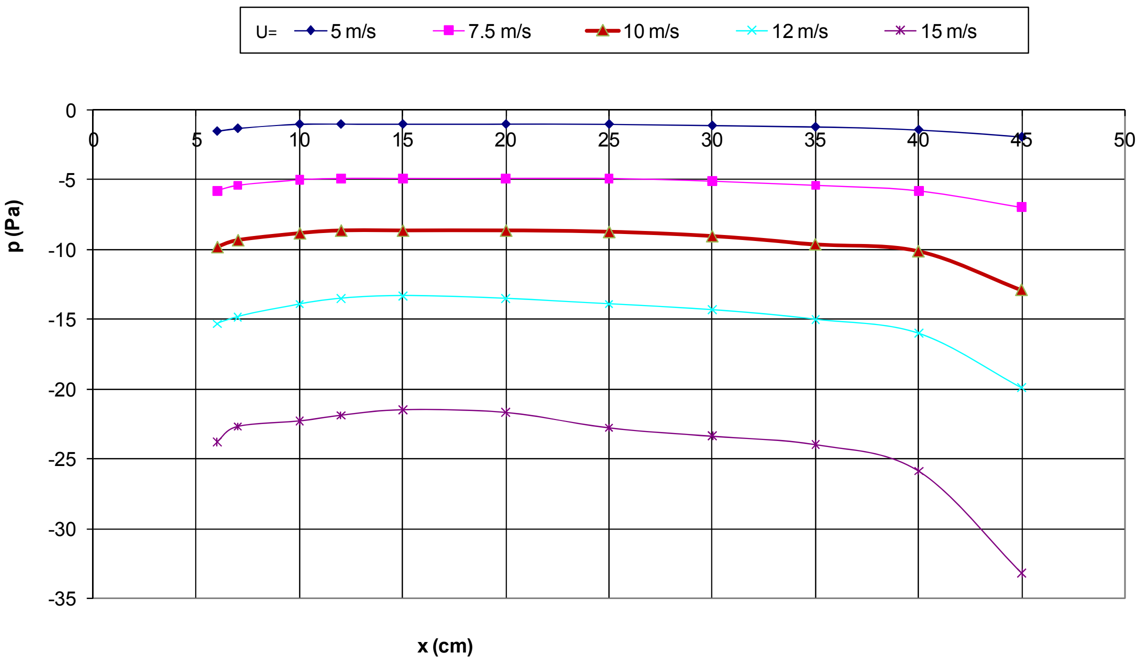

Figure 3. 6 Pressure distribution along the plate x-axis for different flow velocities

It can be seen that the nose and the end of the tunnel had an effect on the pressure field just above the plate. The pressure remained constant in the zone from 10 up to 30 cm from the leading edge. Outside this zone the pressure was lower. So the test area where the conditions of zero pressure gradients are satisfied with acceptable accuracy (close to theoretical) stretches from 10 to 30 cm from the leading edge.

3.3.1 Hot wire anemometry

Hot wire anemometry provides single point measurements at a time. Since this method is analogue, the velocity measurement is continuous and a high frequency response (10-100kHz). This means the signal can be used to do a frequency analysis. The principle of HWA is based on the fact that a heated object will release its heat (by convection, radiation or conduction) to its surroundings. The hot wire anemometer system consists of a hot wire probe connected to the resistance bridge, which is again connected to a computer for recording the data (figure 3.7). The probe (figure 3.8) consists of two prongs which are connected by the actual hot wire(typical values for length and thickness are 1.2 mm and 5 µm.

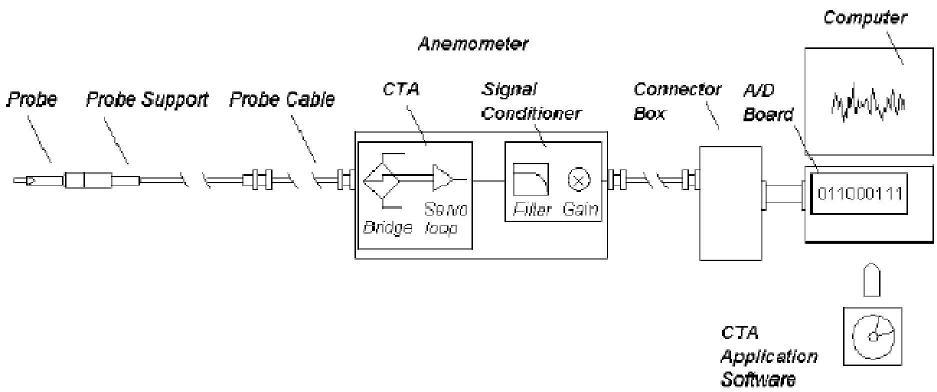

Figure 3. 7 Typical hot wire setup

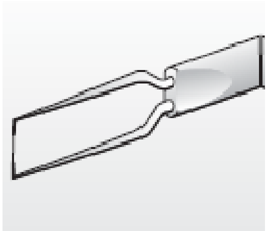

Figure 3. 8 Hot wire probe

In this experiment the constant temperature anemometer (CTA) has been used. Besides several other advantages like a higher frequency and response there is no risk of probe burn-out. This wire forms a part of a Wheatstone bridge and is heated by the electric current through it. The flow will increase the heat transfer from the probe and therefore the voltage over the bridge will increase to compensate this by extra heat dissipation on order to maintain the wire temperature (resistance) constant. (CTA, constant temperature anemometer as used in this experiment). This voltage variation can be related to the flow velocity through calibration and hence the velocity can be calculated from the HWA output signal.

Calibration of HWA

Before doing the calibration the overheat ratio *a* has to be set. This ratio is defined as:

$$a = \frac{R_w - R_0}{R_0} \tag{3.1}$$

R_w is the resistance of the wire in operation and R_0 is the cold resistance of the wire at ambient conditions.
In which the subscript 0 means at ambient conditions. From this the temperature can be calculated:

$$T_w - T_0 = \frac{a}{\alpha_0} \tag{3.2}$$

In which α_0 is the sensor temperature coefficient.
Once the overheat ratio is set the system should be calibrated. This can be done in the following way:

- Expose the wire to a set of known velocities and record the voltage and velocity pairs. Also keep track of the ambient temperature.
- If the ambient temperature changes during the measurements an extra calibration or a correction can be applied to the data using the following expression:
  $E_{corr} = \left(\frac{T_w - T_0}{T_w - T_a} \right)^{0.5} E_a$,(3.8) , in which E_a is the acquired voltage.
- The coefficients can be fitted by using the polynomial curve fitting gives:
  $$U = C_0 + C_1 E_{corr} + C_2 E_{corr}^2 + C_3 E_{corr}^3 + C_4 E_{corr}^4 \tag{3.3}$$
- After the calibration the measurements can start. If during the data acquisition the ambient temperature changes the voltages should be corrected using the same formula.

Errors in HWA
The results from HWA can be affected by several errors. Some possible causes of errors are: calibration errors, changing direction of the flow and errors can arise from ambient temperature changes(when no countermeasures are taken). Calibration errors give quantative errors, however in this investigation qualitative data are the most important. For direction changes in the flow nothing has been done in the HWA campaign, these data are obtained from the PIV results later. The effect of temperature changes have been omitted by doing a calibration for each ambient temperature at the time of measurement.

3.3.3 HWA setup and procedure

The Hot Wire Anemometry measurement is done on the lower side of the plate. The anemometer is always positioned at the centerline of the plate. The horizontal and vertical position of the anemometer is varied by a manual traversing system. The horizontal position can be set at any point in the constant pressure zone. The vertical position can be varied from 0 up to about 7 cm from the plate. The probe is placed normal to the flow and parallel to the plate. Two pictures of the setup can be found in figure 3.9 and 3.10.

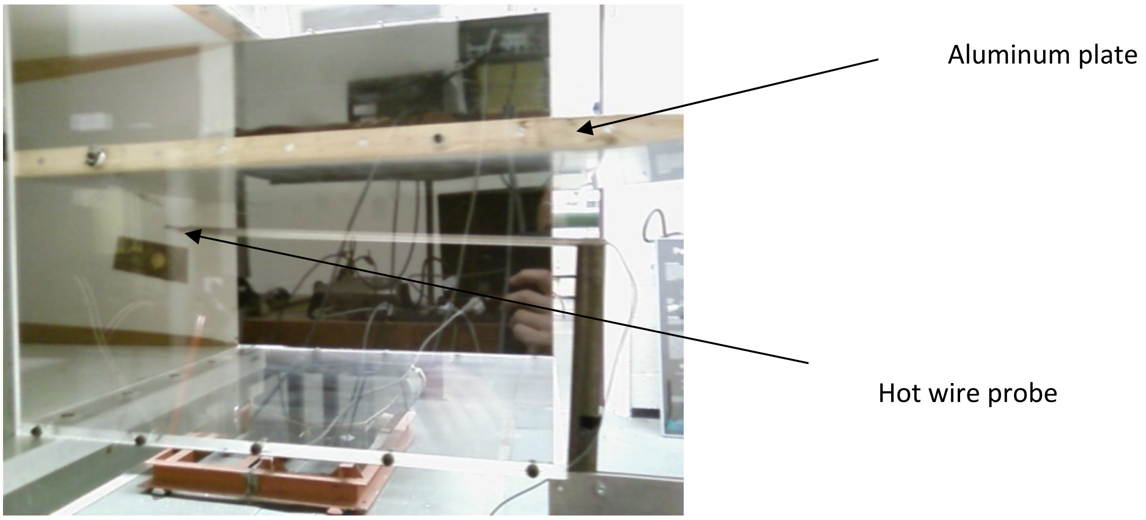

Figure 3.9 HWA setup in the tunnel

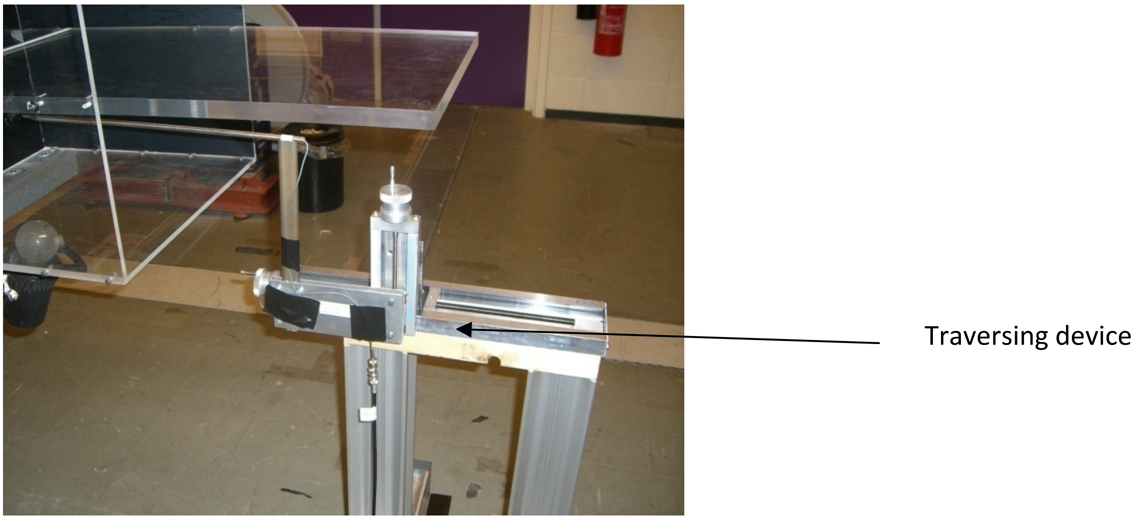

Figure 3. 5 HWA setup in the tunnel

The instrumentation consists of the hot wire probe (Dantec® 9055p0111) connected to a Wheatstone bridge (Dantec 56C17 CTA bridge). The output is transferred by a National Instruments BNC-2110 block connector to a National Instruments (NI PCI-6024E) Data acquisition system to a PC and collected by a program in LABVIEW (see figure 3.11).

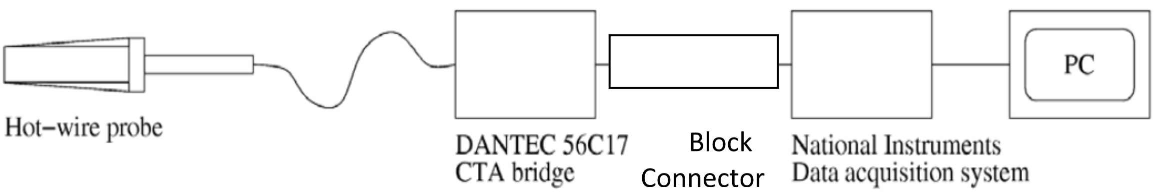

Figure 3. 11 Diagram of HWA setup

Calibration

The calibration of the probe is needed to obtain the voltage velocity relation. Calibration of the velocity is done while the model is still inside the tunnel. Due to this fact there will be a small error. However this error will not give a significant effect to the complete analysis, since the focus is on qualitative results, not on quantitative. The static calibration is done by positioning the anemometer halfway beteen the plate and the tunnel wall. The calibration is performed at velocities in the range of 1 to 20 m/s. The flow velocity in the tunnel is determined with a pitot tube and a static pressure gauge. The procedure starts by setting the tunnel on a specific RPM (or velocity) and taking a 10 second measurement with the anemometer with a 10 kHz sampling rate. The average of the measured data is used to find the voltage corresponding to this specific velocity. When these measurements have been done a calibration curve is fitted onto the measurement data (figure 3.12).

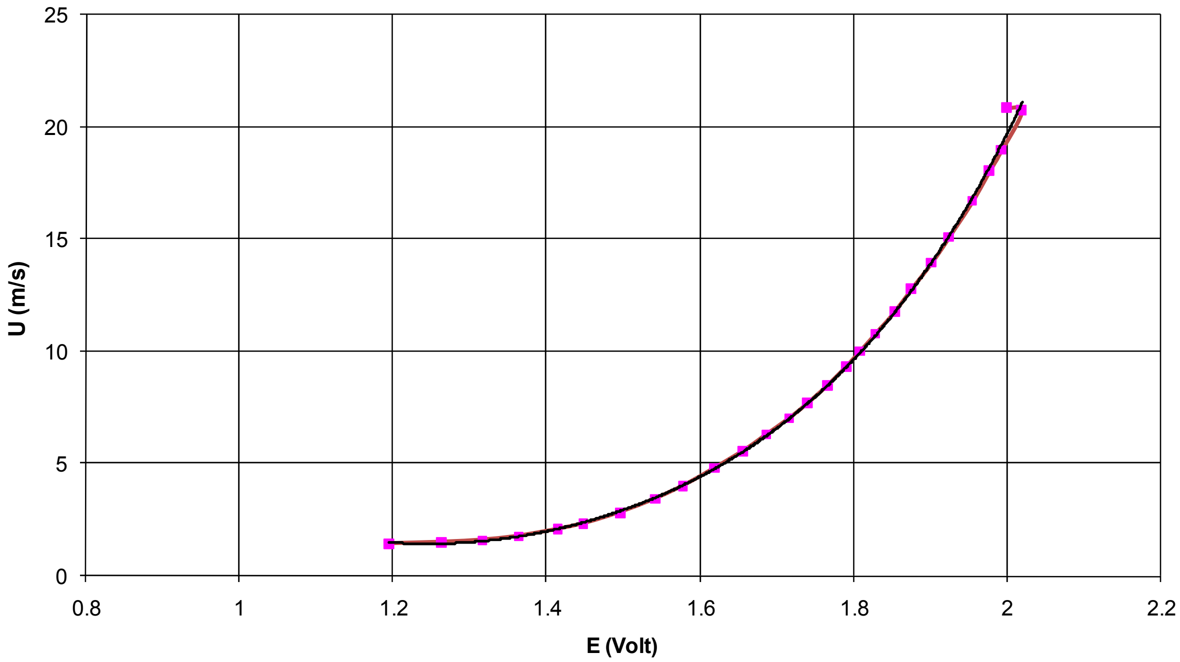

Figure 3.12 Hot wire calibration curve where the voltage is given for a corresponding flow velocity

For this graph the air temperature was 19 degrees Celsius, for all different temperatures at which measurements have been done a similar plot has been made in order to ommit an error due to temperature differences, however these plots are not given here. For data analysis a curve fit of this plot has been used.

The output from the HWA is a voltage which first has to be converted to velocity. This is done by using the calibration function. After that the measurements have been analyzed using the following definitions for the mean velocity, standard deviation and the turbulence respectively:

$$U_{mean} = \frac{1}{N}\sum_{i}^{N} U_i \tag{3.4}$$

$$U_{rms} = \sqrt{\sum_{i}^{N} \frac{\left(U_i - U_{mean}\right)^2}{N-1}} \tag{3.5}$$

$$Tu = \frac{U_{rms}}{U_{free}} \tag{3.6}$$

The boundary layer edge is defined as the distance from the wall where the velocity reaches 99% of the free stream velocity. This free stream velocity is determined by doing a HWA measurement at 7cm above the plate in the same way as all the other points.

The signal aqcuisition frequency of the HWA is set at 3500 Hz. It is expected that the measuremen are uncorrelated since the time-scale of the flow is also very small (order of ms). Also because of the high number of samples (35000) average values will be accurate.

For the velocities and locations mentioned in table 3.1 smooth plate (no strip) measurements have been done (in x-direction, the position in y-direction was changed in small steps from 0.5/0.6mm upward).

Distance	U_∞	U_∞	U_∞	U_∞
6 cm	5 m/s	7.5 m/s	10 m/s	12.5 m/s
10 cm	5 m/s	7.5 m/s	10 m/s	12.5 m/s
15 cm	5 m/s	7.5 m/s	10 m/s	12.5 m/s
25 cm	5 m/s	7.5 m/s	10 m/s	12.5 m/s

Table 3.1 HWA measurement positions on a clean plate at the given distances from the leading edge

For the flow with transition strip zigzag strips were used to induce turbulence. These strips were placed at 10 cm from the leading edge and were 0.95 and 1.45 mm thick. A similar boundary layer measurement as for the laminar flow has been done at 1 cm, 2.5 cm, 5 cm and 10 cm behind the strip. The velocity was set at approximately 9 m/s (from HWA), this velocity was selected sinceat this velocity transition could be triggered with some device (based on the momentum thickness) while still having a thick enough boundary layer to do the measurements in and to be sure the device doesn't protrude de boundary layer. The distance from the leading edge is given in table 3.2.

Distance from leading edge (cm)	Item
10	Leading edge strip
11.1	Trailing edge strip
12.1	HWA 1
13.6	HWA 2
16.1	HWA 3
21.1	HWA 4

Table 3.2 HWA measurement position on a flat plate behind zigzag strips of 0.95mm and 1.45mm thick

In succession to the first HWA measurements a new set of hot-wire tests have been done in order to examine the difference in turbulence creating properties of the different kinds of transition strips. The first set of measurements was done on the aluminium plate which proved to have too little length, since the flow remained laminar till the end of the plate and the boundary layer didn't reach enough thickness for doing the measurements in the boundary layer. The setup is not very different. The aluminium plate has been replaced by a new Plexiglas plate which is geometrically similar to the previous one except for its length (1m). A sketch of the plate with transition strips is given in figure 3.3.

The air flows in x direction as pointed out in figure 3.3. The velocity is approximately 8 m/s. The testing positions are given in table 3.3.

Distance from leading edge (cm)	Item
35	Leading edge strip
36.1	Trailing edge strip
37.1	HWA 1 with strip
38.6	HWA 2 with strip
41.1	HWA 3 with strip
43.6	HWA 4 with strip
48.6	HWA 5 with strip
56.1	HWA 6 with strip

35.6	HWA 1 without strip
40.6	HWA 2 without strip
55.6	HWA 3 without strip

Table 3.3 HWA measurement traversion position for Zigzag strips.

The strips used in this experiment are the zigzag strips of 0.75mm, 0.85mm, 0.90mm and 0.95mm and the straight strips of 1.5mm, 1.6mm and 2.15mm. As can be seen from the table the HWA has been positioned at different locations along the length axis of the plate. Also a traversion in height has been done at each position starting from 0.5mm above the plate, with steps of 0.5mm to characterize the boundary layer. The upper point of such a measurement depends on the local thickness of the boundary layer.

3.3.4 Particle Image Velocimetry

Particle Image Velocimetry (PIV) is a non-intrusive measurement technique, which gives an instantaneous full flow field measurement of the velocity. These properties are clear advantages of PIV, but it comes at a price. PIV is much more complicated and therefore more expensive than for example HWA. Also the data acquisition rate is rather poor (10Hz, modern systems give several kHZ), although recent developments show an improvement. This section is unless mentioned otherwise based on Raffel (2007] and Scarano (2007).

Principles of Particle Image Velocimetry

The basic working principle behind PIV is rather simple and easy to understand. Figure 3.13 gives a sketch of a typical PIV experiment setup. Small tracer particles are added to the flow. In the test section a light sheet is generated by a laser and the required optics. The tracer particles will scatter the laser light in all directions. On one side of the illumination plane there is a camera pointed (in this case) normal to the light sheet. This camera is able to record an image of the scattered light from the particles in the flow. The laser illuminates the flow in pulses, with very short time in between. Now the camera takes at least one image pair (two consecutive recordings). These two images are decomposed into small sections (interrogation windows) and after that cross-correlated during the post-processing. This correlation reveals the displacement of the particles in the time between the two subsequent exposures and hence the velocity vector is known.

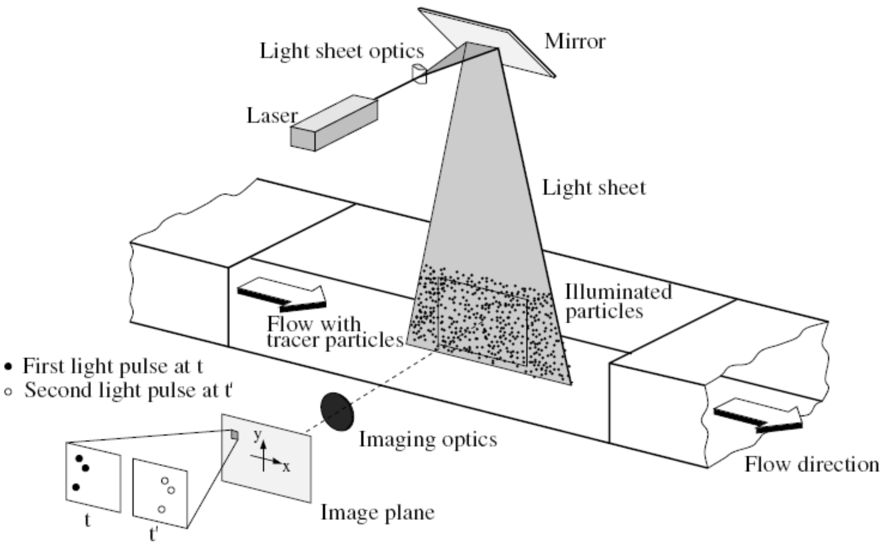

Figure 3. 13 Sketch of a PIV setup [Raffel, 2007]

Seeding
The seeding particles should have certain properties in order to fullfill their function. The seeding should be uniform, the particles should be non-toxic, have good light scattering properties since that is the main reason for using then. They also should have a good ability to follow the flow.

Laser and light sheet optics
The laser produces a narrow circular beam. This laser beam has to be formed into a thin sheet. This is done by an arrangement of lenses and mirrors (to cut corners). This can be done in several ways. In the case that two separate laserbeams are used to produce the two pulses it is important that the laser sheets are in the same position. This is called overlap. An overlap of 100% means the sheets are identical. An overlap of about 80% is acceptable.

Imaging
The light scattered form the particles needs to be imaged on the image plane. The scattered light from a particle does not have the shape of a perfect dot. It is a so-called Airy disc. The diameter of the Airy disc d_{diff} is given by:

$$d_{diff} = 2.44\lambda(1+M)\, f_{\#} \tag{3.7}$$

With: $M = \frac{z_0}{Z_0}$ the magnification factor. And $f_{\#} = \frac{f}{D_a}$ the aperture number (D_a is the aperture diameter.

The next formula is used to obtain the diameter of the particle image:

$$d_{\tau} = \sqrt{(Md_p)^2 + (d_{diff})^2} \tag{3.8}$$

For good cross correlation properties this value needs to be close to 3 pixelsizes. To ensure that the particle images are dots and not streaks the image particle displacement during the pulses themselves should be much smaller than the diameter of the particle, since the pulse of the laser, used in present experiments, only lasts 9 ms this is not an issue in the current investigation

3.3.5 PIV setup and procedure

For the PIV measurement the laser sheet is positioned such that the sheet is coming normal to the flow. The camera takes images from above. The set up is displayed in figure 3.22.

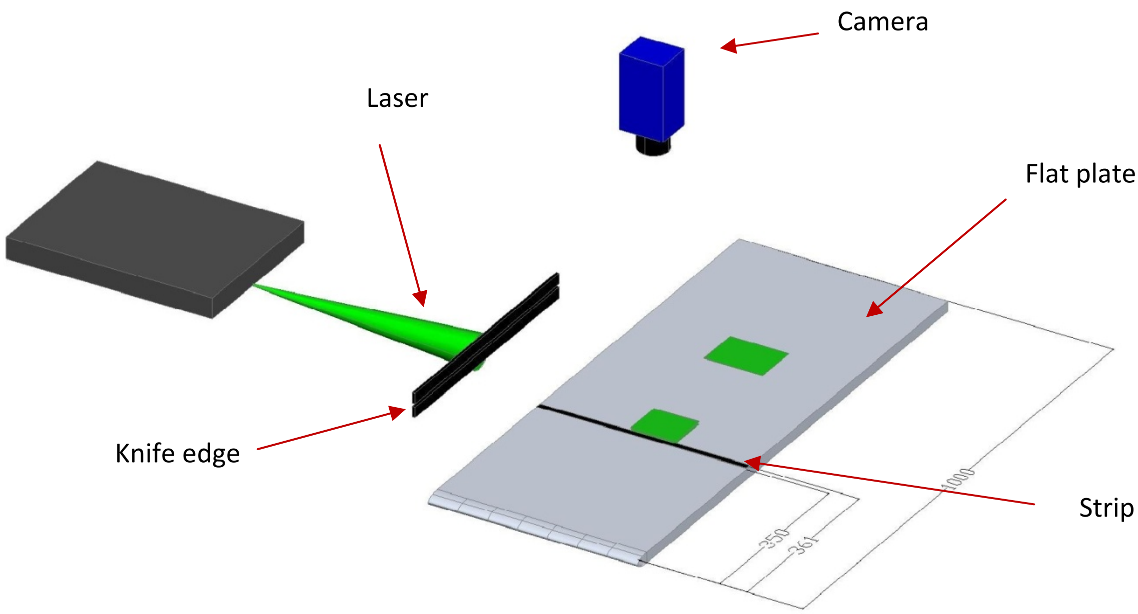

Figure 3.14 Setup with the PIV equipment in the tunnel

The Laser is a double source Nd: YAG consisting out of two cavities which produce infrared light with a wavelength of 1046 nm. A Quantel Twin CFR-2000 is used as the light source. The wavelength is halved by the second harmonic generator resulting in a wavelength of 532 nm, which is visible green light. The maximum power that the laser produces is 200 mJ per pulse. The laser only flashes above a certain threshold which is approximately 60 percent of the maximum power. The pulse duration is 7 ns while the maximum repetition rate of two pulses is 30 Hz. The computer running Davis® controls the flashing rate of the laser as well as the time separation between the laser pulses. The laser sheet is formed by pointing the conical laserbeam from the lenssystem onto the knife edge. Since the light is partially blocked a light sheet is created. The height of this light sheet can be adjusted by moving the knife edge up and down. A picture of the setup is given in figure 15. And a sketch of the knife edge in figure 16.

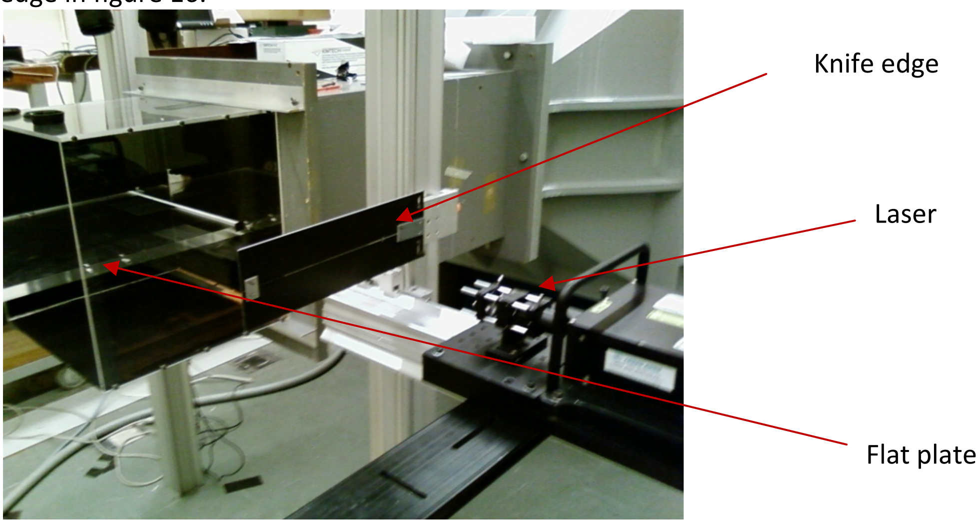

Figure 15 Picture of the PIV setup

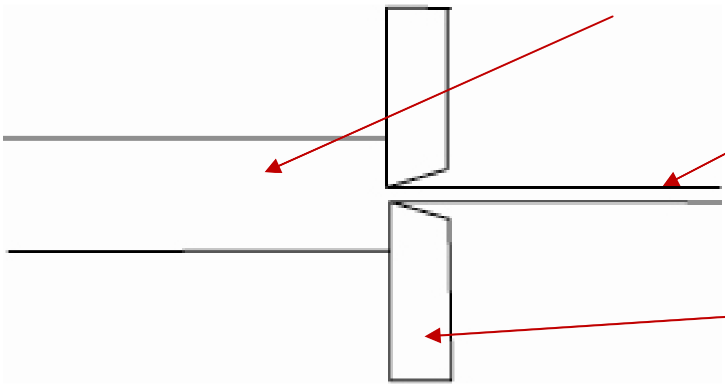

Figure 16 Sketch of the knife edge

The seeding is produced by a SAFEX fog generator which produces a non-toxic water based fog from a fluid named SAFEX normal power mix. The mean diameter of the particles is 1 micrometer. In order to make the seeding condition stable the complete tunnel room was fogged up and then the generator was switched off.

A LaVision Imager intense CCD camera consisting of 1376 times 1040 pixels with 6.45 µm pixel pitch is used to shoot the images. The camera is able to record 12 bit black and white images. The maximum recording rate is 10 Hz. The camera is thus the limiting factor for the measurement frequency. Due to the fact that the exposure in a starting frame is higher than in the follow up frame, the accuracy of the first frame is better than later frames. On the objective a daylight filter is mounted to filter out light with other wavelengths then the laser light. The imaging particle on to the CCD sensor uses a Nikon lens with a focal length of 60 mm. The objective $f_{\#}$ can be set between 2.8 and 32.

The DaVis® software package is used for the image acquisition and analysis. The software controls the camera and laser (ie. Timing of laser and camera shutter). Furthermore it will be able to make an image analysis consisting of FOV analysis, region of interest and cross correlation. The software is also able to do post-processing and data display and output.

Settings of the equipment
The measurements have been done directly behind the strip and 20 cm after the trailing edge of the strip (start of field of view). The Field of View (FOV, w x l, see figure 3.24) is 44x35 mm for the zigzag strips behind the strip and 90x70 mm for the straight strips and the ones at 20 cm. With a focal distance of 60 mm a view on the centre of plate was achieved with the lens at 36.5cm/67cm cm at an aperture number of 8. With this aperture number there was enough light and the particles where imaged as clear dots. An important number for setting this aperture number is the particle image diameter, this diameter is influenced by the aperture number as explained earlier.

$$d_\tau = \sqrt{(Md_p)^2 + (d_{diff})^2}$$

For the particles and lighting conditions and lenses used, d_τ turns out to be $1.2*10^{-5}$m.This is close to an optimum value of 3 pixels ($1.9*10^{-5}$m).

The height of the laser sheet is also varied (the measuring positions are given in appendix B) by moving the knife edge up of down. The heights are chosen such that the required information is obtained. The thickness of the laser sheet is 1mm.

The calibration of the system was performed by putting the calibration panel at approximately the same position as the laser sheet. Now the objective is adjusted such that the plate is in focus and the camera is moved such that the view is perpendicular to the tunnel and the desired field of view (FOV) is obtained. This is done with the laser at continuous lighting.

The calibration plate has been removed from the tunnel. Some seeding is inserted in the test section. This light sheet is needed to focus the camera on the particles in the light sheet. Next the calibration plate is put back and an image is made from it. With this image you can determine the position in space later on in post-processing. The image taken is shown in figure 3.23.

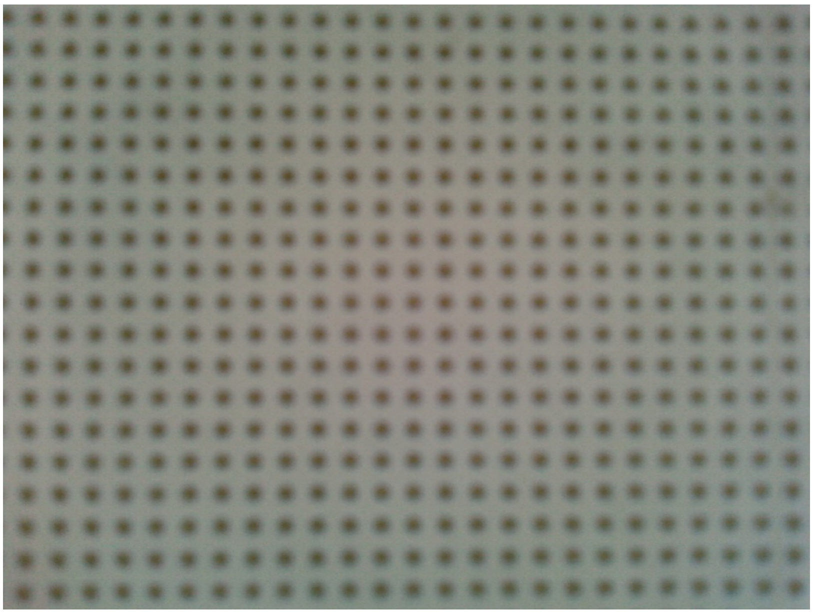

Figure 3. 17 Image of the Calibration plate

The only thing that remains is making sure that the two laser sheets (the two pulses) have sufficient overlap. This is done by pulsing the laser with smallest time increment (at high intensity) and check wehter the images are “identical”.

The different fields of view with their height above the plate are given in figure 3.24 and 3.25.

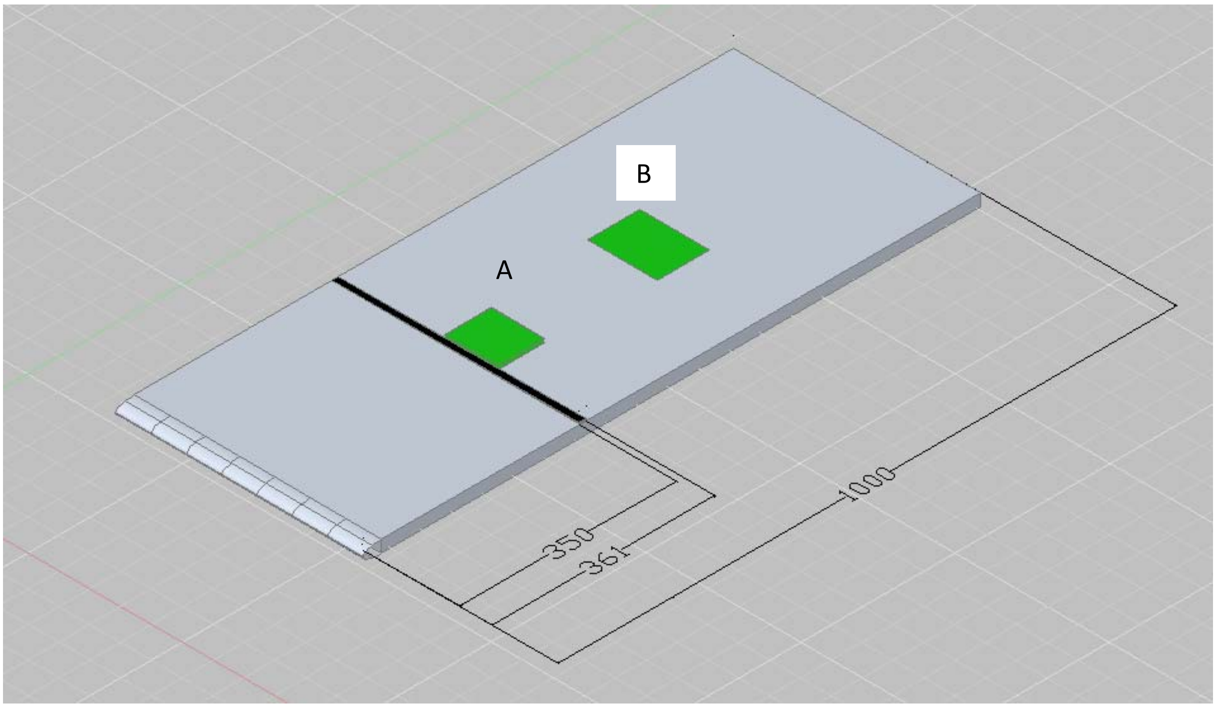

Figure 3. 18 Fields of view

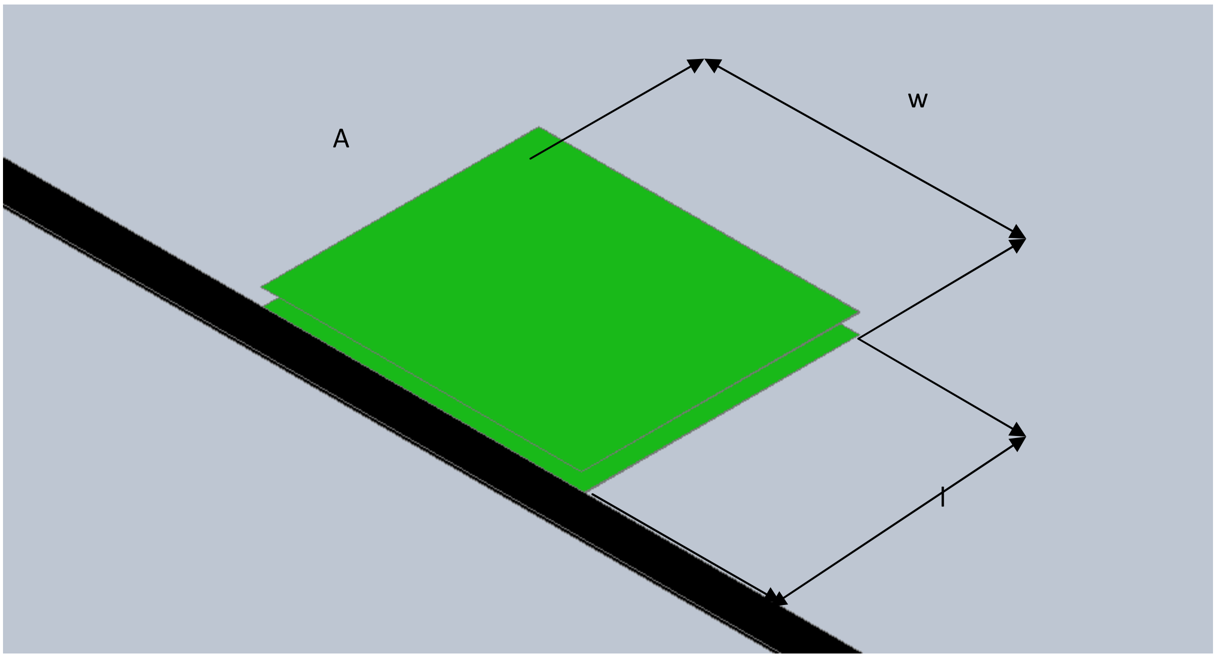

Figure 3. 19 Laser sheet positions (zoom)

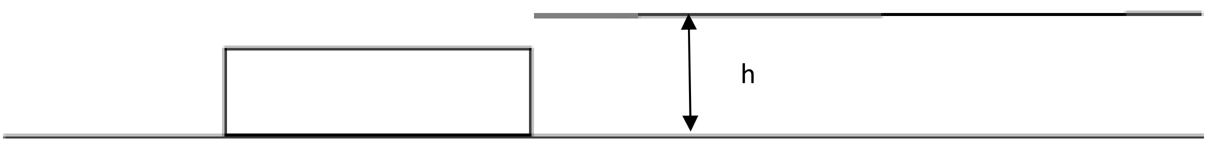

Figure 20 Side view of field of view

4 Results

4.1 Hot wire Anemometry

The velocity profiles for the different cases are determined and for the cases without transition devices they are corrected by extrapolating the lower linear part and setting this to zero (no-slip condition), this offset is the error in height above the plate. The boundary layer profiles are represented in scaled form using the free stream velocity and the boundary layer thickness.
First the results for the smooth plate are given. The velocity profiles should be self similar and are compared with the theoretical Blasius profile in figure 4.1. Only the experimental results for 5 m/s are given, for the other velocities the graph is similar.

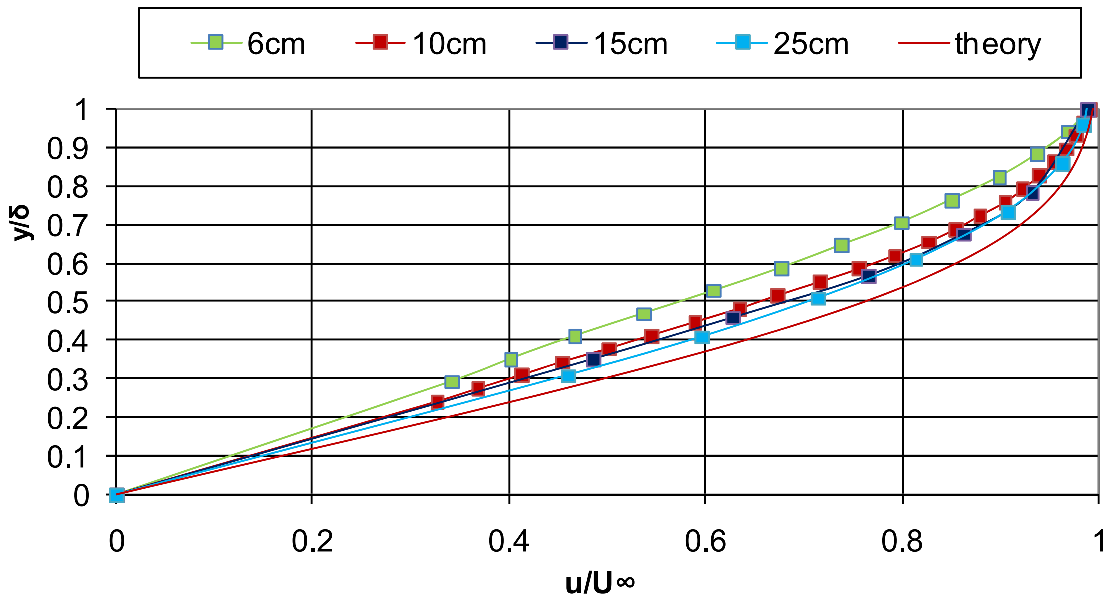

Figure 4. 1 Theoretical velocity profile from Blasius compared to experiments at the given distances behind the leading edge of the strip

It is clear that the traverse taken at 6 cm behind the transition strip is quite influenced by the pressure gradient although the influence becomes smaller with increased distance behind the strip. The others are quite close to each other. The profile has a similar shape to theory.

For the determination of the boundary layer thickness the criterion of a velocity of 99% of the free stream velocity marks the end of the boundary layer for the laminar flow and 98% for the turbulent flow, because the velocity stopped rising over 98%. The experimental results are given in figure 4.2.

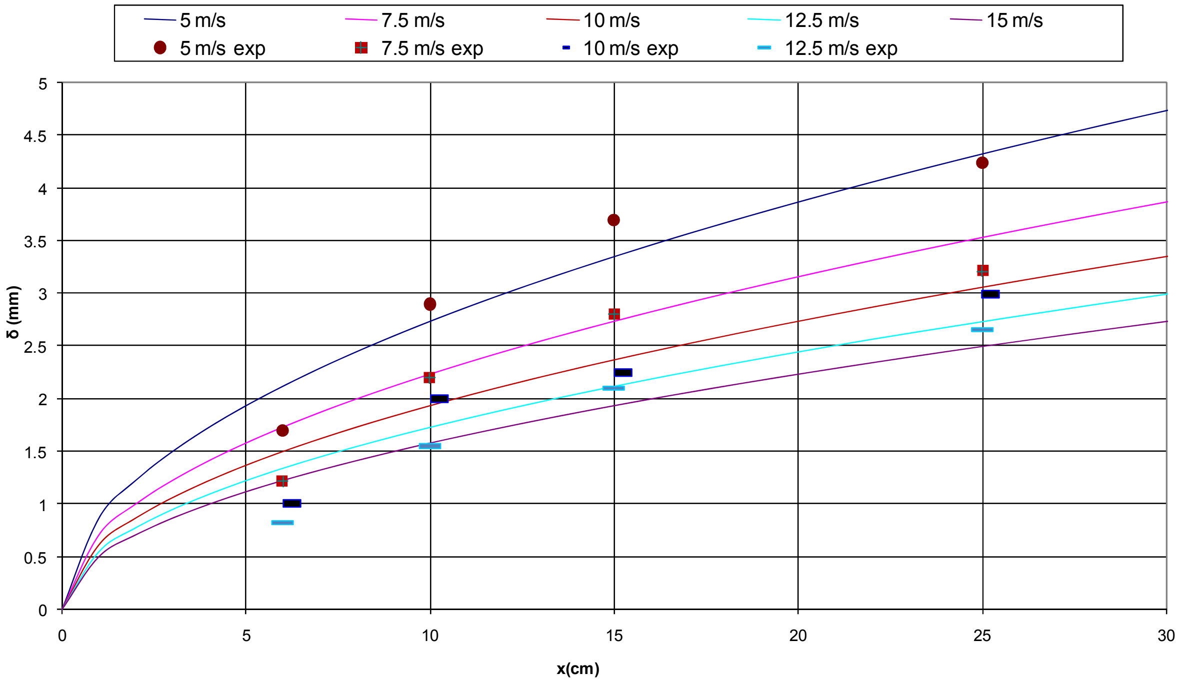

Figure 4. 2 Comparison between the boundary layer thickness from Blasius theory and HWA experiments

From this graph can be concluded that the measurement is most accurate to theory from 10 cm from the leading edge.
Now the results for the flat plate with the 0.95 mm and 1.45 zigzag strips are given.
One can see that the boundary layer is a lot thicker compared to the laminar case as can be seen in figure 4.3.

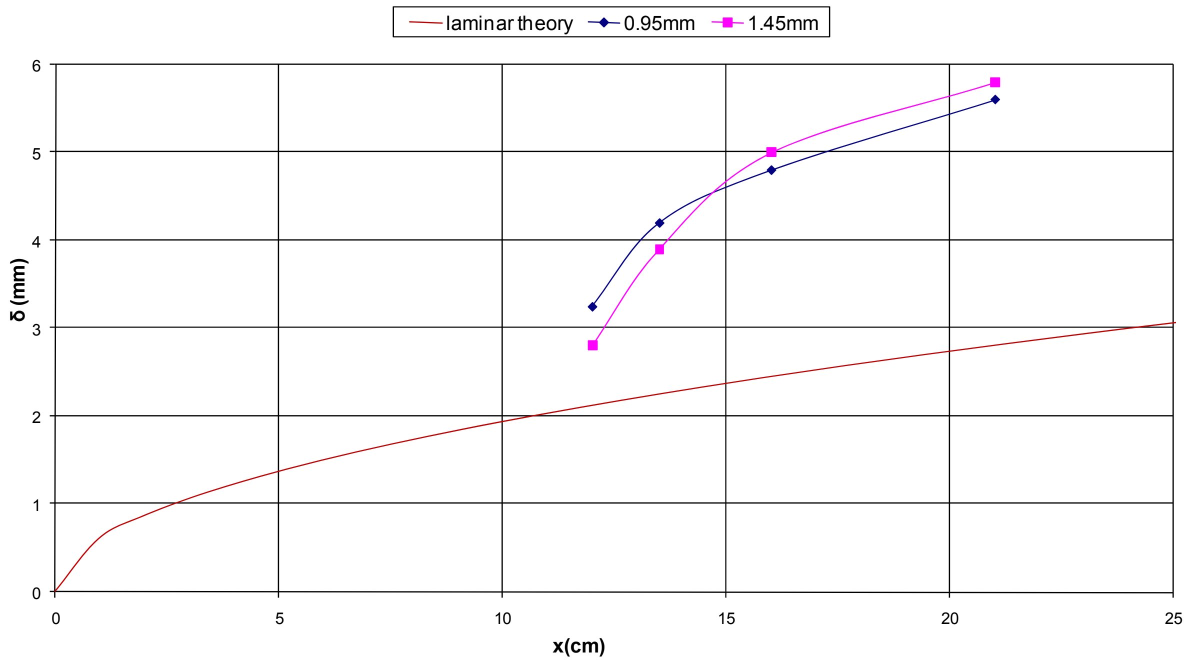

Figure 4. 3 Boundary layer thickness for tripped boundary layer with zigzag stips at 10cm form the leading edge

Turbulence
We take a look at the turbulence intensity in the boundary layer. On the vertical axis,in figure 4.4, the height above the plate is given in non-dimensional form. On the horizontal axis the turbulence intensity is given. For the 0.85mm zigzag strip and the 2.15mm straight strip the measurement has been done twice, with the probe at approximately the same postion (the complete setup has been rebuild) in order to estimate the error and/or reproducibility of the experiment. These second measurements have been marked with "II"in figure 4.4. From these second measurement one can see that the measurement error can be up to 0.04. This is quite high. On the other hand most measurements show quite good similarity. These high errors find their origin in the fact that the spanwise position of the HWA with respect to the strip is random. From the PIV measurements it is clear that the velocity and turbulence profile differ quite a bit in spanwise direction (see figure 4.5), so the spanwise position should be exactly the same with respect to the teeth of the zigzag strip in order to reproduce the results. The "zero velocity" measurement is the noise of the measurement in turbulence equivance. In figures 4.4, 4.6, 4.7 and 4.8 one can see that turbulence increases with the thickness of the strip. One can also see that a zigzag strip produces relatively more turbulence .

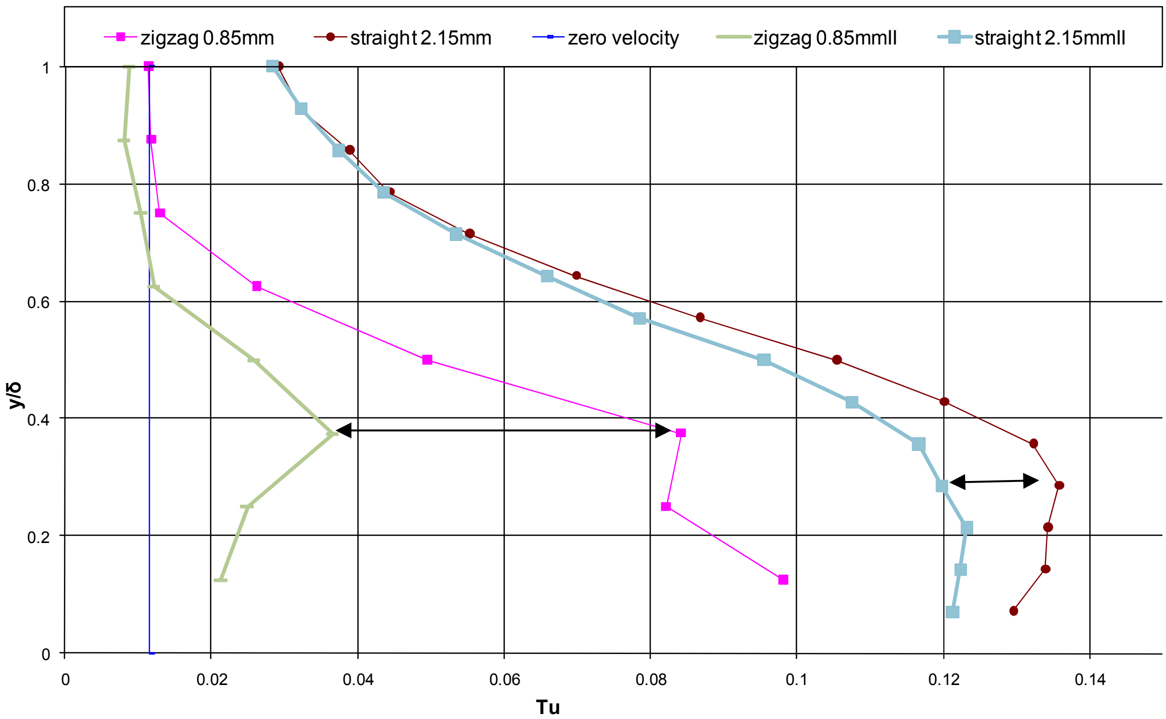

Figuur 4.4 Turbulence intensity behind the various strips at 7.5cm behind the strip (error is marked with arrows)

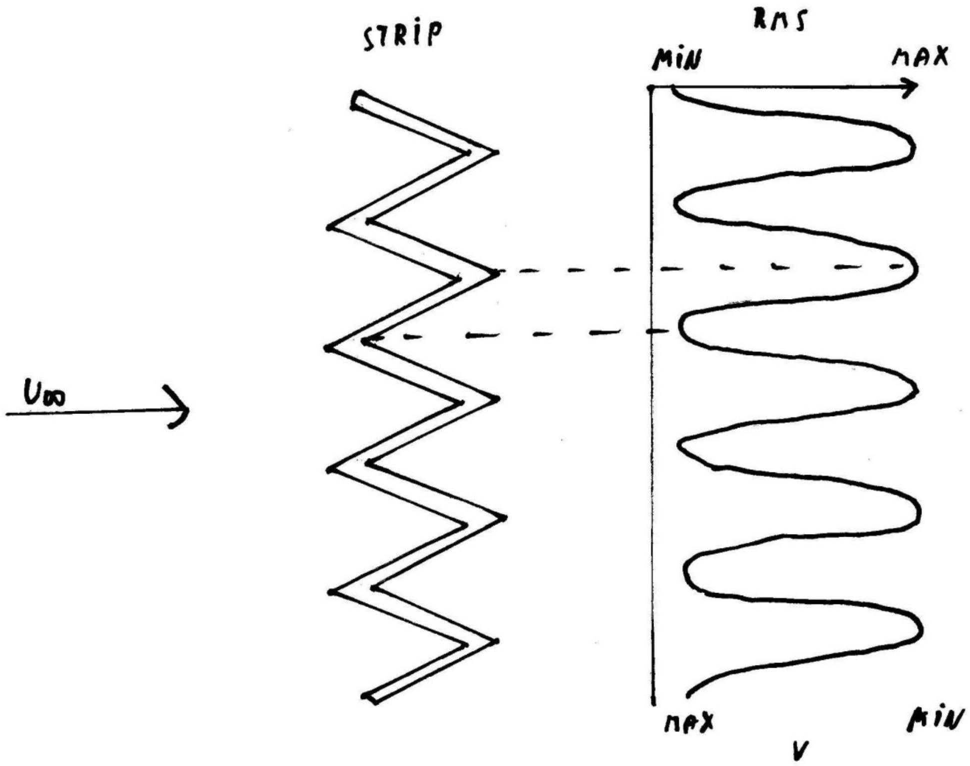

Figuur 4.5 Sketch of top view, suggests how the position of the HWA with respect to the zig zag strip can have a tremendous effect on the measured value

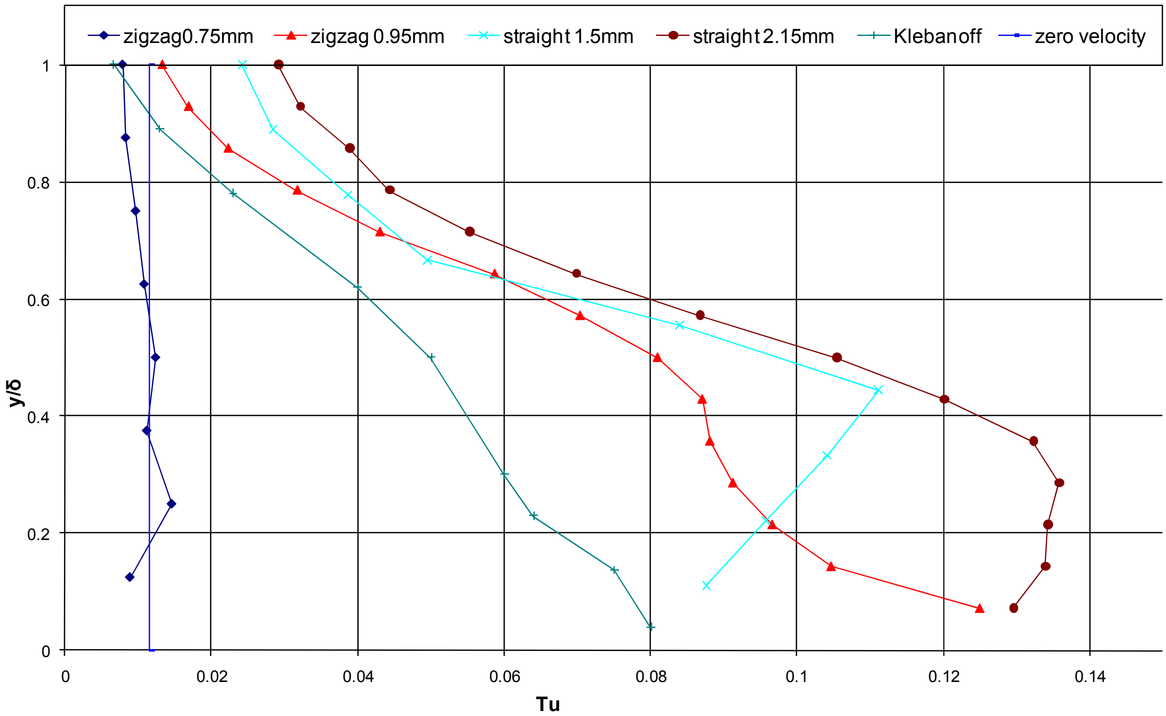

Figure 4. 6 Turbulence intensity behind the various strips at 7.5cm behind the strip

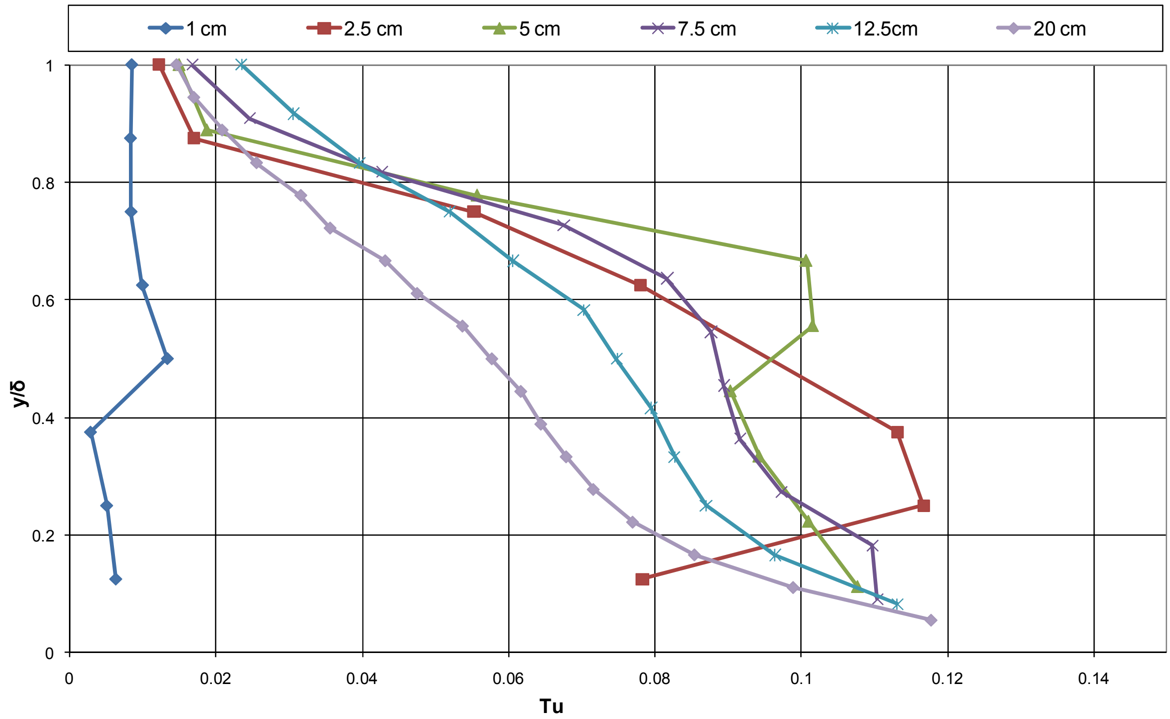

Figure 4. 7 Tubulence intensity behind a 0.9 mm thick zigzag strip

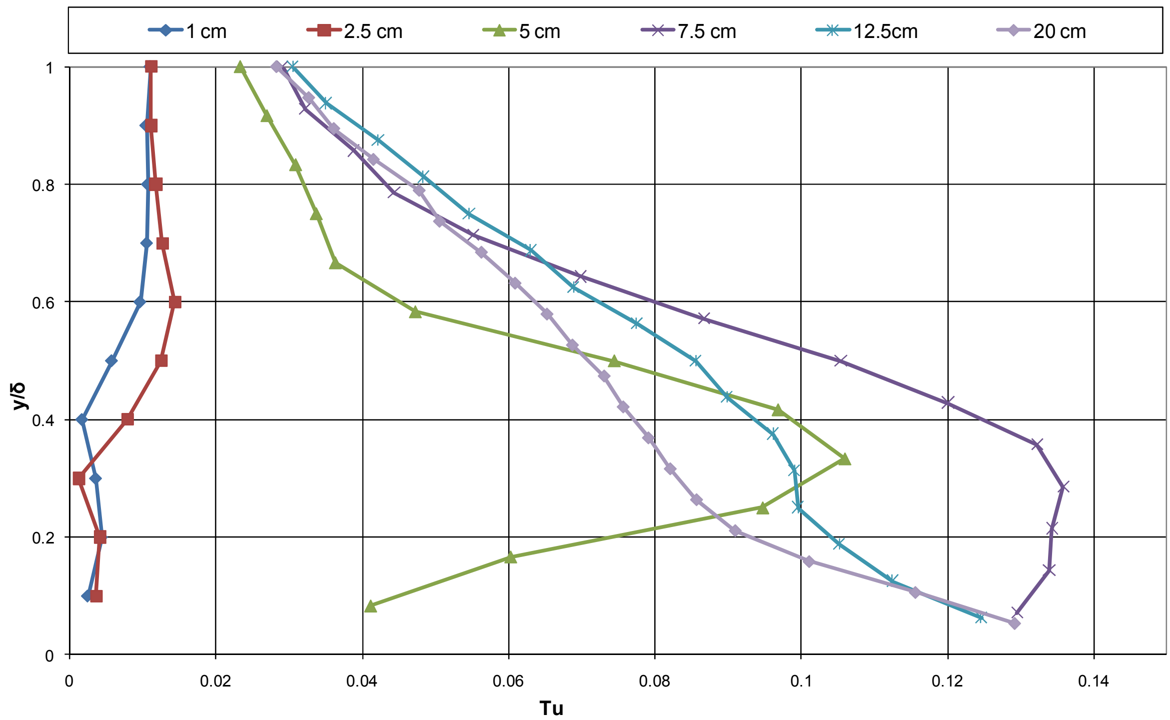

Figure 4. 8 Tubulence intensity behind a 2.15 mm thick straight strip

Figures 4.7 and 4.8 show that the transition to turbulence occurs very quickly with the zigzag tape of 0.9mm (somewhere between 1 and 2.5 cm) and for the 2.15mm straight strip this happens between 2.5 and 5cm. One can also see that turbulence is lower in the wake of the strip since the higher the strips and the closer to it the more the lag in turbulence is, because this area is "shielded" from the free stream.

Velocity profiles

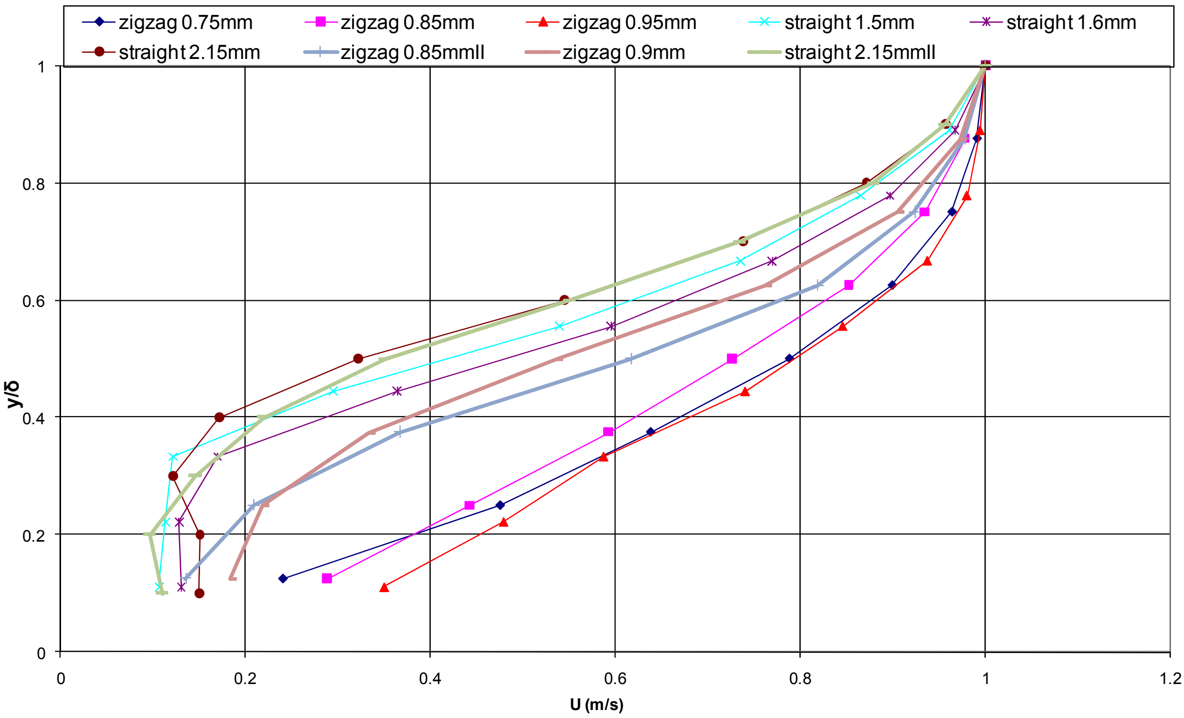

Figure 4. 9 Velocity profile behind the various strips at 2.5cm behind the strip

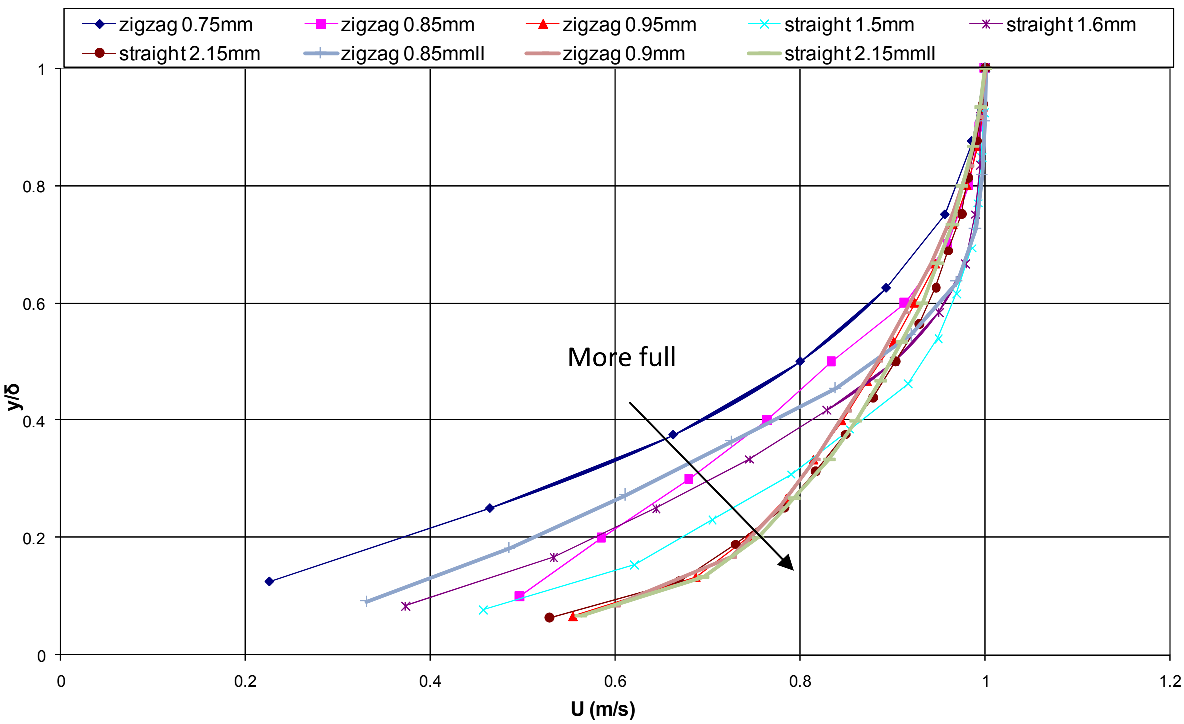

Figure 4. 10 Velocity profile behind the various strips at 12.5cm behind the strip the arrow gives the direction of more full/turbulent velocity profile

In figure 4.9 can be seen that the flow behind an obstable is slowed down near the surface (as it experiences more drag). After some distance turbulence has taken care of the diffence in momentum between the lower and higher regions, by mixing the layers. After this mixing the velocity profiles are similar to the ones in figure 10. The velocity profiles in figure 4.10 show a more “full” profile than for a laminar boundary layer as expected from theory.

Boundary layer thickness
The boundary layer thickness is given in figure 4.11. The boundary layer thickness is important to determine the measurement heights in the upcoming measurement campaign.

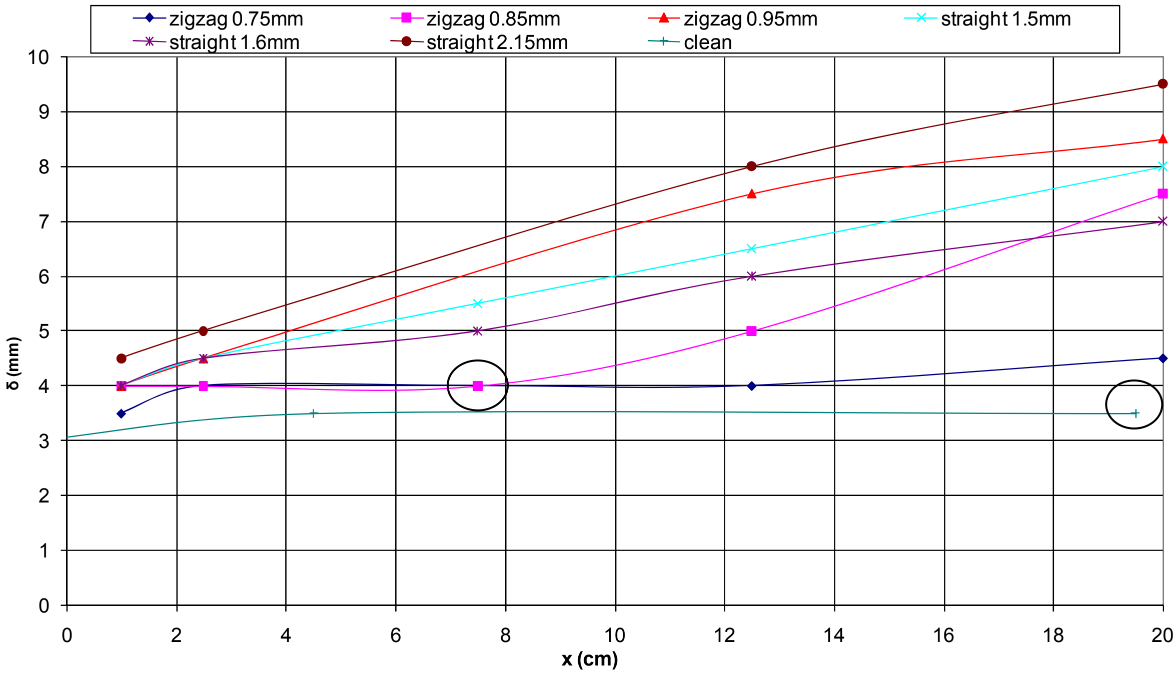

Figure 4. 11 boundary layer thickness behind the various strips not all results are given for reasons of clarity

From figure 4.11 it is evident that the boundary layer is thickened by the strips. There are some peculiarities however. The points marked by a circle would imply now boundary layer growth in that part of the flow. This would be nearly physically impossible having no pressure gradient. This inaccuracy is caused by the fact that the measurement step in the height was rather coarse (0.5mm) with respect to the boundary layer thickness and rate of growth. So the values are rounded to the closest measurement height, which can easily cause this inaccuracy. However from this graph the most important result is clear: in the laminar flow the thickness of the boundary layer is 3mm at the strip position (which is not there yet in the laminar flow). Hence the strips should not be thicker than 3mm (2.75mm because of the inaccuracy discussed before) in order to have boundary layer tripping. When the obstacle protrudes the boundary layer completely one cannot speak about boundary layer tripping anymore.

4.2 PIV experiments

The last experiments which have been performed are the planar PIV measurements. The goal of these measurements are to visualize the main structures in the transitional boundary layer. A sample of the PIV recordings is given in figure 4.12. The images made can be found in appendix C.

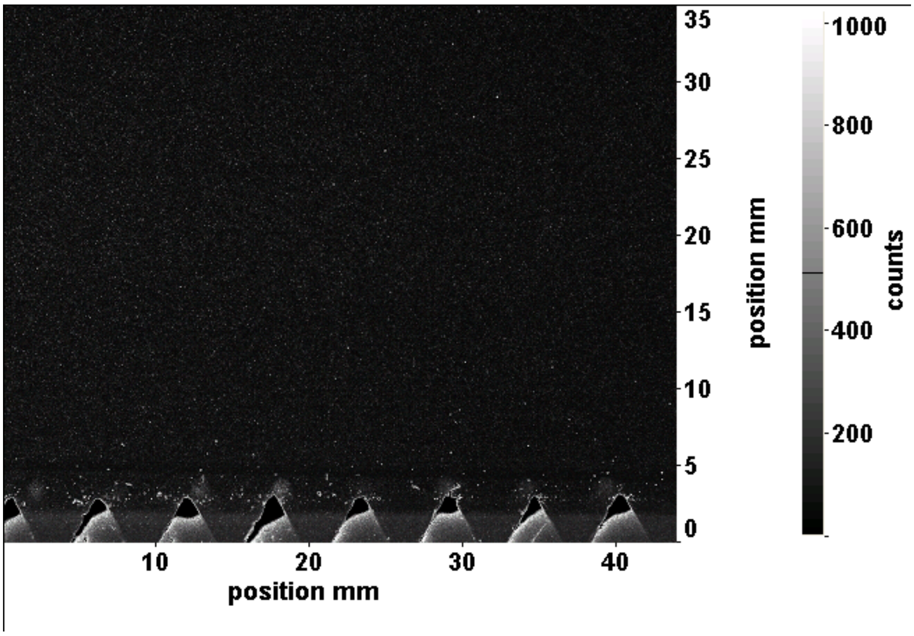

Figure 4. 12 Example of PIV recording of a flow over a 0.9mm thick zig zag strip

When comparing the averaged images of the straight strip (figure 4.14) and the zigzag strip (4.13) it is immediately clear that the flows are very different. Behind the zigzag strip there are long trails with intermitting higher and lower velocities in streamwise direction, even some backflow occurs (figure 4.13, or even clearer in appendix D.11-D12). Whereas the straight strip causes one big region with backflow behind the strip. This effect of the strip gets less intense when looking at a higher level above the plate, because the influence of the strip becomes weaker when getting further away from it.

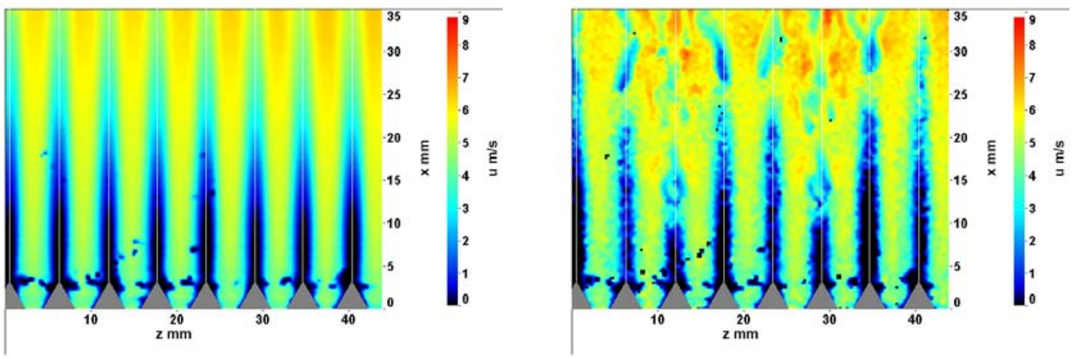

Figure 4.13 Average (left) and instantaneous (right) streamwise velocity behind 0.9mm thick zigzag strip at 1mm height

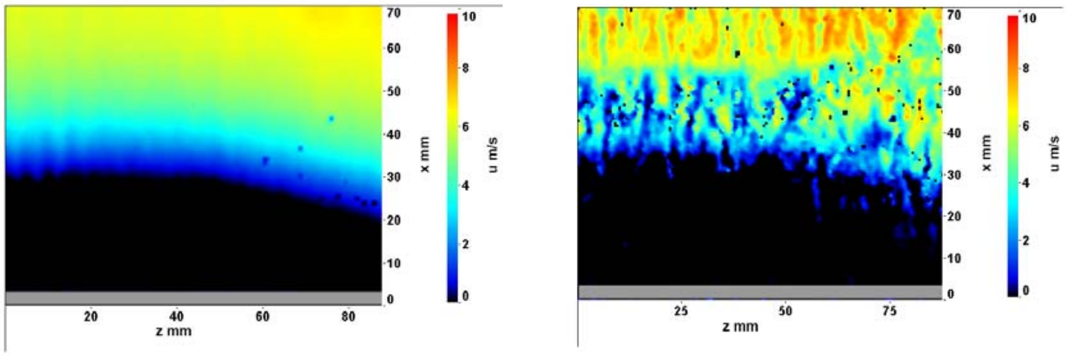

Figure 4.14 Average (left) and instantaneous (right) streamwise velocity behind 2.15mm thick straight strip at 1mm height

One can also see that the wake of the higher straight strip causes a much bigger area with a low velocity, this causes the previously mentioned “shielding” (appendix C). When taking a look at the instantaneous flow fields (figures 4.13 and 4.14, right) one can observe the high and low speed streaks and the turbulent spots, although they look a bit more “structured” in the zigzag case.
In figure 4.15 the spanwise velocity behind a zigzag strip is shown. On the left one can see that the the flow on average flows to the left in some areas and in others to the right. In the image of the instantaneous flow field the high and low speed streaks are visible at the higher x -values. A clear change in flow direction is observed around an x-position of roughly 15mm. What happens here is explained later.

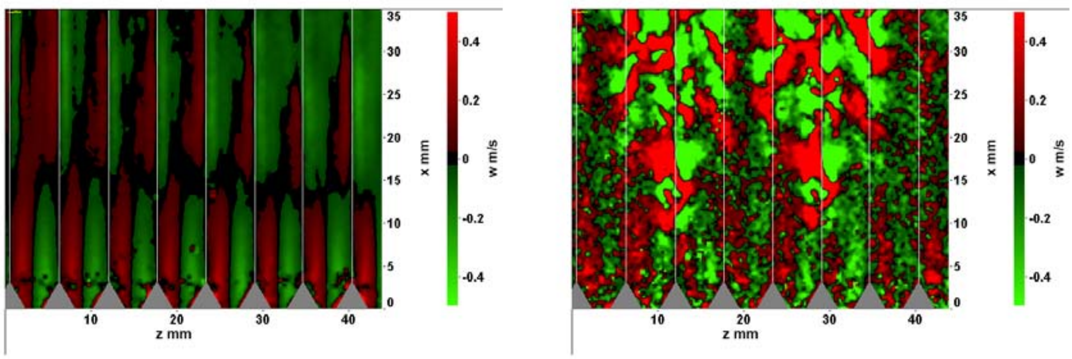

Figure 4.15 Average (left) and instantaneous spanwise velocity behind 0.9mm thickzigzag strip at 1mm height

In figure 4.16 the RMS is given. This is a measure of the turbulence intensity as is defined in equation (3.5) expressed as U_{RMS}. It is clear that turbulence is created in the areas with high velocity gradients, which have been caused by the zigzig strip.

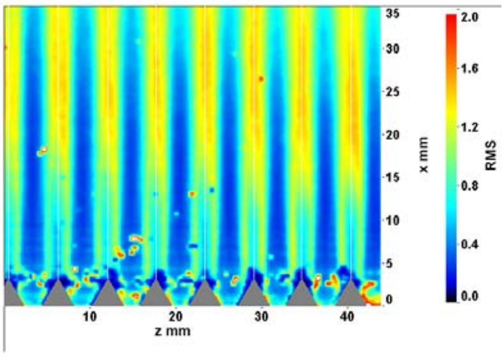

Figure 4.16 RMS behind 0.9mm thick zigzag strip at 1mm height

Now what happens behind the zigzag strip? The shown PIV images are only 2-dimensional, but the flow appears to be highly 3-dimensional. The 2-dimensional results have been combined to show how the 3-dimensional flow looks like. In figure 4.17 a sketch is shown for the zigzag strip. In this sketch a pair of vortices builds up along each tooth of the strip and will separate at the end of the tooth. After that the velocity gradient normal to the plate will tilt the vortices backward causing differences in the planar components of the velocity. The vortices cause more mixing and increase the velocity gradients in the flow and with that generate turbulence. This sketch applies t both the average and instantaneous flow field in that sence that the the instantaneous flow field will have this main structure, but it can fluctuate an deviate from the sketch because of its turbulent nature.

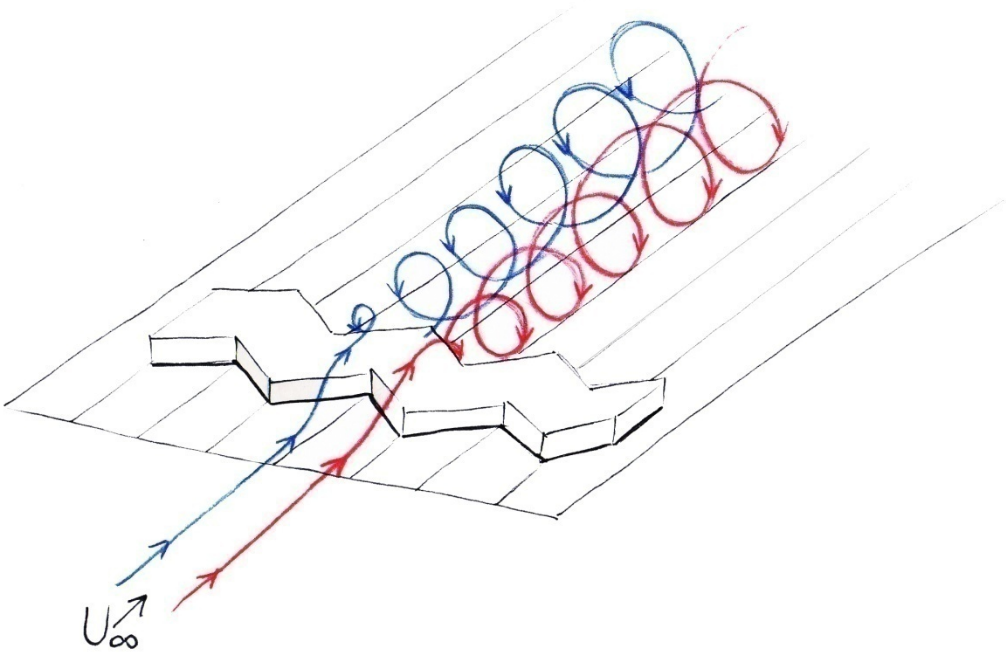

Figure 4. 17 Sketch of the flow over the zigzag strip

These vortices trail quite far into the flow (though the velocity gradients are less rigorous), apparently the vortices are strong enough to avoid being dissipated quickly causing a non-homogeneous turbulent flow (figure 4.18).

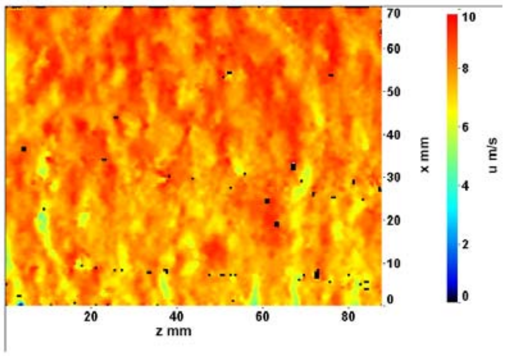

Figure 4.18 Instantanious streamwise velocity behind 0.9mm thick zigzag strip at 4mm height and 20cm

Another peculiarity mentioned earlier is the spanwise velocity change in the 1mm zigzag case. Between 12-17mm behind the strip the spanwise velocity changes sign when travelling downstream. To explain this a sketch of the situation is given in figure 4.19. The diameter of the vortex increases as it is convected downstream. In the 1mm case the laser sheet is positioned such that the laser sheet crosses the vortex axis. This means that in the PIV image you see the upper or lower part of the vortex, depending on the position before or after the crossing.

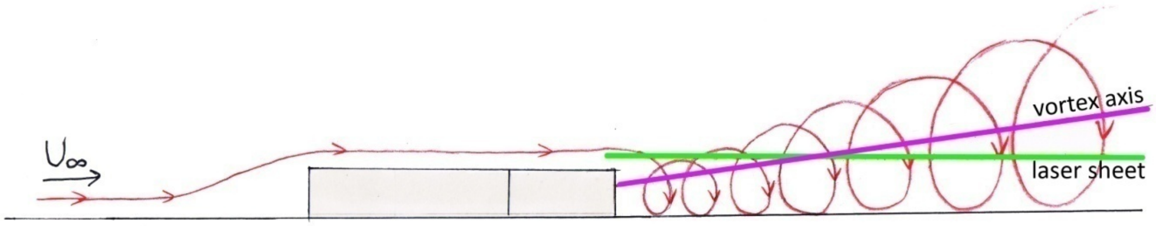

Figure 4. 19 Side view of the flow over a zigzag strip, with laser sheet in position

In figure 4.20 the streamwise velocity for the straight strip is shown, but now filtered differently. It is even clearer that there is a very sharp edge between backflow region and the rest of the flow. This region of backflow is caused by a vortex rolling from the trailing edge of the strip. A sketch of this flow is given in figure 4.21.

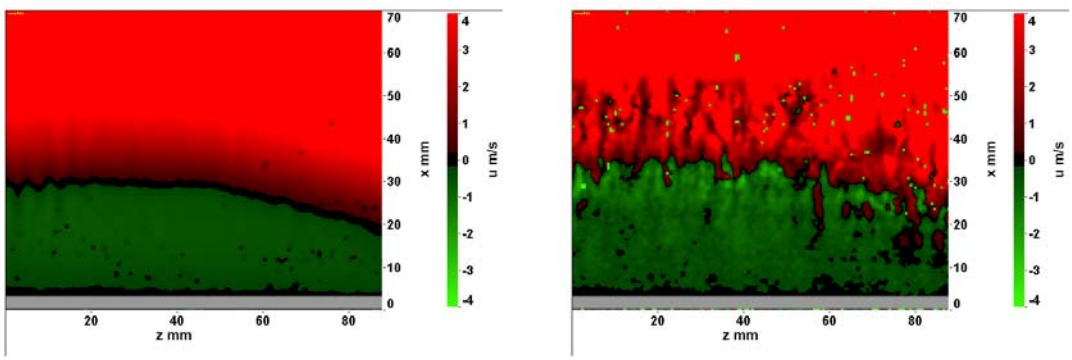

Figure 4.20 Average and instantaneous streamwise velocity behind straight strip at 1mm height

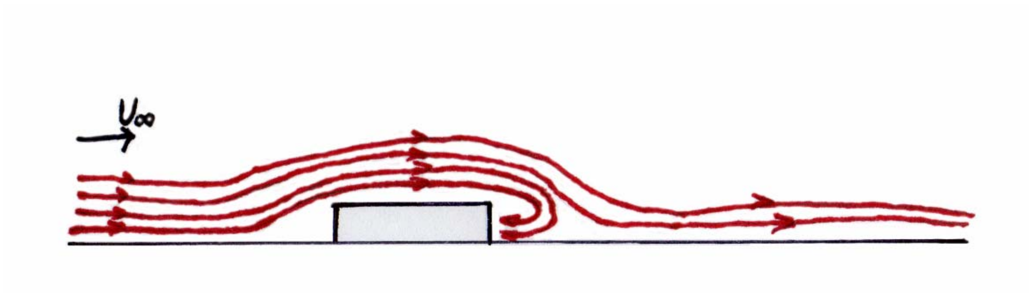

Figure 4.21 Skech of the sideview of the flow over the straight strip

For the production of tubulence the same is true in this case: Turbulence is produced in areas with high velocity gradients as can be seen in figure 4.22.

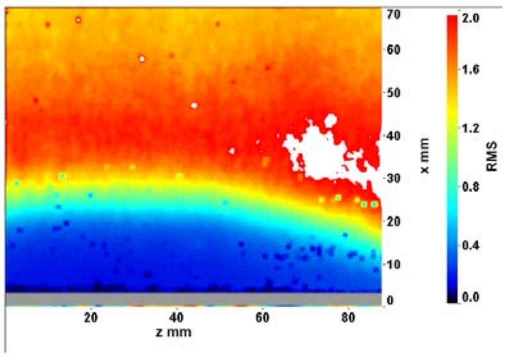

Figure 4.22 RMS behind straight strip at 1mm height

5. Conclusions

5.1 Hot wire anemometer

The HWA measurements had the main goal to assess the transition effect for different strips, in order to select the correct flow conditions for the PIV experiments. The results gave appropriate conditions to continue with the PIV measurements.

The HWA tests showed that at a free stream velocity of 8 m/s transition occurs at about 5-7.5 cm behind the strip for the 2.15mm thick straight strip and the 0.9mm thick zigzag strip. The turbulence and velocity profiles show the expected shapes, but they show a quite high differences between the repeated measurements. This discrepancy can be caused by the exact position behind the zigzag strip, which gives a very different velocity and also RMS. But for the straight strip this is not the case. The more probable cause of this error/bad reproducibility is the sensitivity of the flow to small differences, this is especially true for the zig zag strips. The flow reacts quite strong to thickness changes of 0.05mm so when the thickness of a strip is just 0.01mm off it will probably cause quite a difference in the flow. Also the positioning of the HWA is one of the causes of this difference. The height step is 0.5mm and since it is done by eye, with the help of a cathodometer, there can quite easily be an error of 0.1mm in it, which means 20%. However these errors are not important for the total research plan, as the results are only used to set-up the final experiments from which the main conclusions have been drawn.

5.2 PIV

For the PIV campaign the goal was to investigate the spanwise organisation of the transitional flow, in order to explore the mechanisms of transition behind a straight and zigzag strip and especially the differences. From the planar PIV results one has to imagine what happens in all three dimensions since the third velocity component is missing and the flow seems to be highly three dimensional. For the straight strip it looks like a vortex rolls from the trailing edge of the strip causing the lower part of the flow behind the strip to slow down and even causing backflow near the trailing edge of the strip (figure 4.21). In this part the flow has a very low turbulence intensity. The interaction of the vortex with the outer flow will cause extra mixing in that part of the flow since the viscous forces are increased. This will generate turbulence in a way rather widely described in literature. The case with the zigzag strip is quite different. The teeth of the strip induce strong vortices in the boundary layer (figure 4.17), which give high velocity gradients in the flow and hence will produce turbulence. These vortices also transport particles from different heights and thus different momentum throughout the boundary layer, so there will be strong additional mixing. This explains the difference in boundary layer behind a straight strip and a zigzag strip.

6. Recommendations

The next step in this matter would be extending the PIV measurements into stereo-PIV or even volumetric (tomographic)PIV. This will give a more complete view of the highly three-dimensional flow. Doing the experiments in a thicker boundary layer would make the experiments less difficult concerning accuracy of laser sheet positioning and would require less zoom from the lenses, because in the current situation everything is on a miniature scale and small errors in positioning and dimension become relatively large.

Additional HWA measurements would not give any more information about coherent structures in the boundary layer as it is only possible to measure the absolute velocity at one given point in time.

Difficulties for PIV measurements are severe between the teeth of the zigzag strip. This is because there will be a lot of shadows. One option would be aiming the laser sheet upstream such that the laser light will be able to reach this area. Then care has to be taken to minimize the light scatter from the strip itself.

References

[1] Abbas, F. (2008). *Aerodynamics of multiple bluff body front-edge interference.* Delft: MSc Thesis, Faculty of Aerospace engineering, Delft University of Technology.

[2] *Aerodynamic tuning of a nimbus 4D model*. (sd). Opgeroepen op 11 4, 2008, van http://pagesperso-orange.fr/scherrer/matthieu/aero/nimbus4e.html

[3] Brandt, L. &. (2002). *Transition of streamwise streaks in zero-pressure-gradient boundary layers.* Stockholm.

[4] Braslow, A. L. (1960). *Review of the effect of distibuted surface roughness on boundary-layer transition.* London: NASA Langley Research Center.

[5] Elsinga, G., Schrijer, F., & Scarano, F. (2006). Experimental aerodynamics, laboratory exercise on HWA and PIV measurement techniques. Delft.

[6] *http://boojum.as.arizona.edu/~jill/NS102_2006/Lectures/Lecture12/turbulent.html*. (2006).

[8] Kachanov, Y. s. (1994). Annu. Rev. fluid mech.

[9] Klebanoff, P. (1955). *Characteristics of turbulence in a boundary layer with zero pressure gradient.* NACA 1247.

[10] Preston, J. (1957). *The minimum Reynolds number for a turbulent boundary layer and the selection of a transition device.* Liverpool

.

[11] Raffel, M., Willert, C. E., Wereley, S. T., & Kompenhans, J. (2007). *Particle image velocimetry.* Gottingen: Springer.

[12] Robinson, S. K. (1991). *Coherent motions in the turbulent boundary layer.* Virginia.

[13] Scarano, F. (2007). Experimental aerodynamics. Delft.

[14] Scott, J. (2005, february 13). *http://www.aerospaceweb.org/question/aerodynamics/q0215.shtml*.

[15] Smith, C. a. (1983). The characteristics of low-speed streaks in the near-wall region of a turbulent boundary layer. In *J. fluid Mech. vol 129* (pp. 27-54). Bethlehem.

[16] White, F. M. (1991). *Viscous fluid flow.* McGraw-Hill, Inc.

Appendix A technical specifications

Hot wire anemometer:

- Dantec 9055p0111 probe
- Dantec 56C17 CTA bridge
- BNC-2110 block connector
- National Instruments NI PCI-6024E data acquisition board

PIV:

- Camera: Lavision Imager Intense
  Pixel size: 6.45x6.45µm
  Sensor size: 1376x1040 pixels
  Read out noise: <5 [e^-]
  Max. Frame rate [1/s]: 10
- Laser: Quantel Twin CFR-2000
  Wavelength: 532nm
  Power per pulse: 200mJ
  Repetion rate: 30Hz

Appendix B Measurement positions

6 cm	5 m/s	7.5 m/s	10 m/s	12.5 m/s
10 cm	5 m/s	7.5 m/s	7.5 m/s	7.5 m/s
15 cm	5 m/s	7.5 m/s	7.5 m/s	7.5 m/s
25 cm	5 m/s	7.5 m/s	7.5 m/s	7.5 m/s

Table B 1 HWA measurement positions on a clean plate at the gievn distances from the leading edge

Distance from leading edge (cm)	Item
10	Leading edge strip
11.1	Trailing edge strip
12.1 (1 cm behind trailing edge of strip)	HWA 1
13.6 (2.5 cm behind trailing edge of strip)	HWA 2
16.1 (5 cm behind trailing edge of strip)	HWA 3
21.1 (10 cm behind trailing edge of strip)	HWA 4

Table B 2 HWA measurement position on a flat plate behind zigzag strips of 0.95mm and 1.45mm thick

Distance from leading edge (cm)	Item
35	Leading edge strip
36.1	Trailing edge strip
37.1 (1 cm behind trailing edge of strip)	HWA 1 with strip
38.6 (2.5 cm behind trailing edge of strip)	HWA 2 with strip
41.1 (5 cm behind trailing edge of strip)	HWA 3 with strip
43.6 (7.5 cm behind trailing edge of strip)	HWA 4 with strip
48.6 (12.5 cm behind trailing edge of strip)	HWA 5 with strip
56.1 (20 cm behind trailing edge of strip)	HWA 6 with strip
35.6	HWA 1 without strip
40.6	HWA 2 without strip
55.6	HWA 3 without strip

Table B 3 HWA measurement traversion position for Zigzag strips of 0.75mm, 0.85mm,0.9mm and 0.95mm for which 0.85mm has been done twice for error estimate. Straight strips of 1.5mm, 1.6mm and 2.15mm, the last one being done twice.

Straight strip		Zig zag strip	
Height [mm]	Distance behind strip [cm]	Height [mm]	Distance behind strip [cm]
1	0	1	
2.5	0	2	
4	0		
5	20	4	20

Table B 4 Measurement positions of PIV campaign

Appendix C Results of HWA measurements

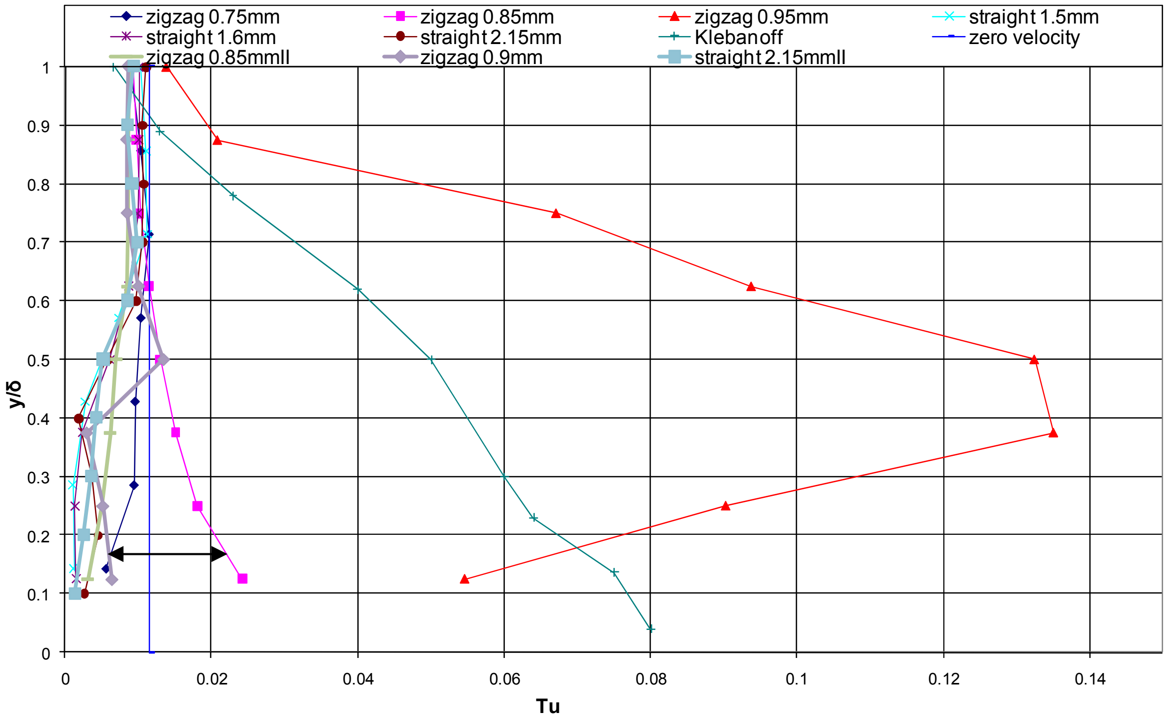

Figure C.1Turbulence intensity behind the various strips at 1cm behind the strip (error is marked with arrows)

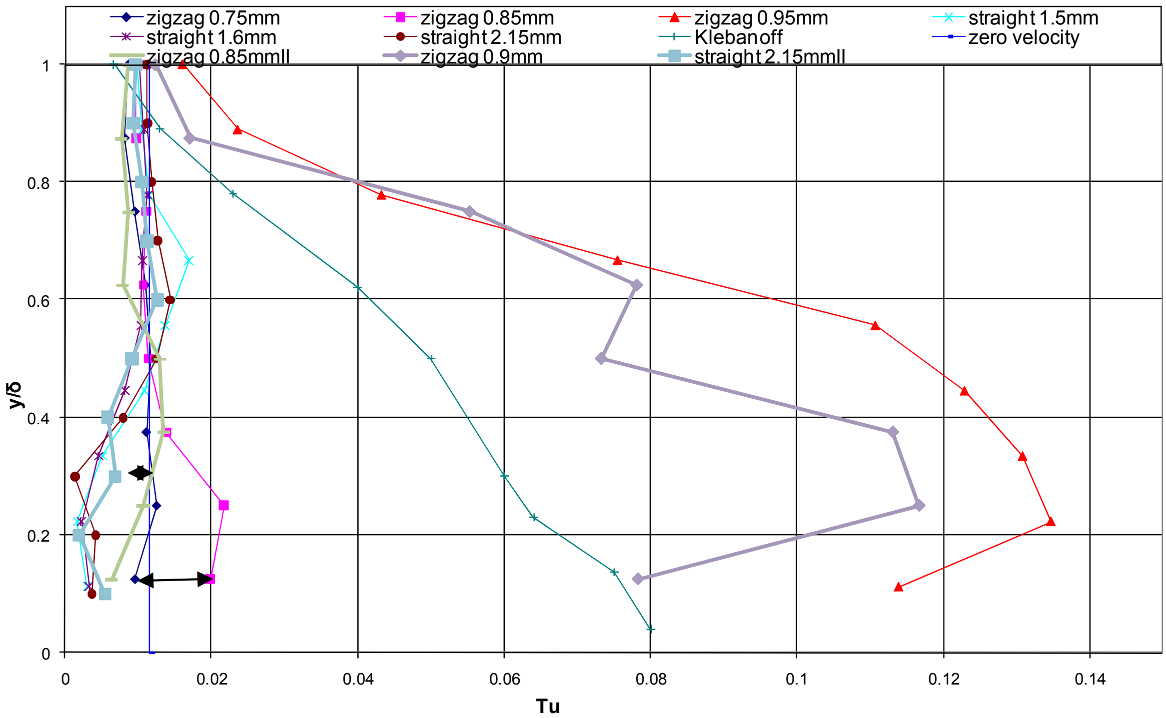

Figure C.2 Turbulence intensity behind the various strips at 2.5cm behind the strip (error is marked with arrows)

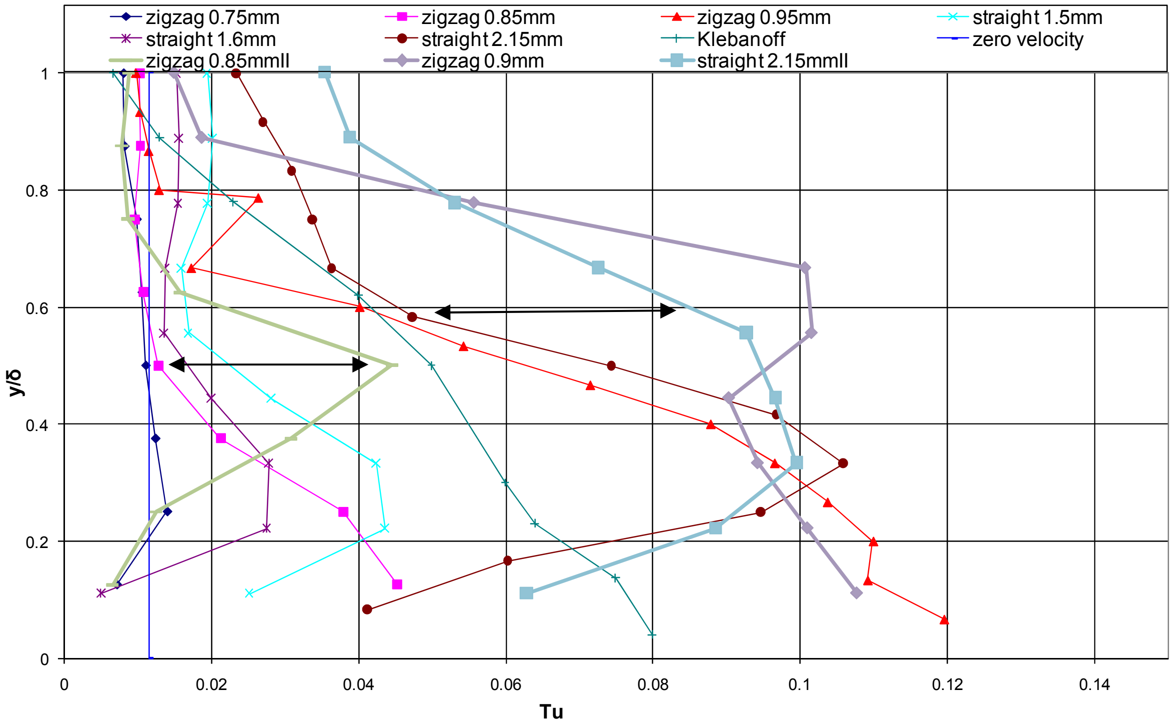

Figure C.3 Turbulence intensity behind the various strips at 5cm behind the strip (error is marked with arrows)

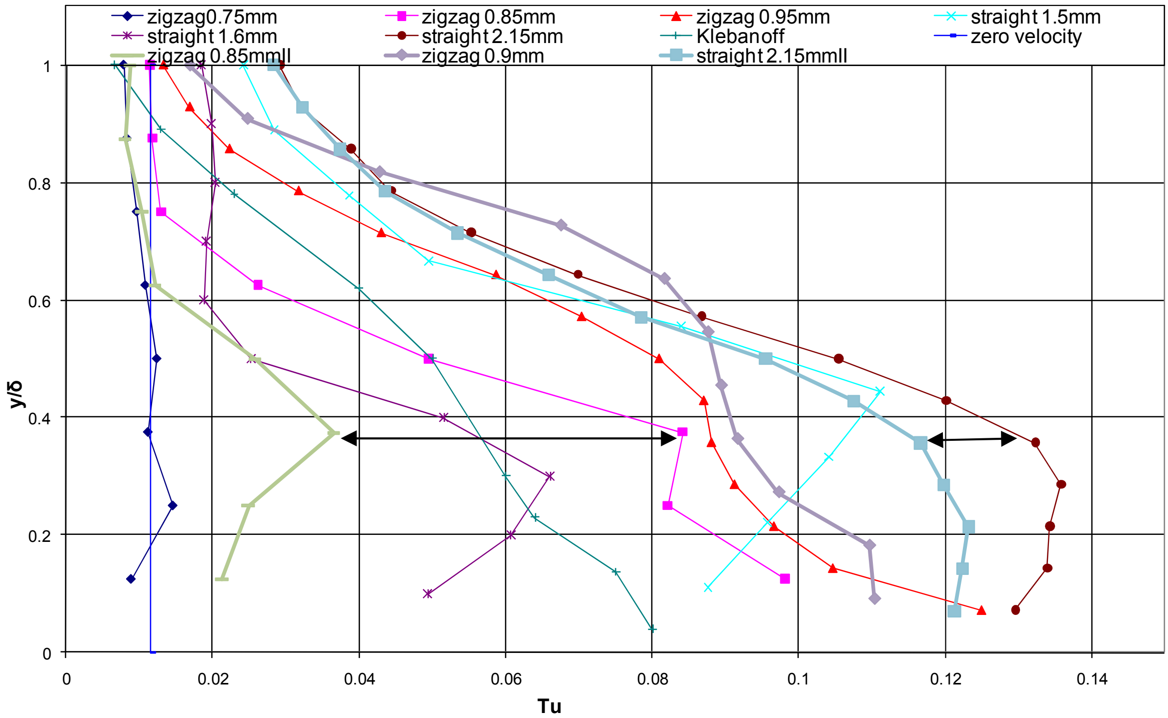

Figure C.4 Turbulence intensity behind the various strips at 7.5cm behind the strip (error is marked with arrows)

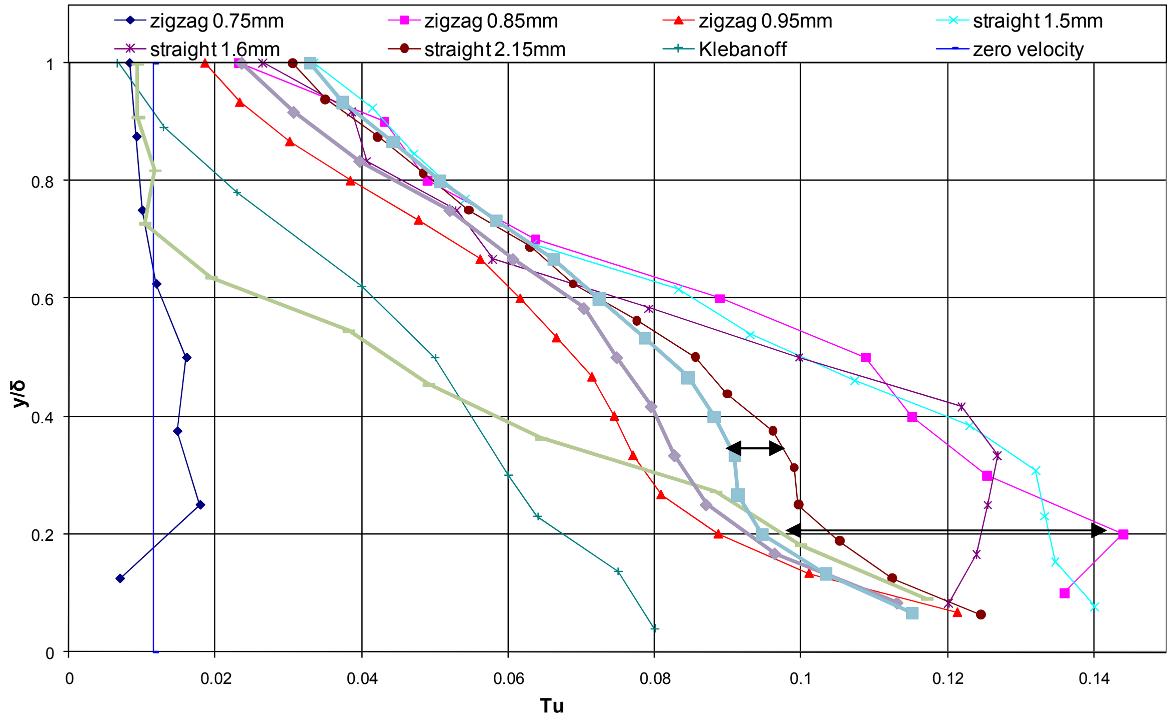

Figure C.5 Turbulence intensity behind the various strips at 12.5cm behind the strip (error is marked with arrows)

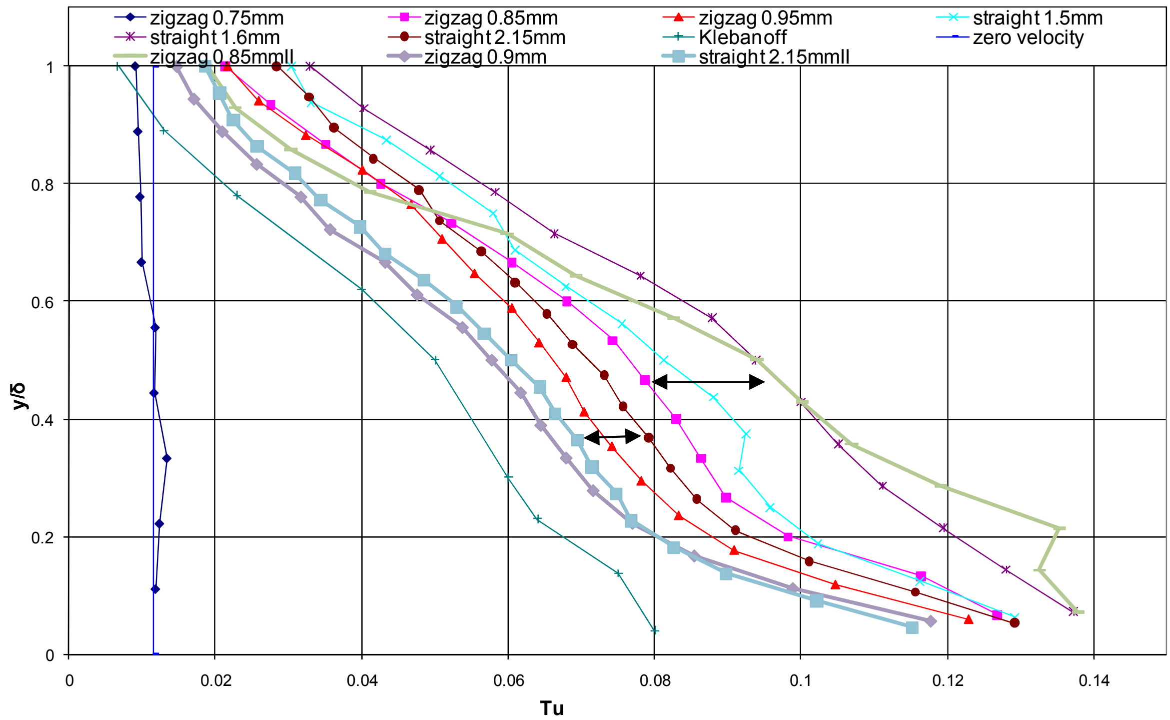

Figure C.6 Turbulence intensity behind the various strips at 20cm behind the strip (error is marked with arrows)

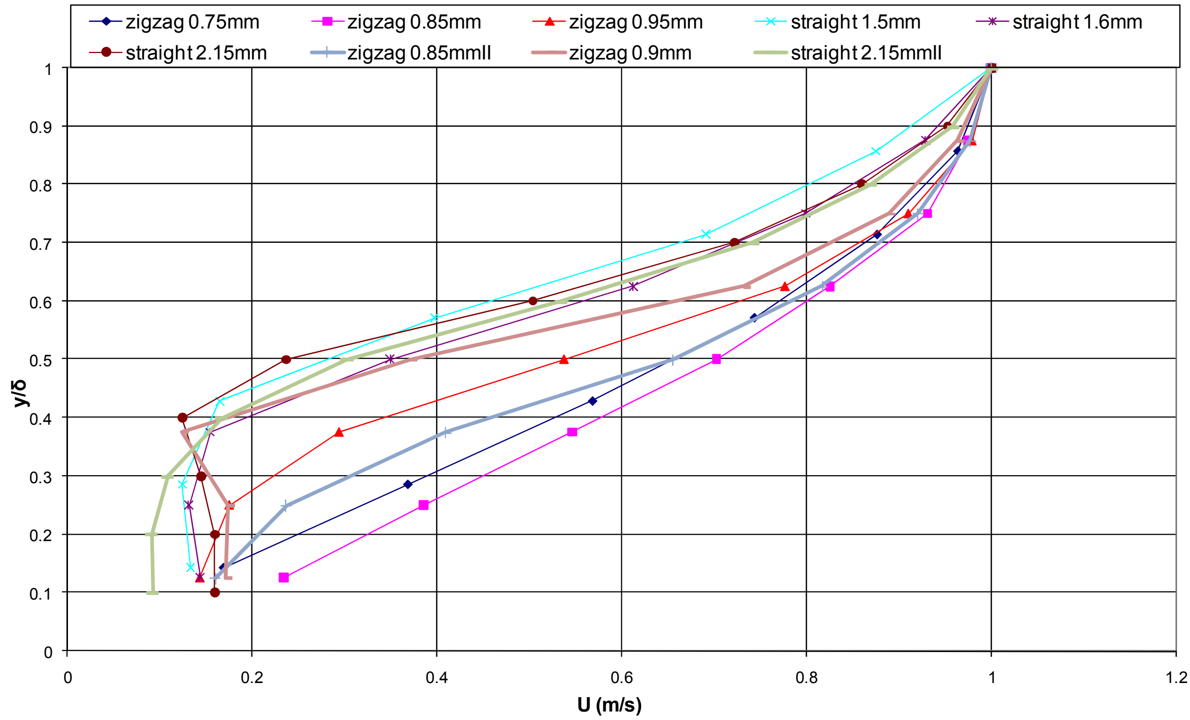

Figure C.7 Velocity profile behind the various strips at 1cm behind the strip

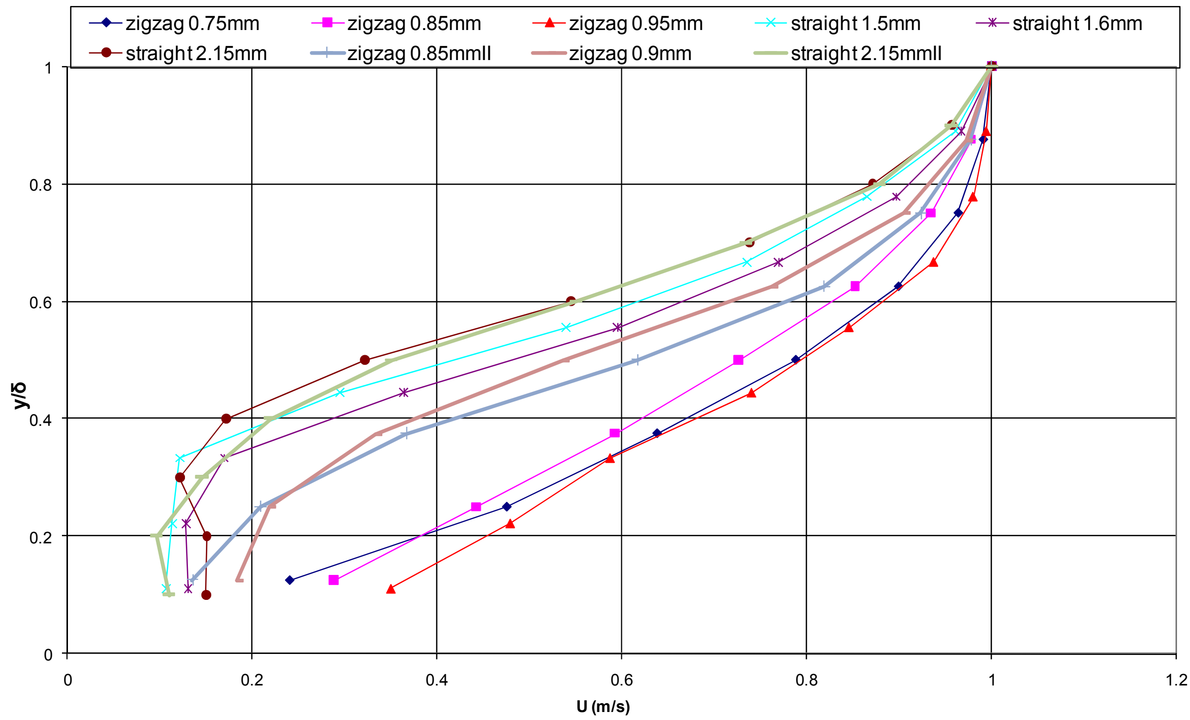

Figure C.8 Velocity profile behind the various strips at 2.5cm behind the strip

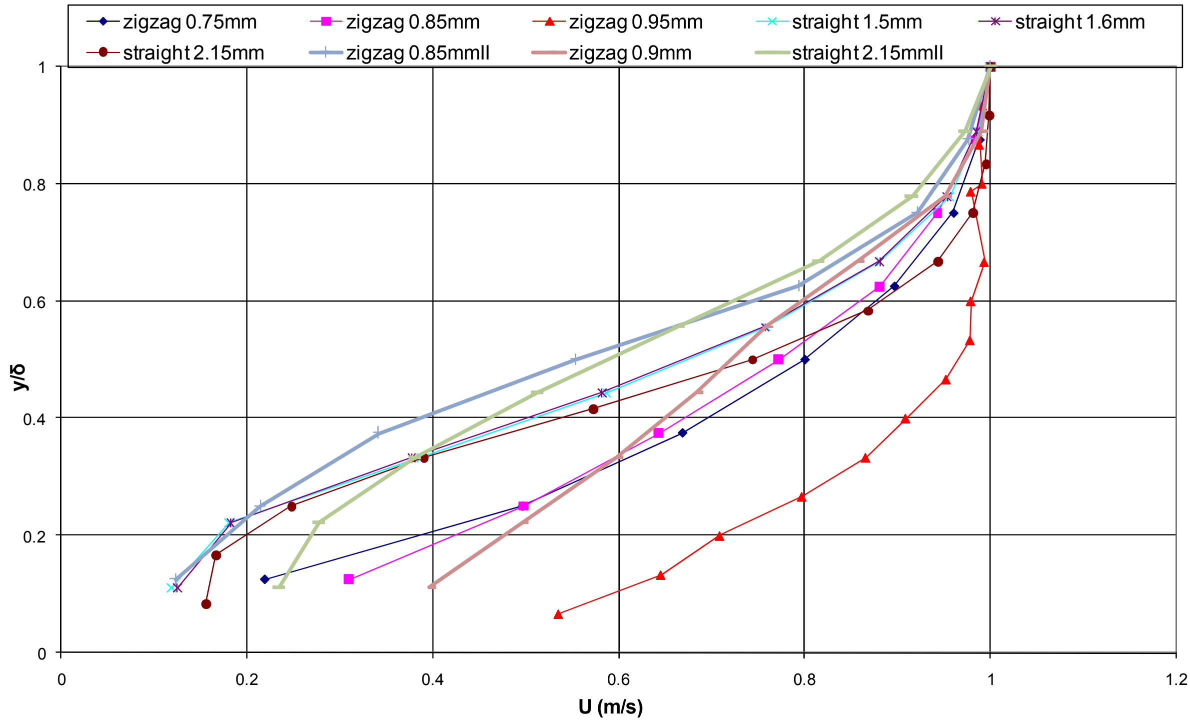

Figure C.9 Velocity profile behind the various strips at 1cm behind the strip

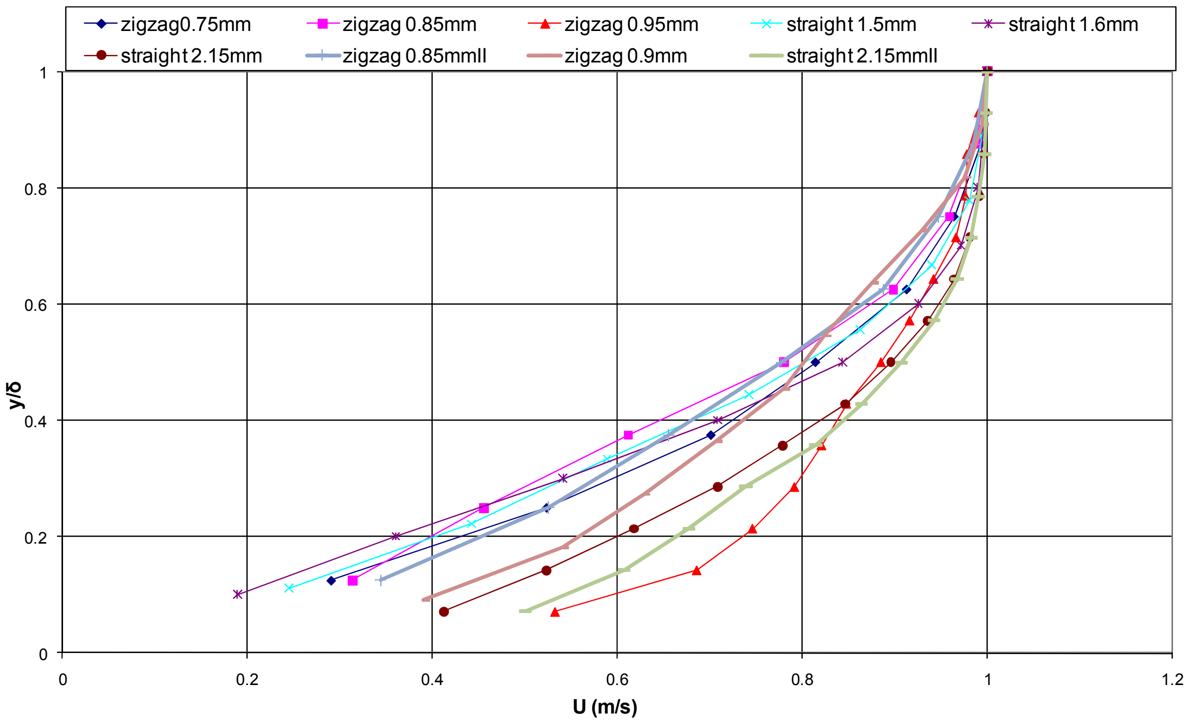

Figure C.10 Velocity profile behind the various strips at 7.5cm behind the strip

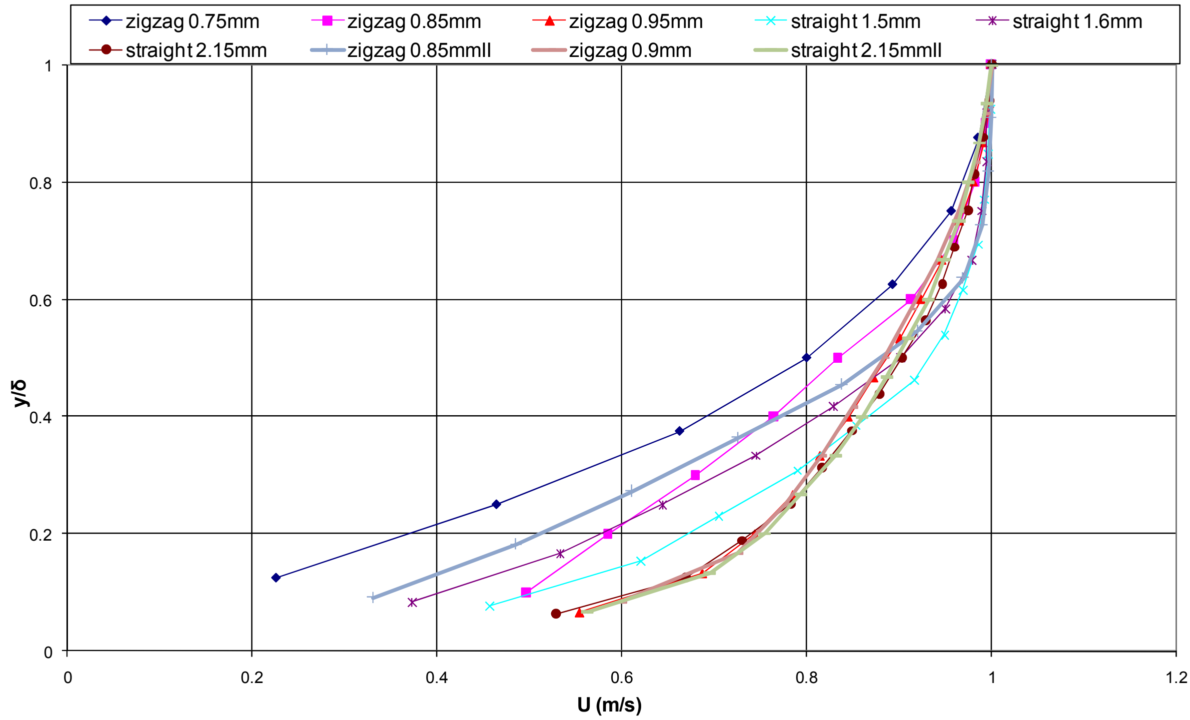

Figure C.11 Velocity profile behind the various strips at 12.5cm behind the strip

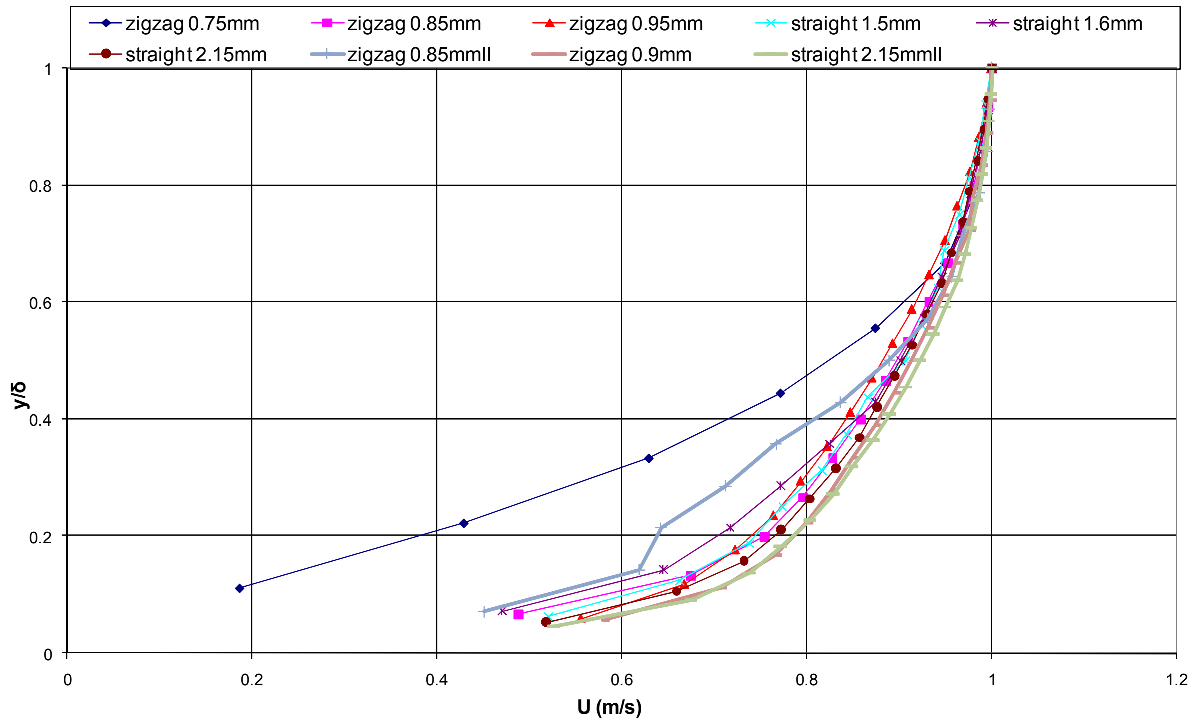

Figure C.12 Velocity profile behind the various strips at 20cm behind the strip

Appendix D Results of PIV measurements

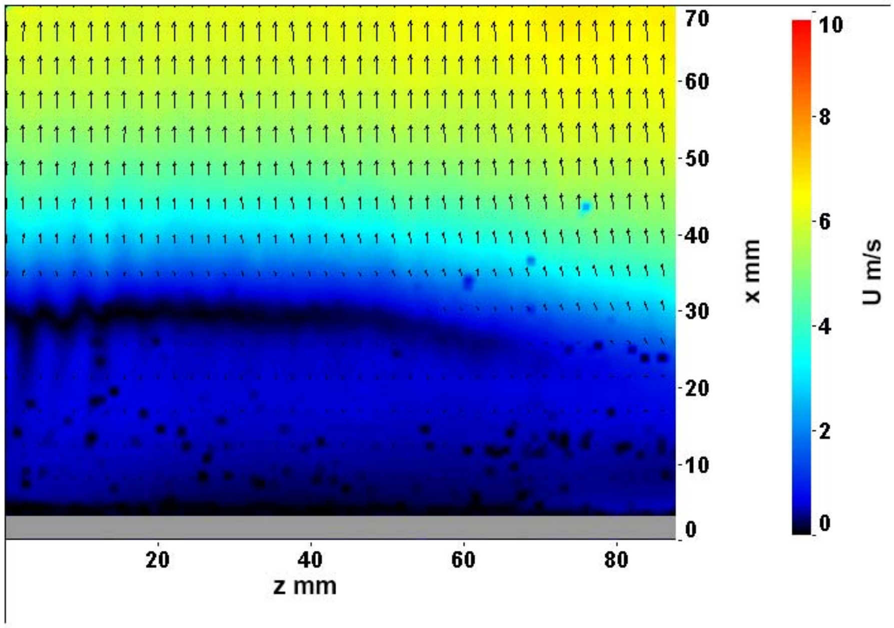

Figure D.1 Average Velocity behind straight strip at 1mm height

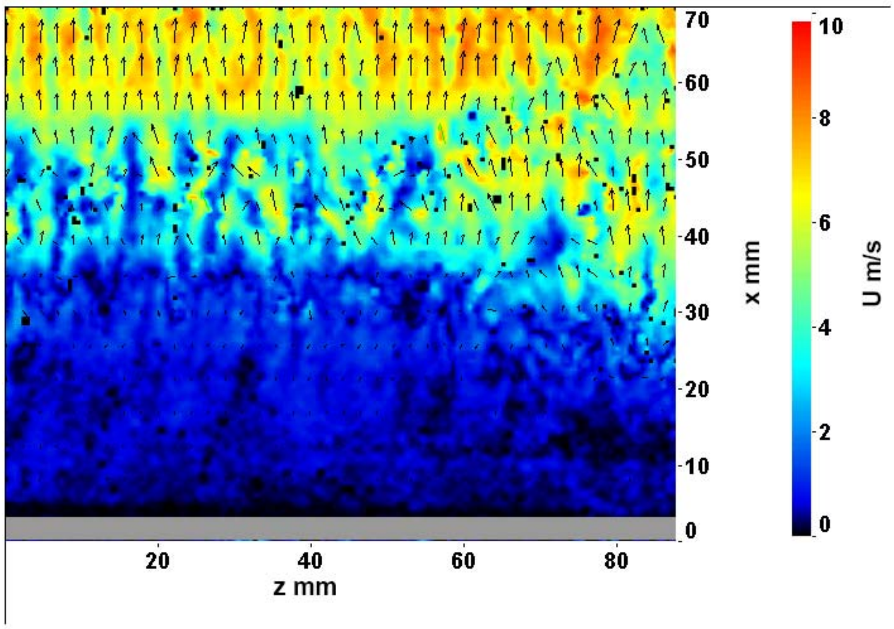

Figure D.2 Instantanious velocity behind straight strip at 1mm height

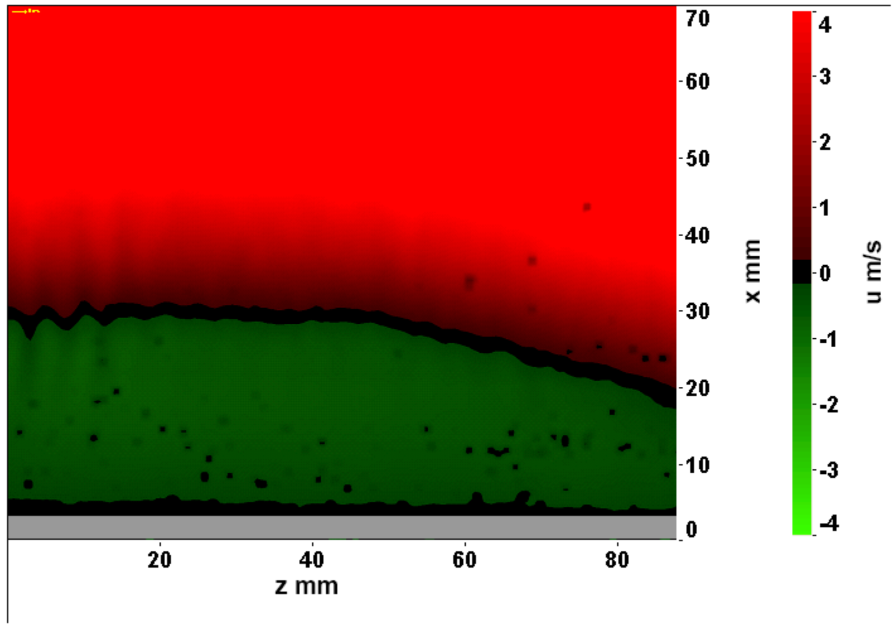

Figure D.3 Average streamwise velocity behind straight strip at 1mm height

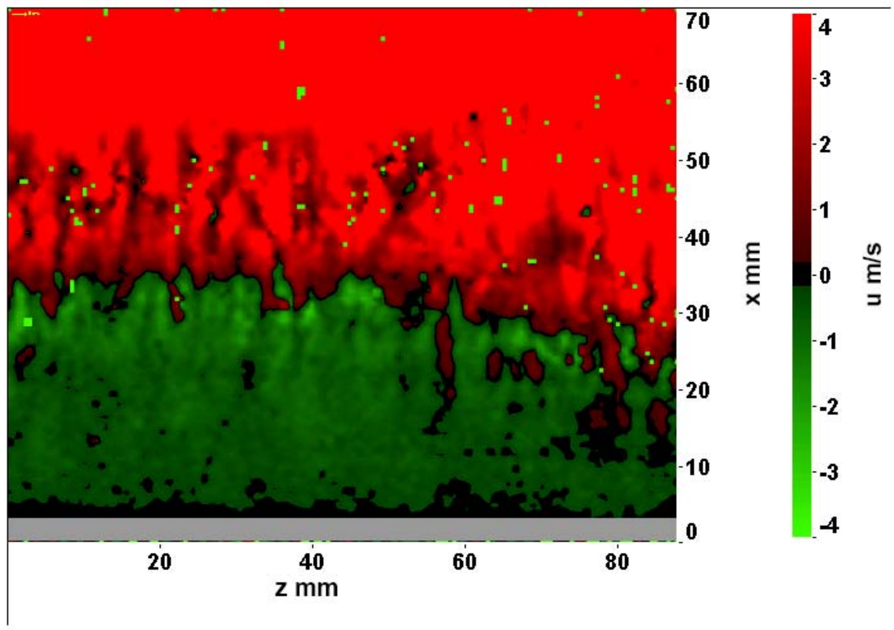

Figure D.4 Instantanious steamwise velocity behind straight strip at 1mm height

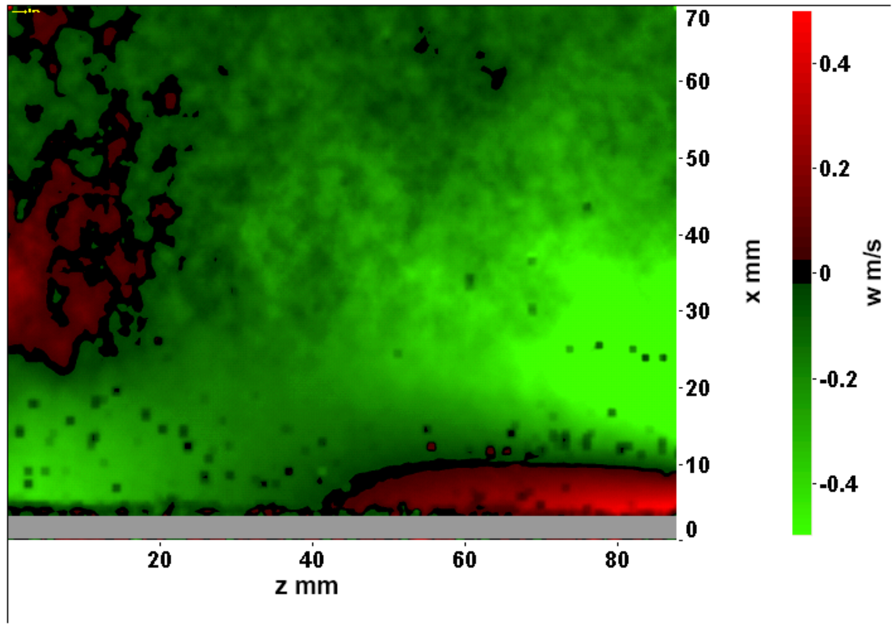

Figure D.5 Average spanwise velocity behind straight strip at 1mm height

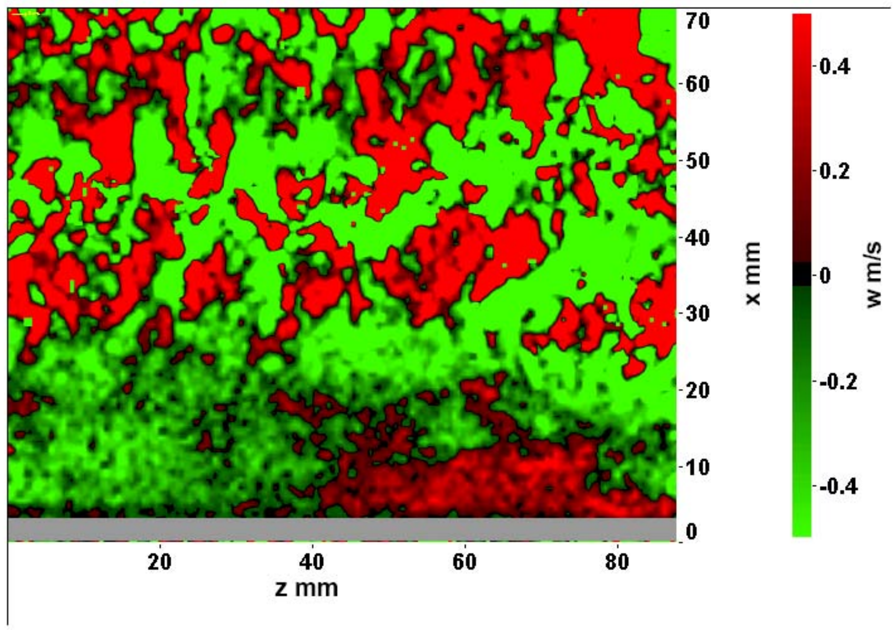

Figure D.6 Instantanious spanwise velocity behind straight strip at 1mm height

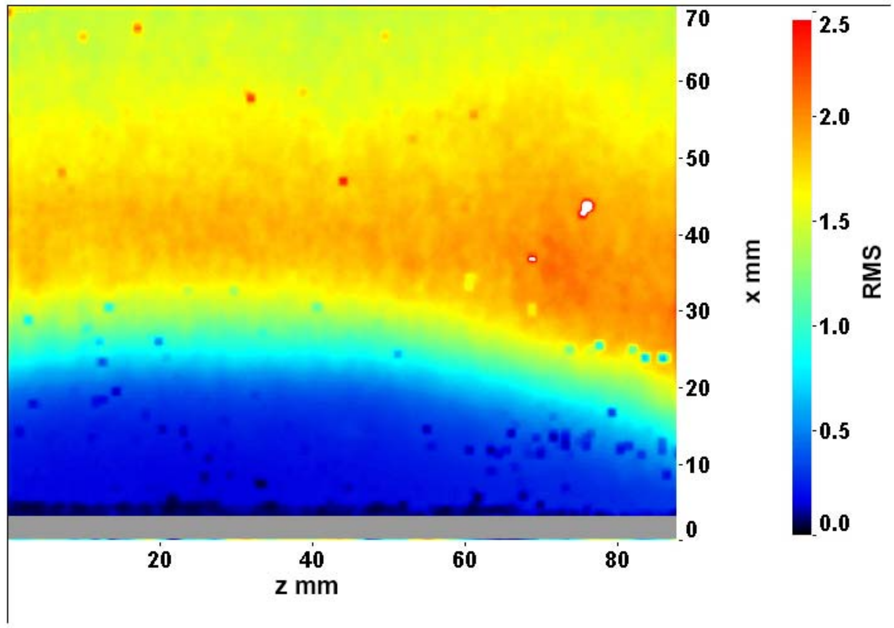

Figure D.7 RMS behind straight strip at 1mm height

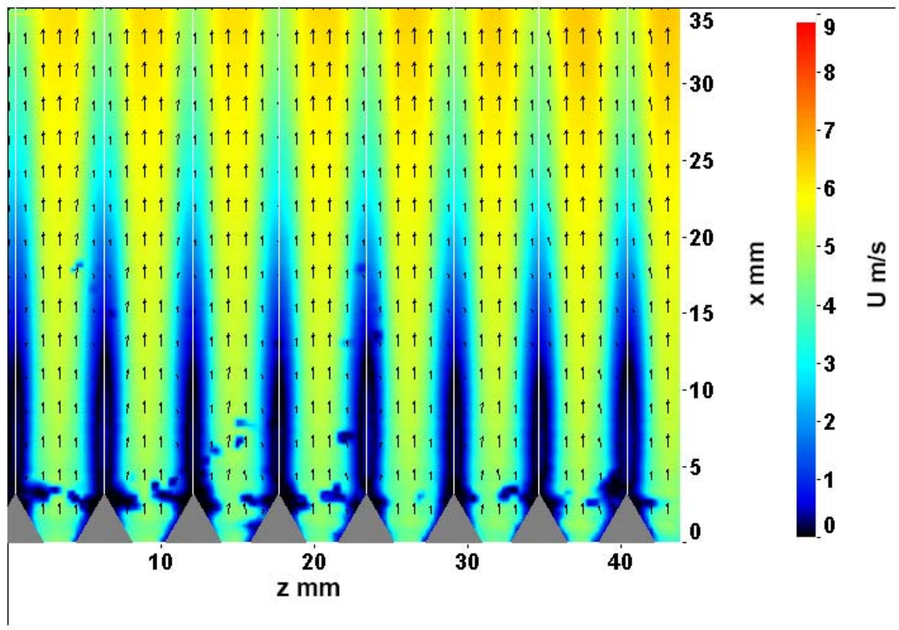

Figure D.8 Average velocity behind zigzag strip at 1mm height

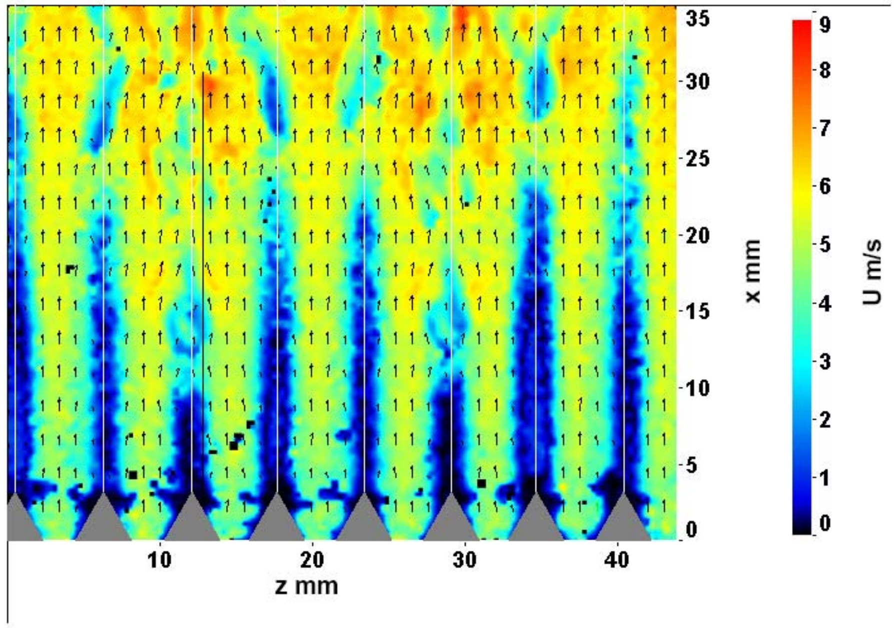

Figure D.9 Instantanious velocity behind zigzag strip at 1mm height

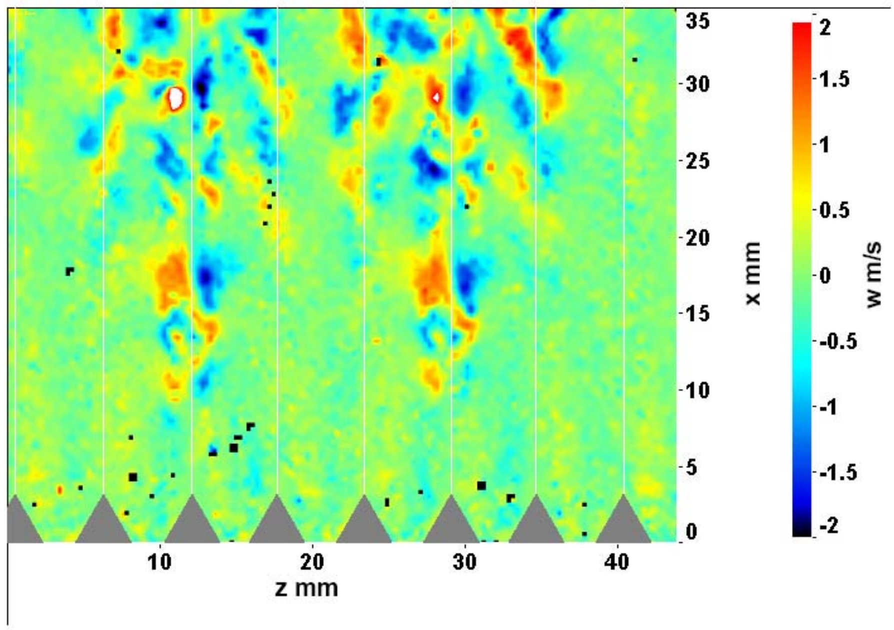

Figure D.10 Instantanious spanwise velocity behind zigzag strip at 1mm height

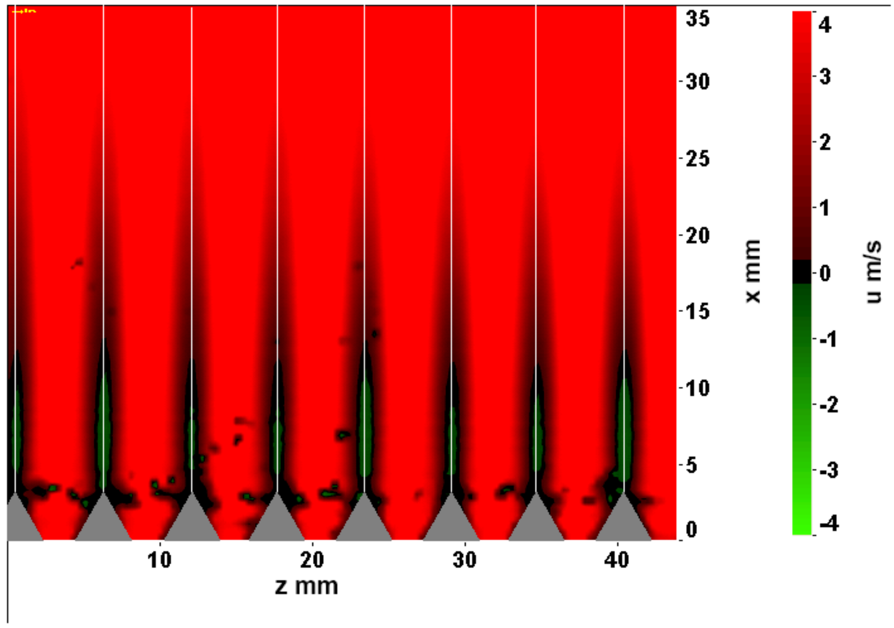

Figure D.11 Average streamwise velocity behind zigzag strip at 1mm height

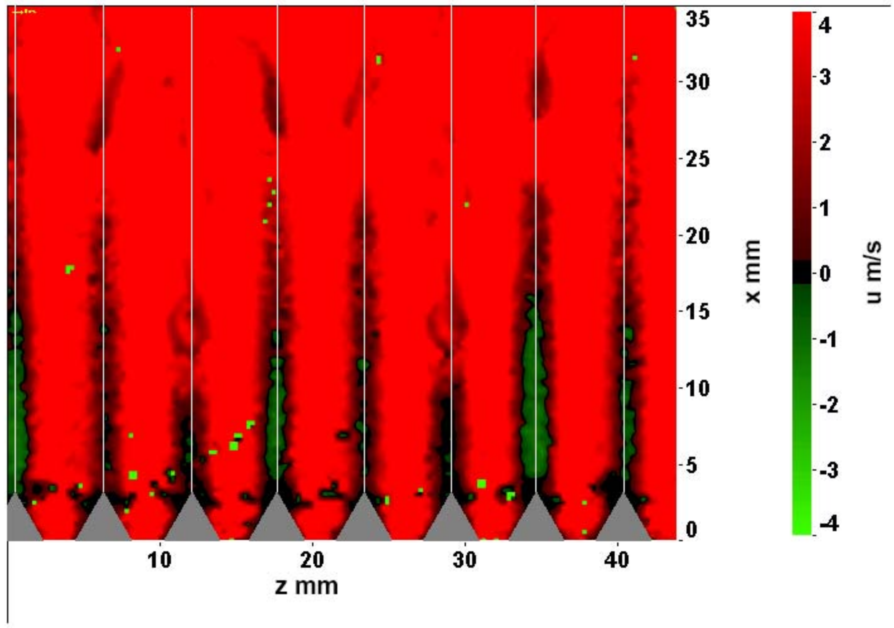

Figure D.12 Instantanious streamwise velocity behind zigzag strip at 1mm height

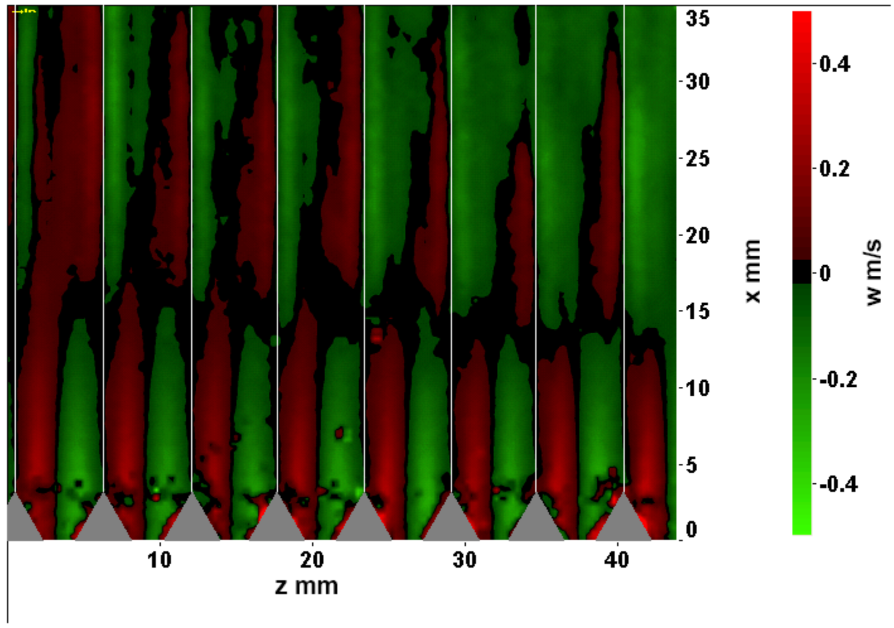

Figure D.13 Average spanwise velocity behind zigzag strip at 1mm height

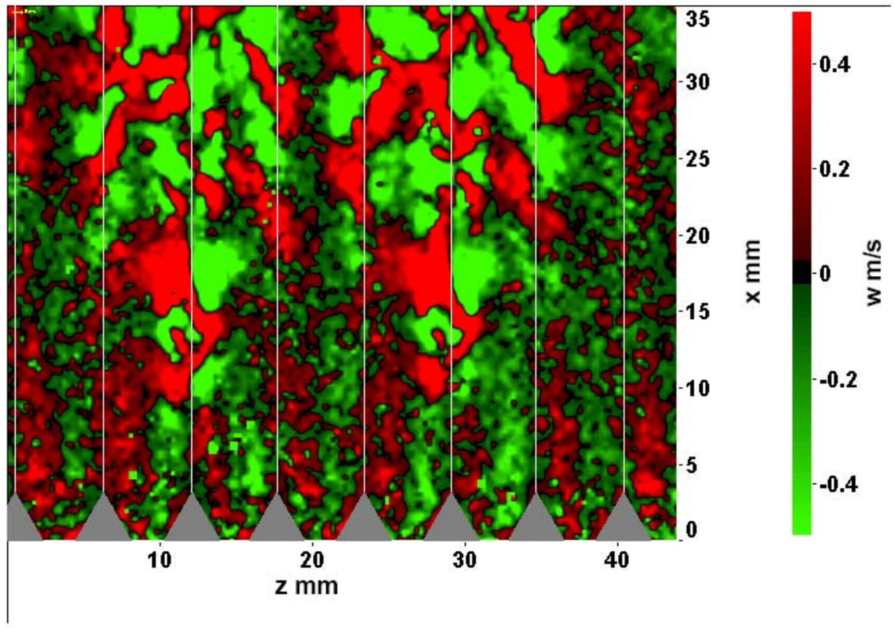

Figure D.14 Instantanious spanwise velocity behind zigzag strip at 1mm height

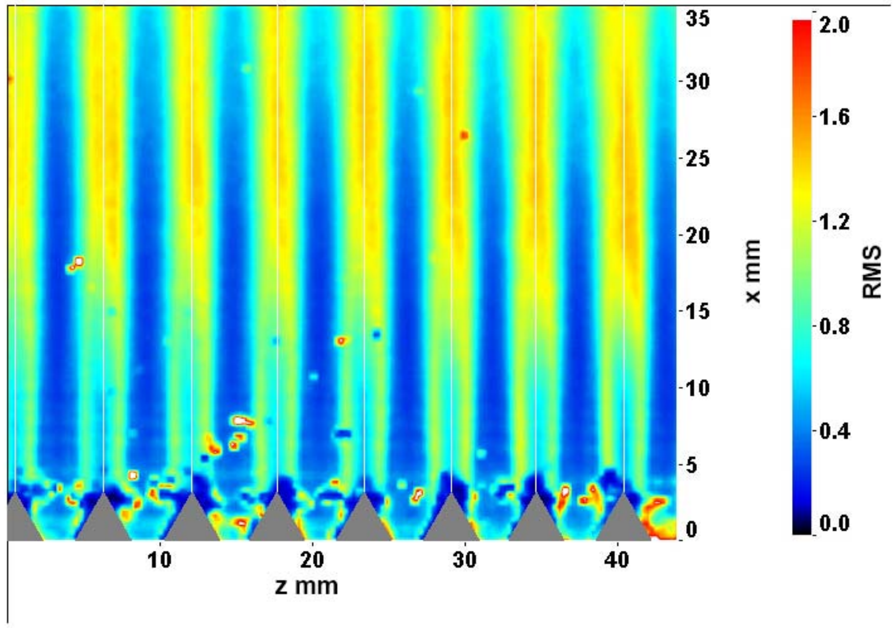

Figure D.15 RMS behind zigzag strip at 1mm height

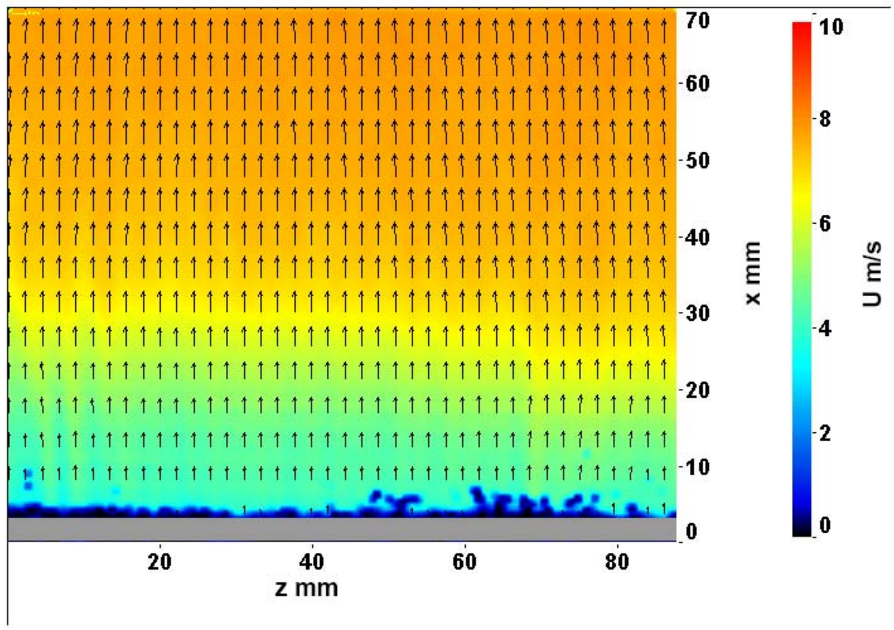

Figure D.16 Average velocity behind straight strip at 2.5mm height

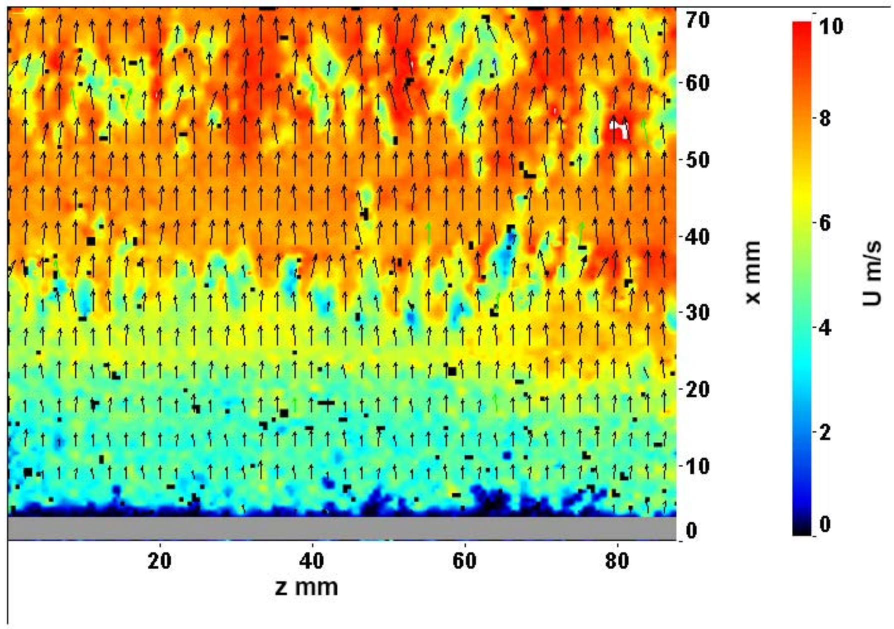

Figure D.17 Instantanious velocity behind straight strip at 2.5mm height

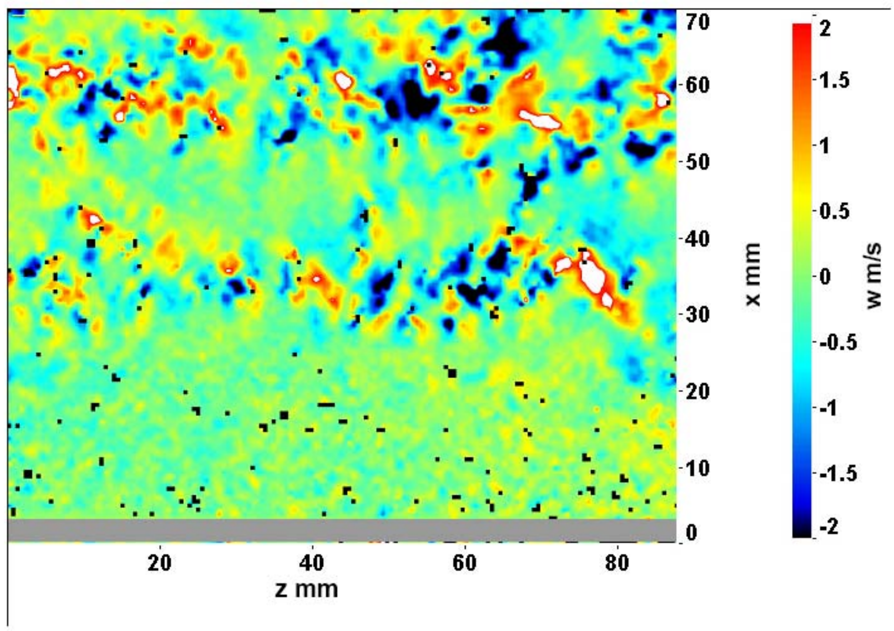

Figure D.18 Instantanious spanwise velocity behind straight strip at 2.5mm height

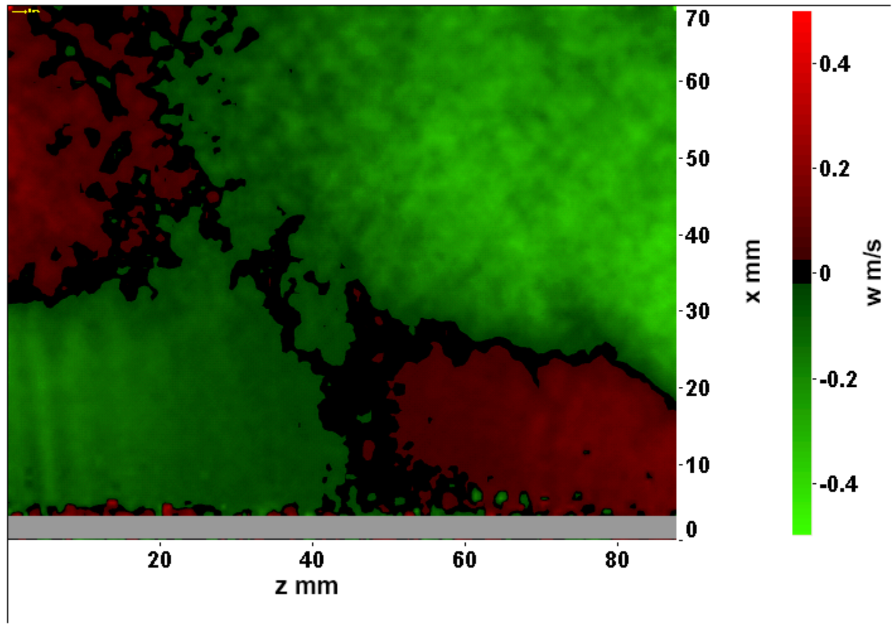

Figure D.19 Average spanwise velocity behind straight strip at 2.5mm height

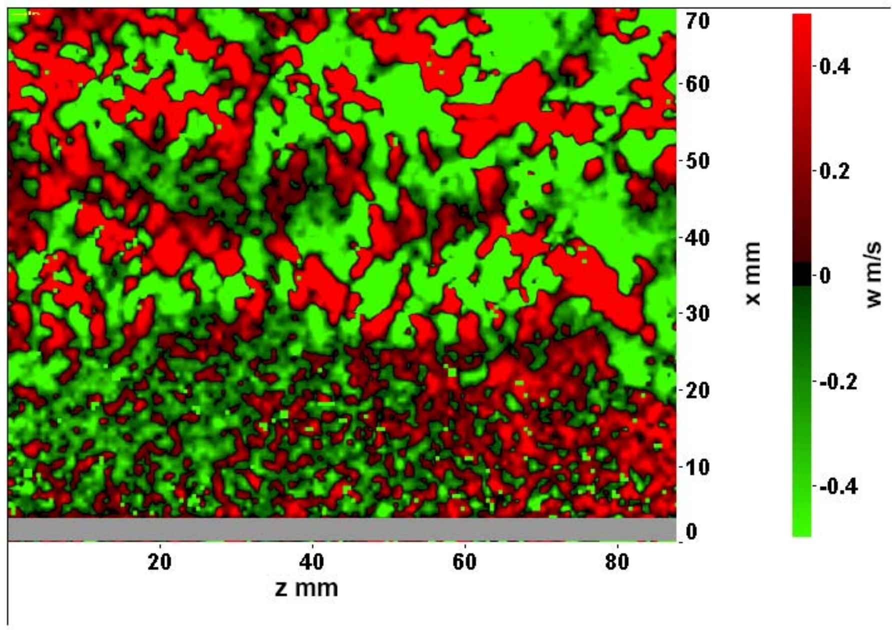

Figure D.20 Instantanious spanwise velocity behind straight strip at 2.5mm height

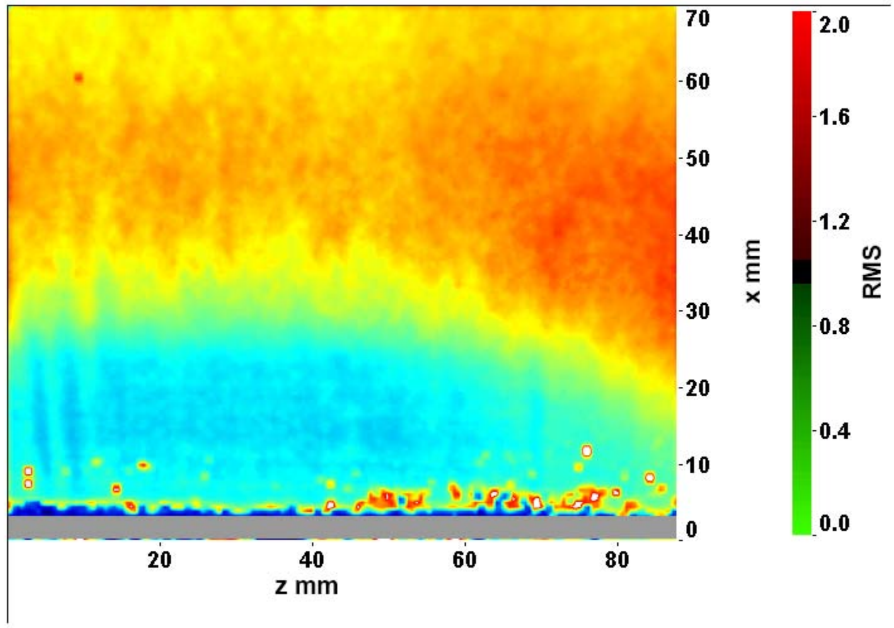

Figure D.21 RMS behind straight strip at 2.5mm height

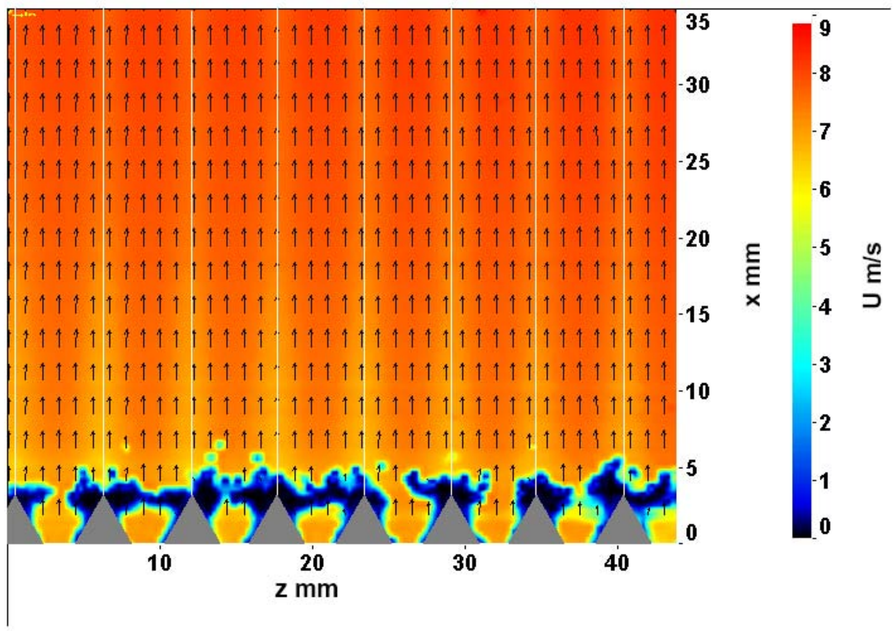

Figure D.22 Average velocity behind zigzag strip at 2mm height

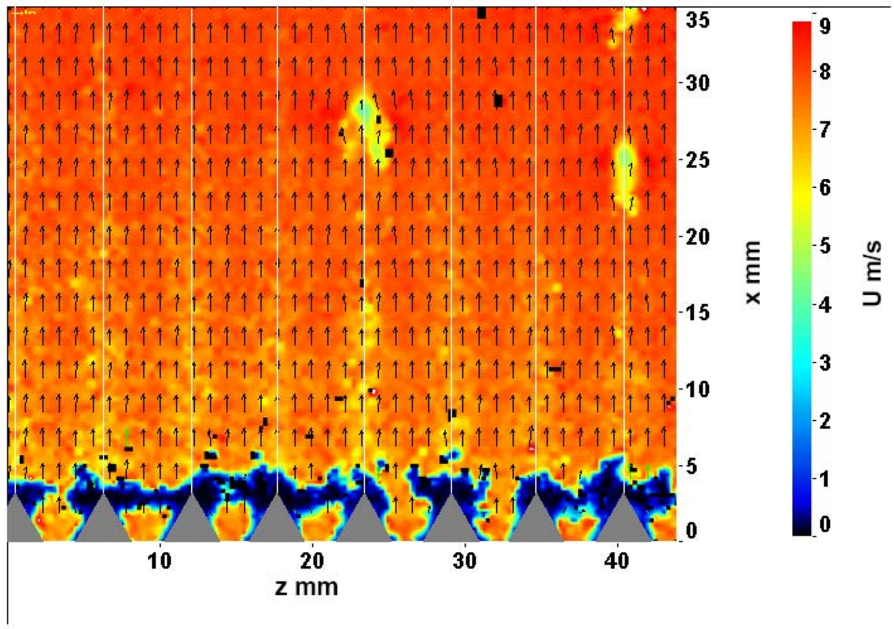

Figure D.23 Instantanious velocity behind zigzag strip at 2mm height

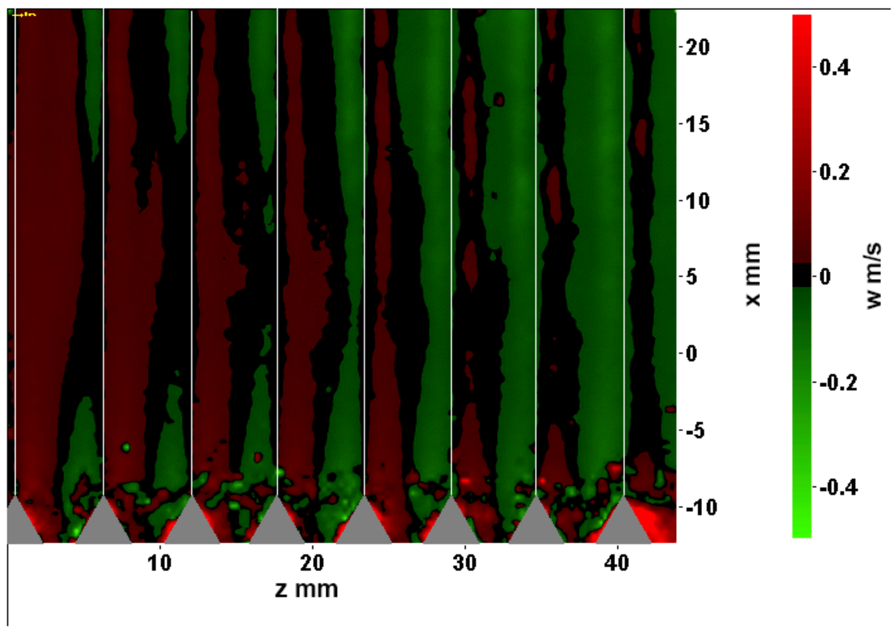

Figure D.24 Average spanwise velocity behind zigzag strip at 2mm height

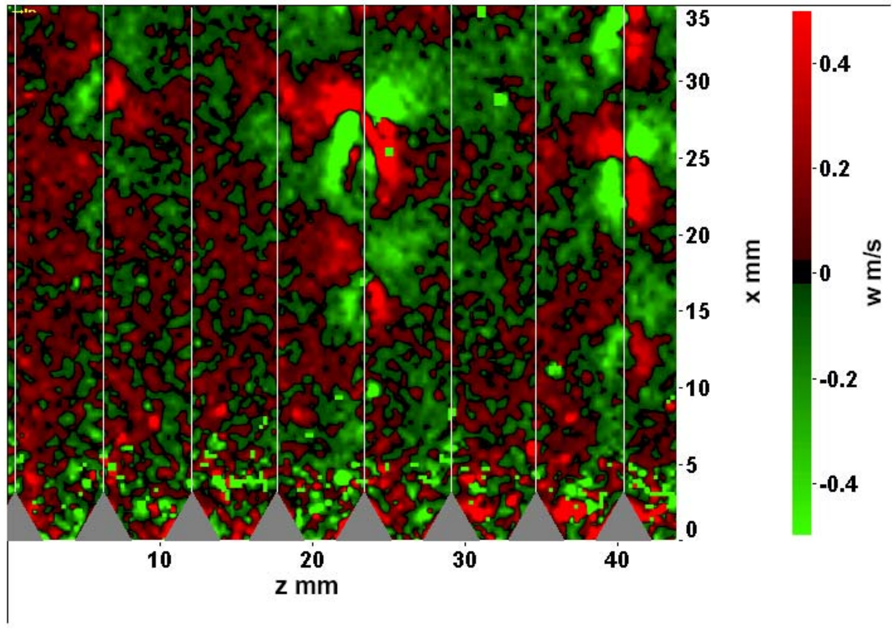

Figure D.25 Instantanious spanwise velocity behind zigzag strip at 2mm height

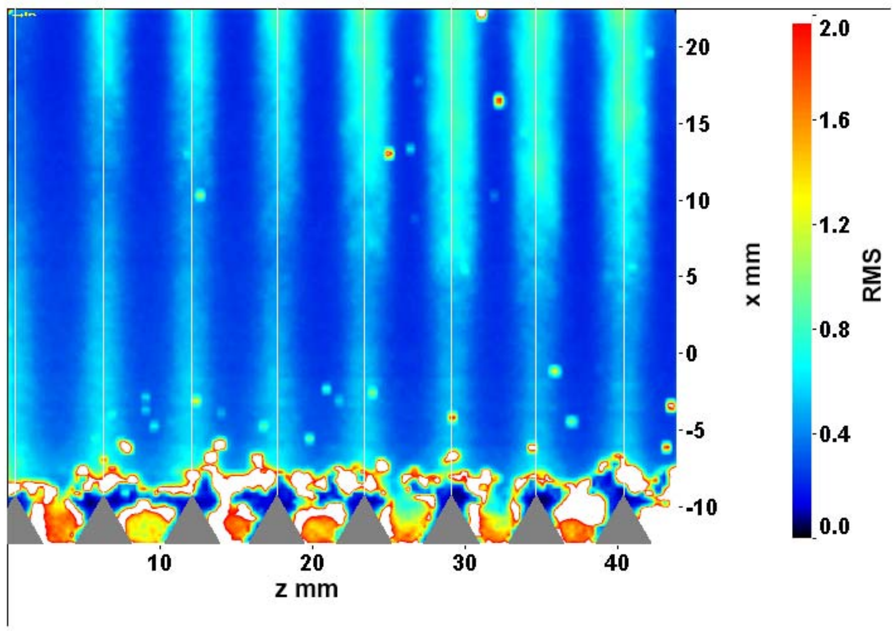

Figure D.26 RMS behind zigzag strip at 2mm height

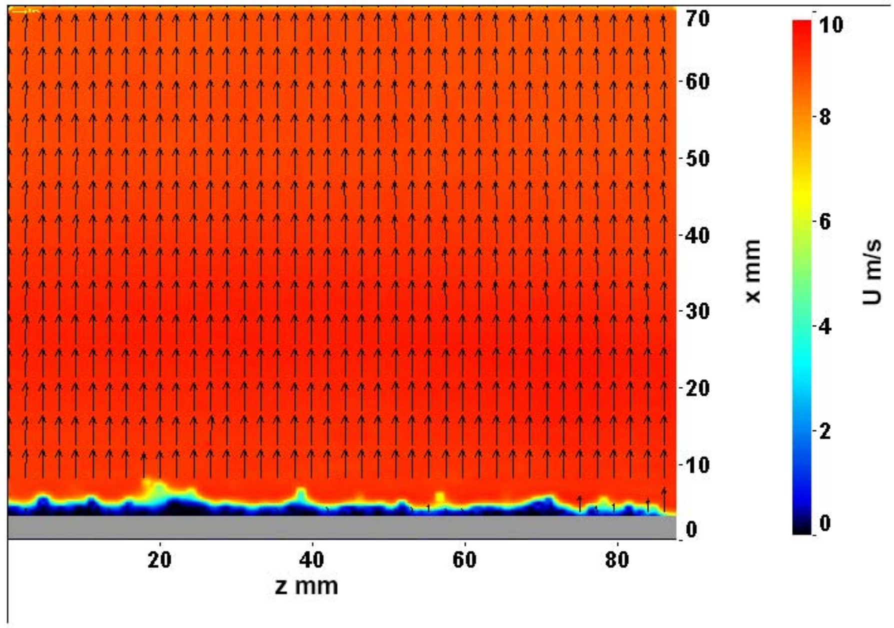

Figure D.27 Average velocity behind straight strip at 4mm height

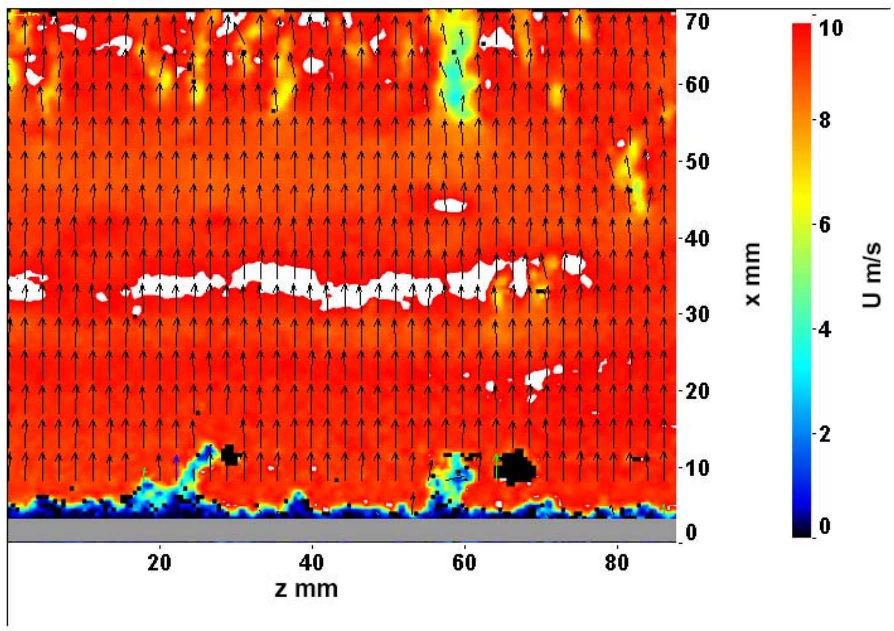

Figure D.28 Instantanious velocity behind straight strip at 4mm height

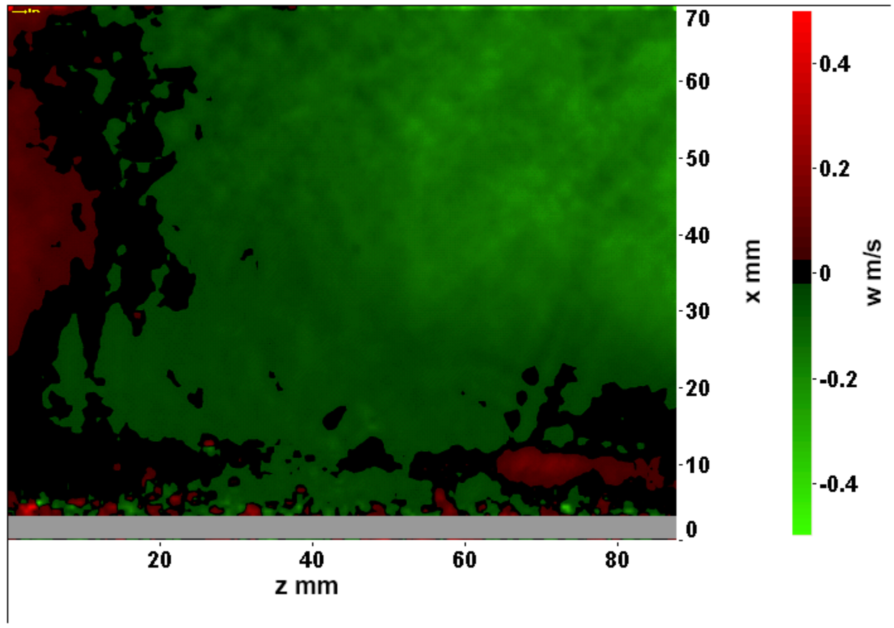

Figure D.29 Average spanwise velocity behind straight strip at 4mm height

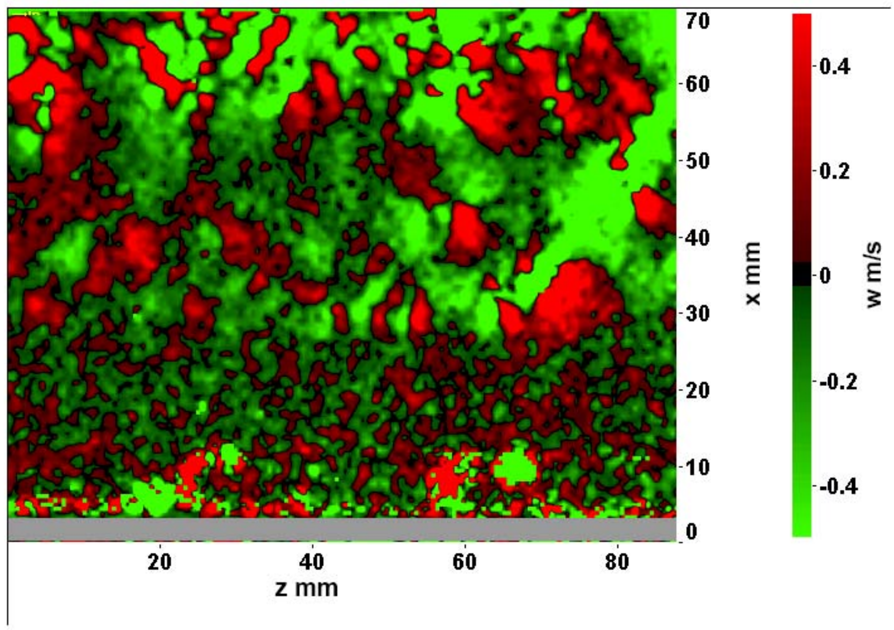

Figure D.30 Instantanious spanwise velocity behind straight strip at 4mm height

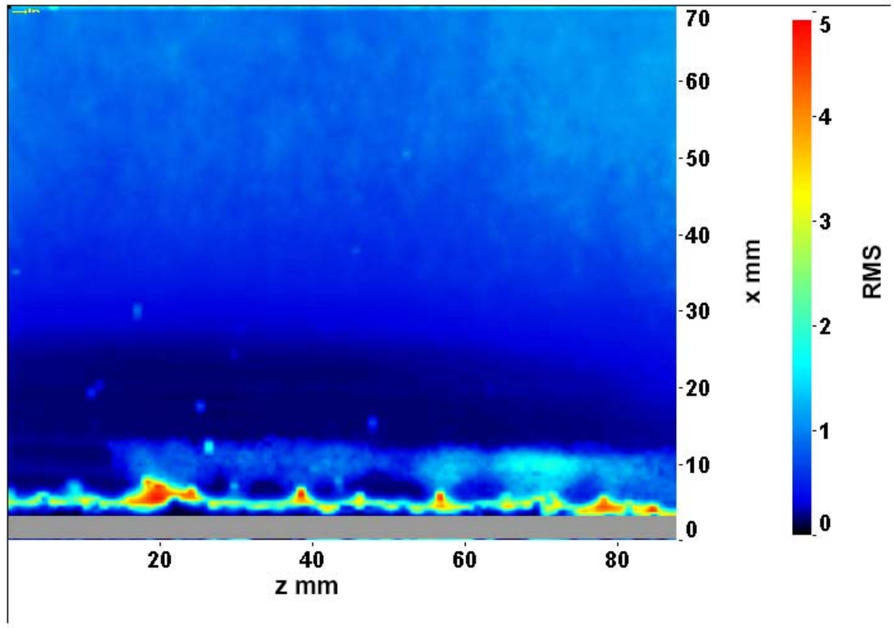

Figure D.31 RMS behind straight strip at 4mm height

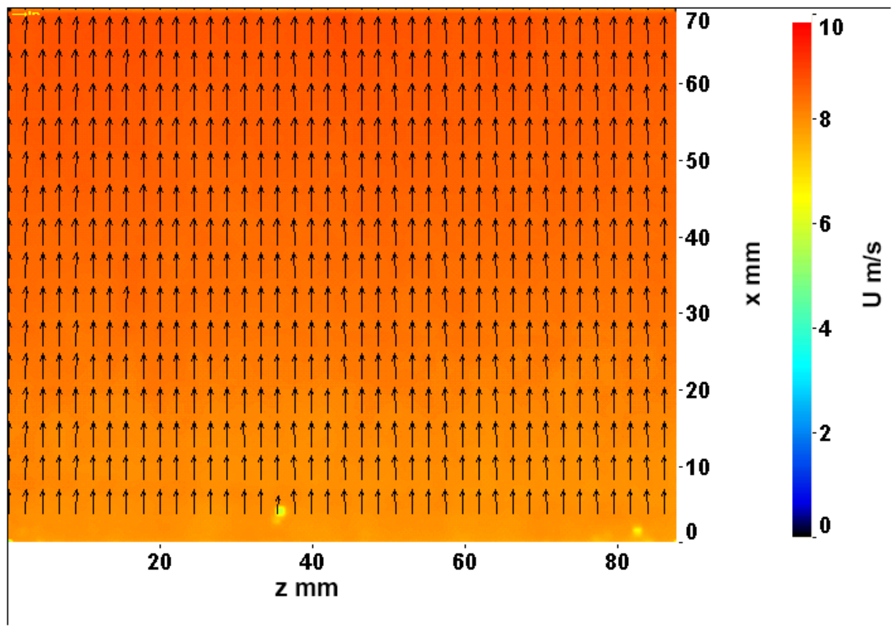

Figure D.32 Average velocity behind straight strip at 5mm height

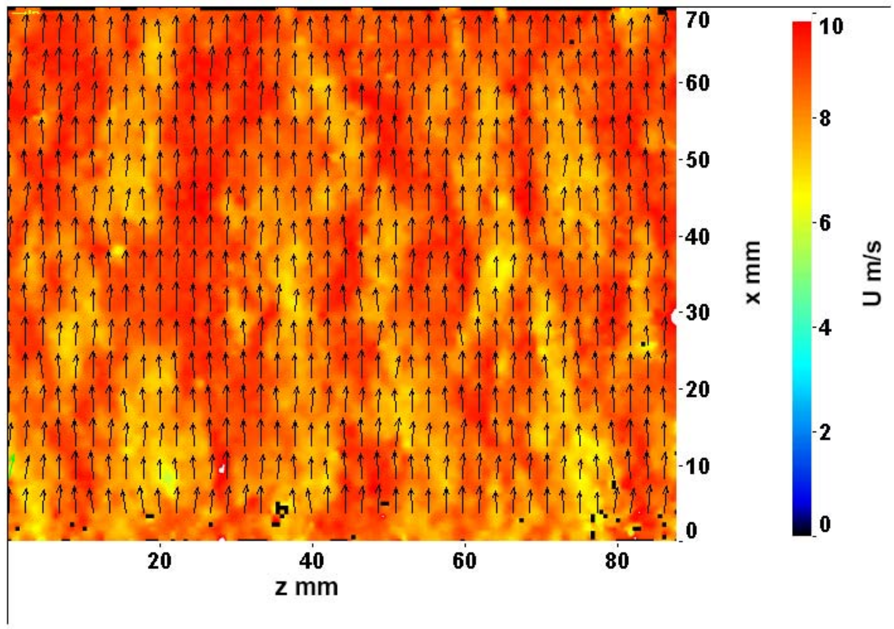

Figure D.33 Instantanious velocity behind straight strip at 5mm height

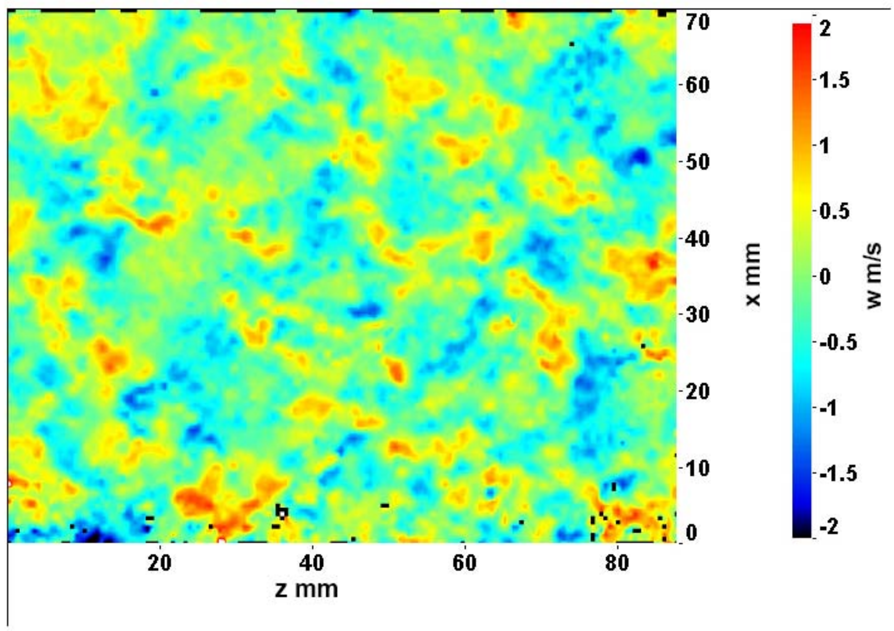

Figure D.34 Instantanious spanwise velocity behind straight strip at 5mm height

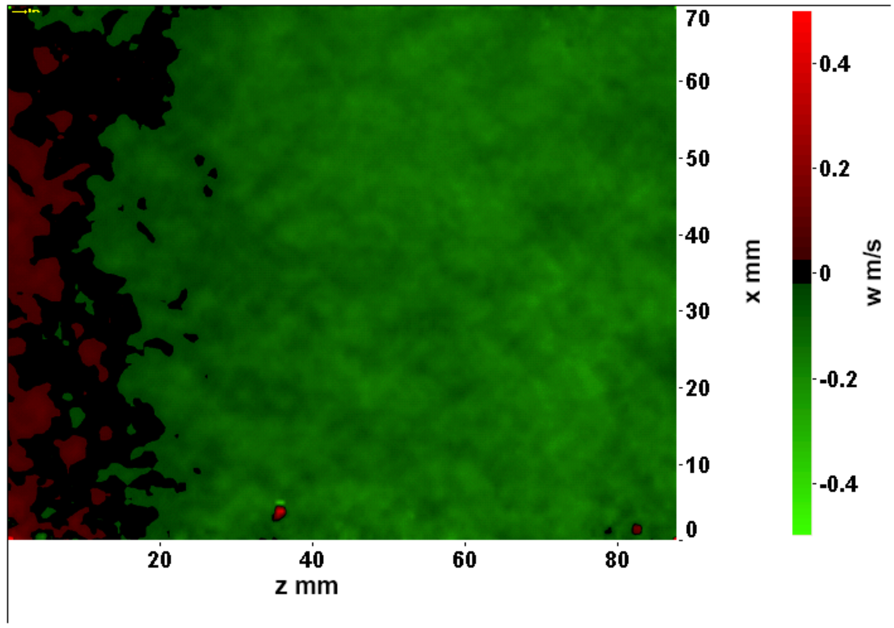

Figure D.35 Average spanwise velocity behind straight strip at 5mm height

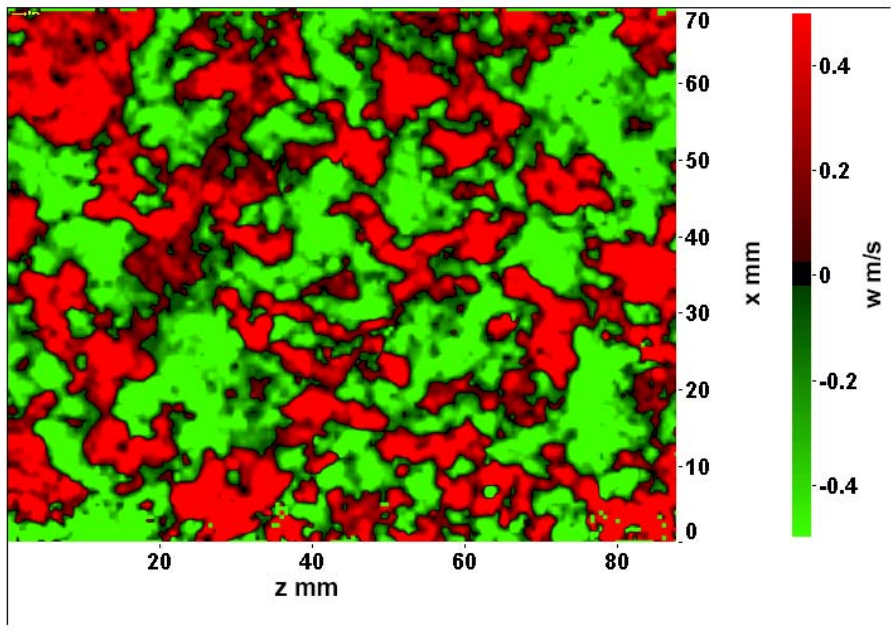

Figure D.36 Instantanious spanwise velocity behind straight strip at 5mm height

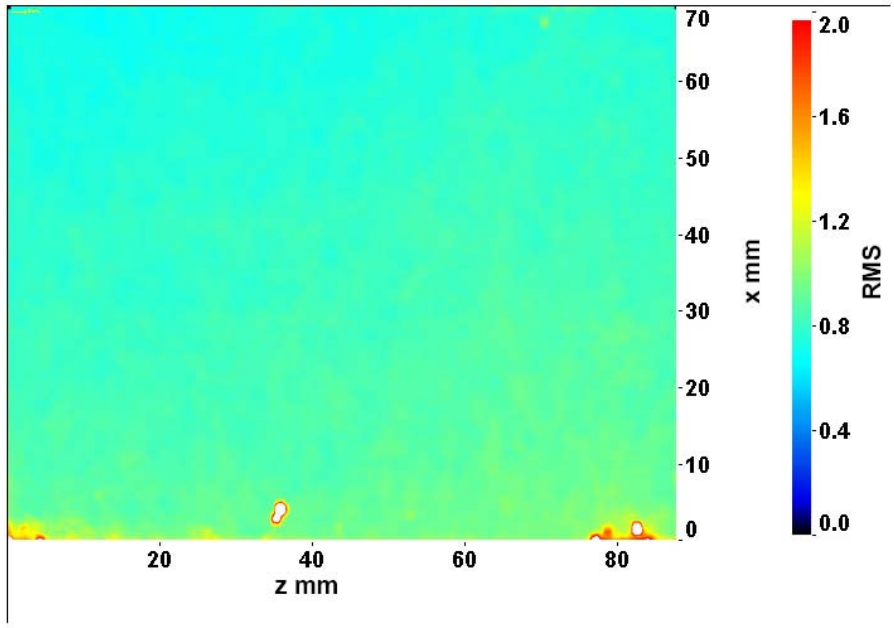

Figure D.37 RMS behind straight strip at 5mm height

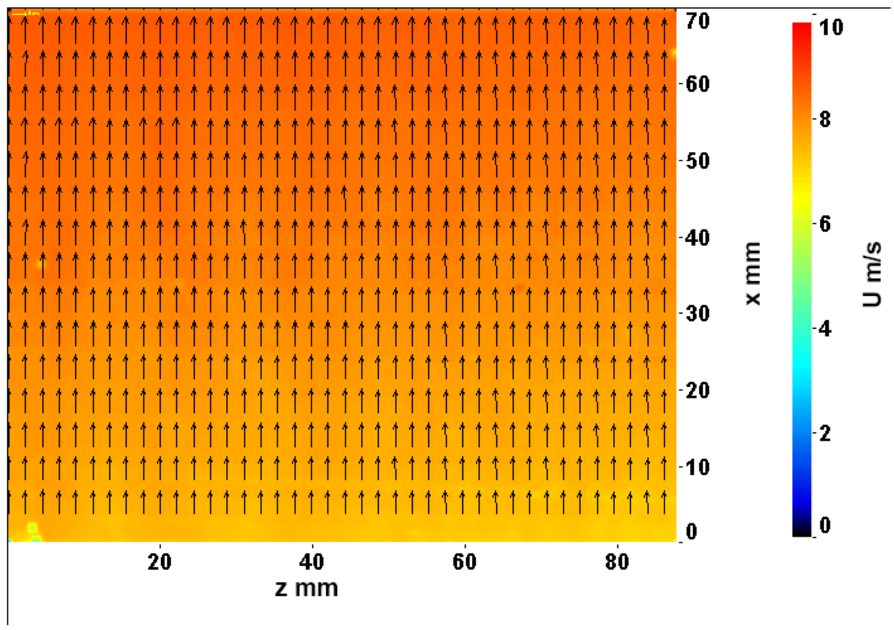

Figure D.38 Average velocity behind zigzag strip at 4mm height and 20cm

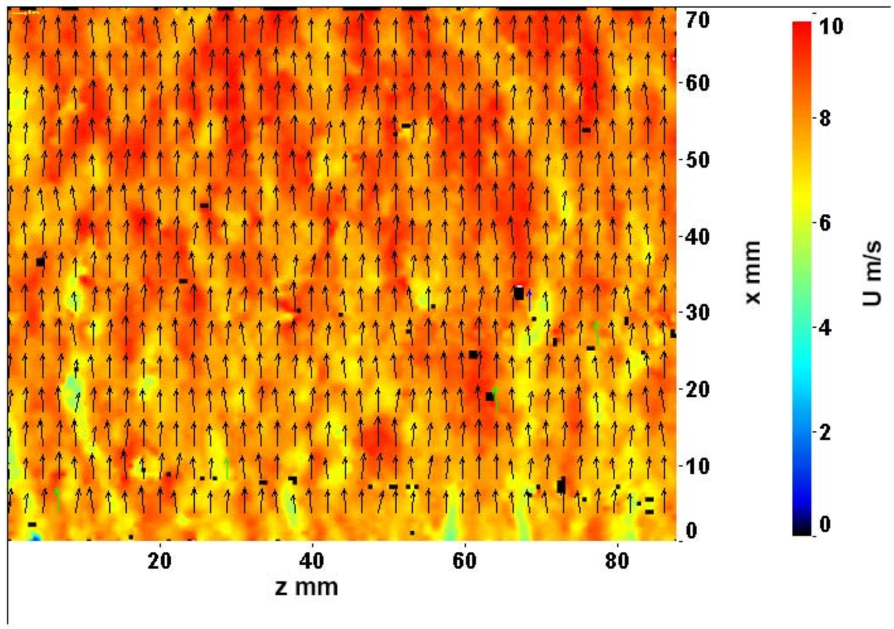

Figure D.39 Instantanious velocity behind zigzag strip at 4mm height and 20cm

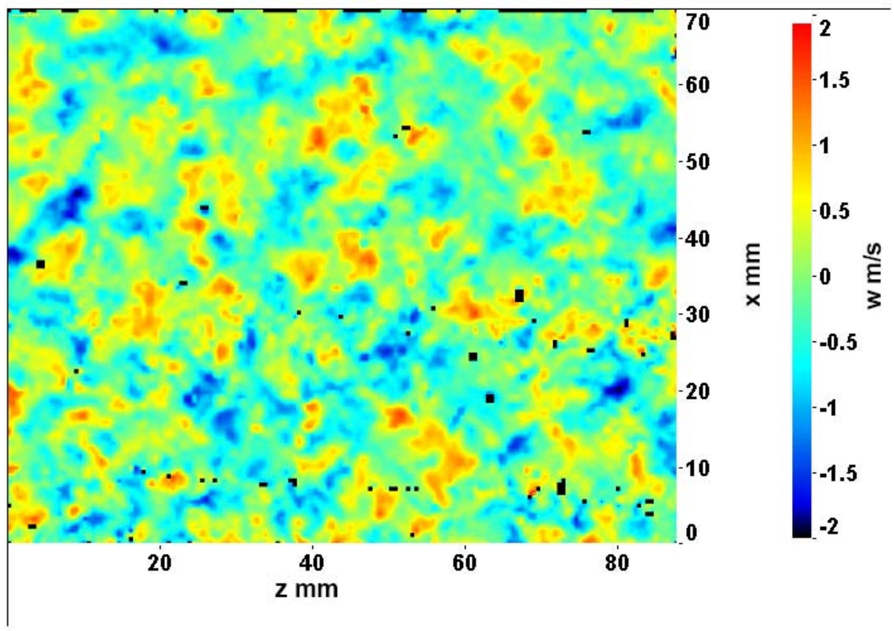

Figure D.40 Instantanious spanwise velocity behind zigzag strip at 4mm height and 20cm

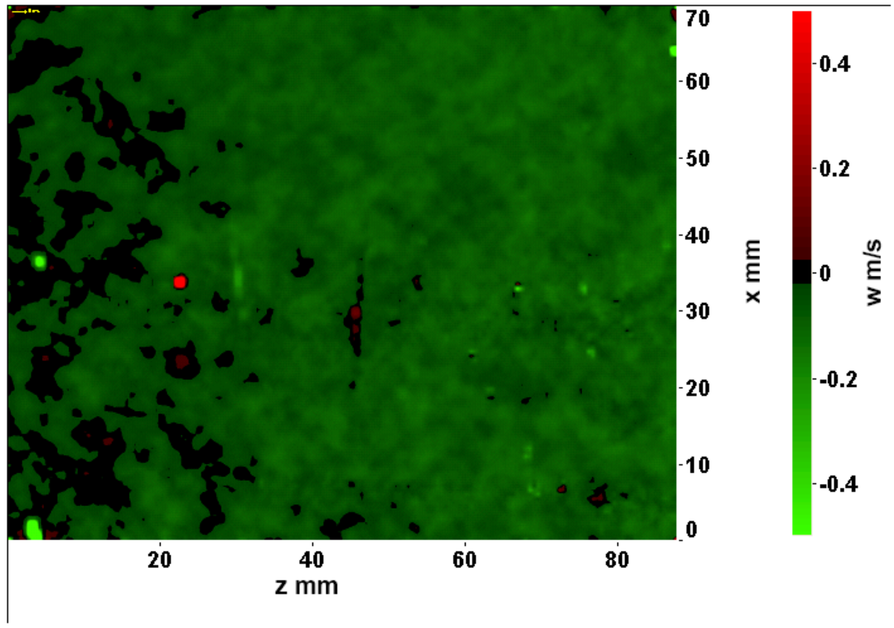

Figure D.41 Average spanwise velocity behind zigzag strip at 4mm height and 20cm

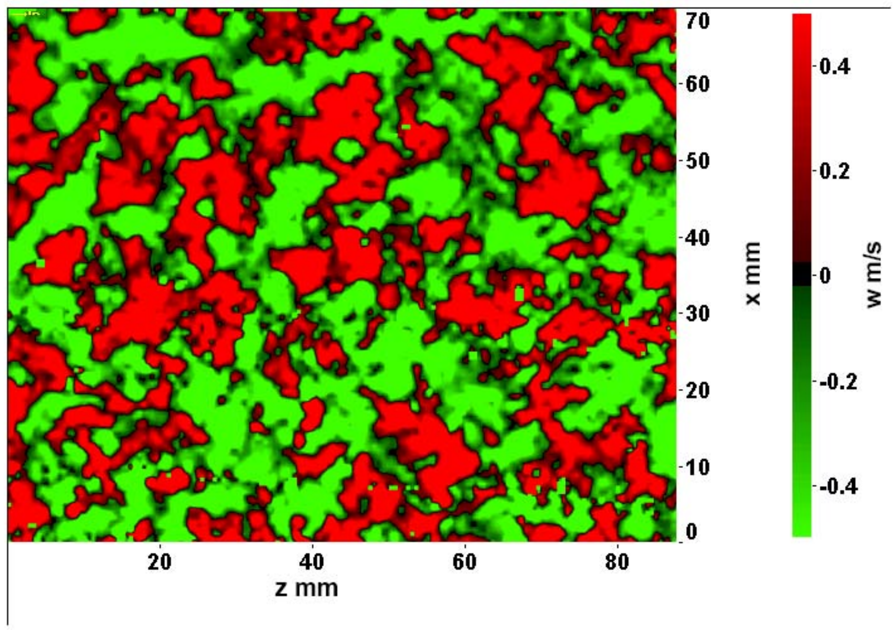

Figure D.42 Instantanious spanwise velocity behind zigzag strip at 4mm height and 20cm

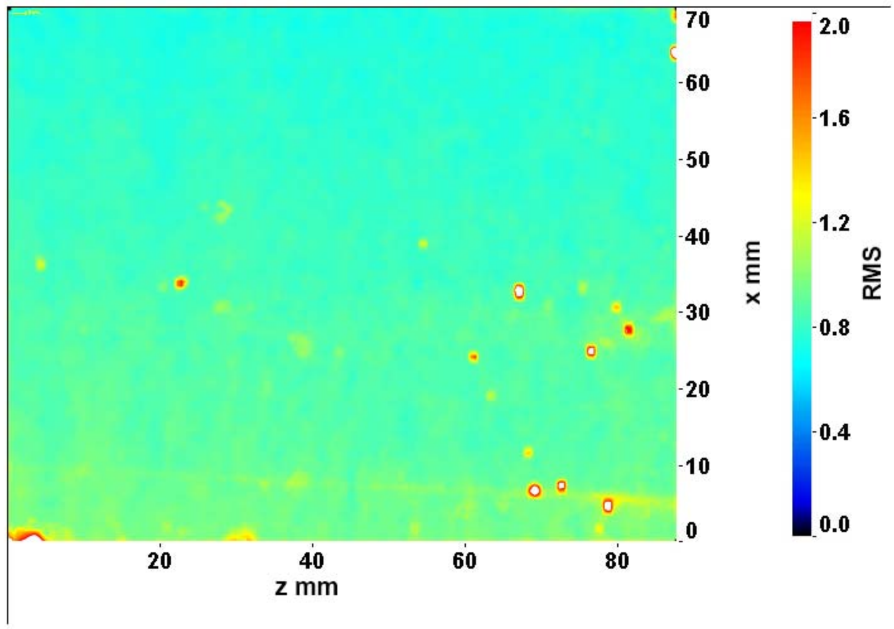

Figure D.43 RMS behind zigzag strip at 4mm height and 20cm

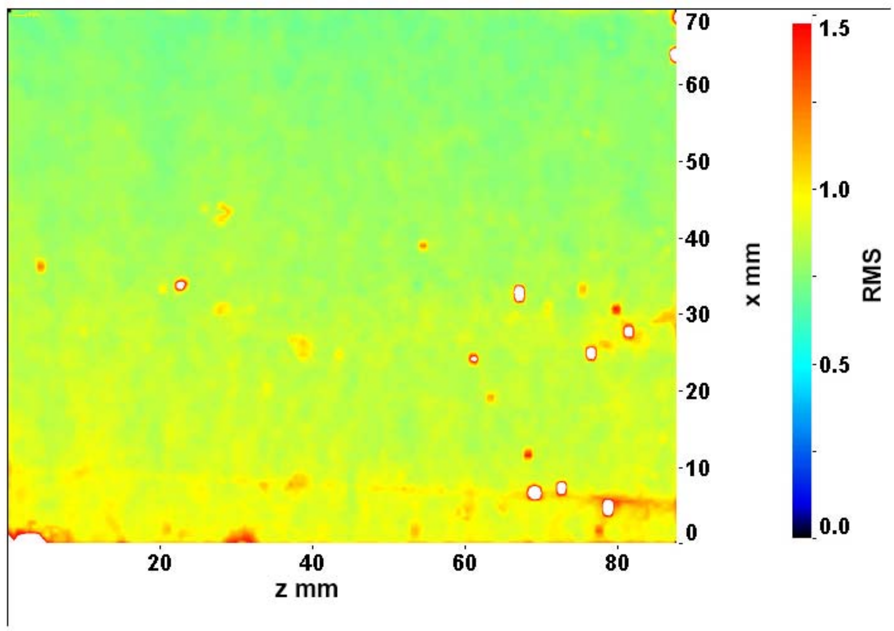

Figure D.44 RMS behind zigzag strip at 4mm height and 20cm

Appendix E King's law

Working principles of HWA (CTA)
Assuming that the wire only loses its heat through convection to the fluid the equilibrium of power yields:

$$\frac{dE_c}{dt} = W - H$$

With:

$$E_c = C_w T_s$$

$$W = I^2 R_w$$

$$R_w = f(T_w)$$

In which E_c is the thermal energy in the wire, C_w is the heat capacity of the wire, T_s is the temperature of the surroundings and R_w is the electrical resistance of the wire. Assuming the wire is at equilibrium at the instant means $\frac{dE_c}{dt} = 0$. Hence:

$$W = H$$

When we assume the following:

- The velocity is normal to the wire
- The temperature of the wire is the same everywhere on the wire
- Fluid has a constant temperature and density

We can convert (3.2) into:

$$I^2 R_w = \frac{NuAk_f}{d}\left(T_w - T_s\right)$$

Where A is outside wire area and k_f is the heat conductivity of the fluid and d the diameter of the wire. For forced convection:

$$Nu = A_1 + B_1 \operatorname{Re}^n = A_2 + B_2 U^n$$

Combining the last two yields:

$$I^2 R_w^2 = E^2 = \left(T_w - T_s\right)\left(A + BU^n\right)$$

This result is known as King's law.

Appendix F Particle Stokes number

The particle stokes number S_k is a good number to check whether you are within acceptable numbers. It is defined as:

$$S_k = \frac{\tau_p}{\tau_f}$$

In which τ_f is the characteristic time of the flow. This Stokes number should be below 0.1 in order to have 1% accuracy.

$$\tau_p = \frac{d_p^2 \rho}{18\mu} = \frac{0.9^2 \cdot 1000}{18 \cdot 1.83 \cdot 10^{-5}} = 3.5 \cdot 10^{-6}$$

$$\tau_f = \frac{\delta_{99\%}}{U_\infty} = \frac{0.008}{8} = 0.001$$

$$\Rightarrow S_k = 3.5 \cdot 10^{-3}$$

As can be seen from this calculation the Stokes number is well below the needed value.